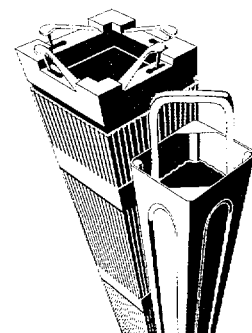


# SIEMENS

EMF-2328(NP)  
Revision 0

## PWR Small Break LOCA Evaluation Model, S-RELAP5 Based

January 2000

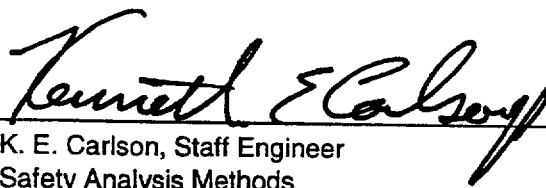


Siemens Power Corporation  
Nuclear Division

---

**PWR Small Break LOCA Evaluation Model, S-RELAP5 Based**

Prepared:

  
K. E. Carlson, Staff Engineer  
Safety Analysis Methods

1/10/00  
Date

Contributors:

H. Chow, S. E. Jensen, A. B. Meginnis, W. T. Nutt, D. L. Caraher, W. S. Yeung

Concurred:

  
J. F. Mallay, Director  
Regulatory Affairs

1/10/00  
Date

**U.S. Nuclear Regulatory Commission  
Report Disclaimer**

**Important Notice Regarding Contents and Use of This Document**

***Please Read Carefully***

This technical report was derived through research and development programs sponsored by Siemens Power Corporation. It is being submitted by Siemens Power Corporation to the U.S. Nuclear Regulatory Commission as part of a technical contribution to facilitate safety analyses by licensees of the U.S. Nuclear Regulatory Commission which utilize Siemens Power Corporation fabricated reload fuel or technical services provided by Siemens Power Corporation for light water power reactors and it is true and correct to the best of Siemens Power Corporation's knowledge, information, and belief. The information contained herein may be used by the U.S. Nuclear Regulatory Commission in its review of this report and, under the terms of the respective agreements, by licensees or applicants before the U.S. Nuclear Regulatory Commission which are customers of Siemens Power Corporation in their demonstration of compliance with the U.S. Nuclear Regulatory Commission's regulations.

Siemens Power Corporation's warranties and representations concerning the subject matter of this document are those set forth in the agreement between Siemens Power Corporation and the Customer pursuant to which this document is issued. Accordingly, except as otherwise expressly provided in such agreement, neither Siemens Power Corporation nor any person acting on its behalf:

- a. makes any warranty, or representation, express or implied, with respect to the accuracy, completeness, or usefulness of the information contained in this document, or that the use of any information, apparatus, method, or process disclosed in this document will not infringe privately owned rights;

or

- b. assumes any liabilities with respect to the use of, or for damages resulting from the use of, any information, apparatus, method, or process disclosed in this document.

### Nature of Changes

Item	Page	Description and Justification
1.	All	This is a new document.

### **Abstract**

A Pressurized Water Reactor (PWR) Small Break Loss of Coolant Accident (SBLOCA) Emergency Core Cooling System (ECCS) evaluation model is presented that incorporates S-RELAP5 as the systems analysis code. A fuel rod model based on the NRC approved RODEX2 code has been integrated into S-RELAP5 to calculate the fuel rod heat-up portion of the SBLOCA. The revised evaluation model replaces the NRC approved evaluation model defined by Reference 1 which utilized the ANF-RELAP and TOODEE2 codes for system analysis and hot rod heat up.

A number of benchmark cases have been analyzed to demonstrate that S-RELAP5 is capable of modeling a SBLOCA. The benchmarks consist of two-dimensional flow tests, the Semiscale S-UT-8 test, the LOFT LP-SB-03 test, a loop seal clearing test in the UPTF, and an integral test in the BETHSY facility. In addition, an example problem is provided to demonstrate the application of the evaluation model.

## Contents

1.0	Introduction.....	1-1
2.0	Summary .....	2-1
3.0	Small Break LOCA Evaluation Model Description.....	3-1
3.1	Event Description.....	3-1
3.1.1	Limiting Break Conditions.....	3-1
3.2	Limiting Break Scenario .....	3-3
3.3	Methodology Description.....	3-4
3.3.1	System Modeling.....	3-6
3.3.1.1	Loop Seal Modeling.....	3-6
3.3.1.2	Main Coolant Piping.....	3-7
3.3.1.3	Reactor Coolant Pumps .....	3-8
3.3.1.4	Downcomer Modeling.....	3-8
3.3.1.5	Upper Vessel .....	3-9
3.3.2	Core Modeling.....	3-9
3.3.2.1	General Hydraulic Modeling .....	3-9
3.3.2.2	Radial Loss Coefficients.....	3-9
3.3.2.3	Heat Structures .....	3-10
3.4	SBLOCA Analysis .....	3-10
4.0	Model Description .....	4-1
5.0	Benchmark Calculations .....	5-1
5.1	Two-Dimensional Flow Test .....	5-2
5.1.1	Test Facility Description .....	5-2
5.1.2	S-RELAP5 Model Description.....	5-3
5.1.3	Boundary Conditions .....	5-4
5.1.4	Comparison to Data .....	5-4
5.1.4.1	Test 1 – 1100/550 .....	5-4
5.1.4.2	Test 2 – 1500/0 .....	5-5
5.1.4.3	Test 3 – 1300/0 .....	5-5
5.1.5	Comparison to Core Flow Distribution Codes .....	5-6
5.1.6	Conclusions.....	5-6
5.2	Semiscale Test S-UT-8 .....	5-24
5.2.1	Test Facility Description .....	5-24
5.2.2	S-RELAP5 Model Description.....	5-25
5.2.3	Boundary Conditions .....	5-26
5.2.4	Comparison to Data .....	5-26
5.2.5	Conclusions.....	5-27
5.3	LOFT LP-SB-03 .....	5-35
5.3.1	Test Facility Description .....	5-35
5.3.2	S-RELAP5 Model Description.....	5-35
5.3.3	Event Description .....	5-36
5.3.4	Comparison to Data .....	5-37
5.3.5	Conclusions.....	5-38
5.4	UPTF Loop Seal Clearing .....	5-43

5.4.1	Test Facility Description .....	5-43
5.4.2	S-RELAP5 Model Description.....	5-45
5.4.3	Boundary Conditions .....	5-45
5.4.4	Comparison to Data .....	5-45
5.4.5	Sensitivities .....	5-47
5.4.6	Conclusions.....	5-47
5.5	BETHSY.....	5-58
5.5.1	Test Facility Description .....	5-58
5.5.2	S-RELAP5 Model .....	5-59
5.5.3	Boundary Conditions .....	5-59
5.5.4	Comparison to Data .....	5-60
5.5.5	Conclusions.....	5-62
6.0	Methodology Example .....	6-1
6.1	S-RELAP5 Model .....	6-1
6.2	Break Spectrum .....	6-2
6.3	2-Inch Break Base Case .....	6-3
6.4	Sensitivity Studies .....	6-4
6.4.1	Time Step Size .....	6-4
6.4.2	Restart .....	6-5
6.4.3	Loop Seal Biasing .....	6-5
6.4.4	Pump Model .....	6-5
6.4.5	Radial Flow Form Loss Coefficients .....	6-6
6.4.6	Nodalization Studies.....	6-6
6.4.7	Summary.....	6-7
7.0	References .....	7-1
Appendix A	Core Radial Loss Coefficient Development.....	A-1

## Tables

2.1	Comparison Between Previous and Proposed Methodologies .....	2-2
2.2	Sensitivity Studies Summary .....	2-4
5.1	Experiment Summary .....	5-1
5.1.1	Flow Boundary Conditions for the Cases Evaluated .....	5-7
5.2.1	Sequence of Events for Semiscale Test S-UT-8 .....	5-25
5.2.2	Summary of Calculated PCTs. ....	5-27
5.3.1	Event Sequence.....	5-36
5.5.1	Chronology of Main Events .....	5-63
5.5.2	Initial Conditions for BETHSY Test 9.1b.....	5-64
6.1	Break Spectrum Results Summary.....	6-8
6.2	Event Sequence for 2.0-Inch Break.....	6-9
6.3	Sensitivity Studies .....	6-10

## Figures

3.1	Schematic of Old and New SPC Small Break Models .....	3-5
5.1.1	Test Rig for Flow Blockage Tests Showing Location of Perforated Plate.....	5-3
5.1.2	Cross Sectional View of Test Assemblies Without Perforated Plate Between Test Assemblies .....	5-9
5.1.3	Cross Sectional View of Test Assemblies with Perforated Plate Between Test Assemblies .....	5-10
5.1.4	Nodalization Diagram for S-RELAP5 Modeling of Westinghouse Flow Blockage Tests .....	5-11
5.1.5	Form Loss for Lateral Flow (Typical) .....	5-12
5.1.6	Axial Velocities at 7.5-Inches for Asymmetric Flow (1138/512).....	5-12
5.1.7	Axial Velocities at 12.5-Inches for Asymmetric Flow (1138/512).....	5-13
5.1.8	Axial Velocities at 17.5-Inches for Asymmetric Flow (1138/512).....	5-13
5.1.9	Axial Velocities at 22.5-Inches for Asymmetric Flow (1138/512).....	5-14
5.1.10	Axial Velocities at 27.5-Inches for Asymmetric Flow (1138/512).....	5-14
5.1.11	Axial Velocities at 32.5-Inches for Asymmetric Flow (1138/512).....	5-15
5.1.12	Axial Flow Fractions for Asymmetric Flow (1138/512) .....	5-15
5.1.13	Axial Velocities at 7.5-Inches for Asymmetric Flow (1281/0) .....	5-16
5.1.14	Axial Velocities at 12.5-Inches for Asymmetric Flow (1281/0).....	5-16
5.1.15	Axial Velocities at 17.5-Inches for Asymmetric Flow (1281/0).....	5-17
5.1.16	Axial Velocities at 22.5-Inches for Asymmetric Flow (1281/0) .....	5-17
5.1.17	Axial Velocities at 27.5-Inches for Asymmetric Flow (1281/0) .....	5-18
5.1.18	Axial Velocities at 32.5-Inches for Asymmetric Flow (1281/0) .....	5-18
5.1.19	Axial Flow Fractions for Asymmetric Flow–Blocked Inlet Comparison of S-RELAP5 to Flow Data and Flow Fractions Based on Velocities .....	5-19



5.1.20	Axial Velocities at 7.5-Inches for Asymmetric Flow (1300/0) – Blocked Exit for Assembly B .....	5-19
5.1.21	Axial Velocities at 12.5-Inches for Asymmetric Flow (1300/0) – Blocked Exit for Assembly B .....	5-20
5.1.22	Axial Velocities at 17.5-Inches for Asymmetric Flow (1300/0) – Blocked Exit for Assembly B .....	5-20
5.1.23	Axial Velocities at 22.5-Inches for Asymmetric Flow (1300/0) – Blocked Exit for Assembly B .....	5-21
5.1.24	Axial Velocities at 27.5-Inches for Asymmetric Flow (1300/0) – Blocked Exit for Assembly B .....	5-21
5.1.25	Axial Velocities at 32.5-Inches for Asymmetric Flow (1300/0) – Blocked Exit for Assembly B .....	5-22
5.1.26	Comparison of S-RELAP5 with THINC-IV for Asymmetric Flow (1138/512).....	5-22
5.1.27	Comparison of S-RELAP5 with THINC-IV for Asymmetric Flow (1500/0) .....	5-23
5.2.1	Isometric of the Semiscale Mod-2A Facility .....	5-29
5.2.2	S-RELAP5 Nodalization for S-UT-8 Simulations .....	5-30
5.2.3	Primary System Pressure (Upper Plenum).....	5-31
5.2.4	Secondary Side Pressures .....	5-31
5.2.5	Integrated Break Flow .....	5-32
5.2.6	Collapsed Level in the Intact SG Upflow Tubes.....	5-32
5.2.7	Collapsed Level in the Intact SG Downflow Tubes .....	5-33
5.2.8	Collapsed Level in the Core .....	5-33
5.2.9	Core Mid-Plane Cladding Temperature .....	5-34
5.3.1	LOFT Reactor Vessel Assembly. ....	5-39
5.3.2	Primary System Nodalization .....	5-40
5.3.3	S-RELAP5 Mixture Level Using Two-Dimensional Core Model Compared to LOFT Data and ANF-RELAP Calculation.....	5-41
5.3.4	S-RELAP5 Clad Temperatures at the 49-Inch Elevation Using Two-Dimensional Core Model Compared to LOFT Data and ANF-RELAP Calculation .....	5-41
5.3.5	S-RELAP5 Clad Temperatures at the 28-Inch Elevation Using Two-Dimensional Core Model Compared to LOFT Data and ANF-RELAP Calculation .....	5-42
5.3.6	S-RELAP5 Steam Temperatures at the Core Exit Using Two-Dimensional Core Model Compared to LOFT Data and ANF-RELAP Calculation .....	5-42
5.4.1	Upper Plenum Test Facility .....	5-48
5.4.2	Configuration and Instrumentation for Loop 2.....	5-49
5.4.3	UPTF Loop 2 Loop Seal Configuration and Instrumentation.....	5-50
5.4.4	Loop Seal Nodalization with 13 Volumes .....	5-51
5.4.5	Cold-Leg Outlet Pressure Boundary Condition for S-RELAP5 Model UPTF Test A5RUN11E .....	5-52
5.4.6	Cross-Over Leg Inlet Steam and Water Injection Mass Flow Rate Boundary Conditions for S-RELAP5 Model UPTF Test A5RUN11E .....	5-52
5.4.7	Cross-Over Leg Inlet Steam and Water Injection Temperature Boundary Conditions for S-RELAP5 Model UPTF Test A5RUN11E .....	5-53

5.4.8	Comparison of Loop Seal Collapsed Liquid Level to Data from UPTF Test A5RUN11E-Base Model 10 ms Time Step .....	5-53
5.4.9	Comparison of Differential Pressure Across Loop Seal to Data from UPTF Test A5RUN11E-Base Model with 10 ms Time Step .....	5-54
5.4.10	Loop Seal Nodalization with 10 Volumes .....	5-54
5.4.11	Comparison of Loop Seal Collapsed Liquid Level to Data from UPTF Test A5RUN11E-Alternative Model with 10 ms Time Step .....	5-55
5.4.12	Comparison of Differential Pressure Across Loop Seal to Data from UPTF Test A5RUN11E-Alternative Model with 10 ms Time Step .....	5-55
5.4.13	Calculated Comparison of Loop Seal Collapsed Liquid Level to Data from UPTF Test A5RUN11E-Base Model with 100 ms Time Step .....	5-56
5.4.14	Comparison of Differential Pressure Across Loop Seal to Data from UPTF Test A5RUN11E-Base Model with 100 ms Time Step .....	5-56
5.4.15	Calculated Comparison of Loop Seal Collapsed Liquid Level to Data from UPTF Test A5RUN11E - Base Model with 5 ms Time Step .....	5-57
5.4.16	Comparison of Calculated Differential Pressure Across Loop Seal to Data from UPTF Test A5RUN11E - Base Model with 5 ms Time Step .....	5-57
5.5.1	Schematic of BETHSY 3-Loop Configuration .....	5-65
5.5.2	S-RELAP5 Nodalization of BETHSY Facility .....	5-66
5.5.3	S-RELAP5 Core Power Compared to Experimental Data .....	5-67
5.5.4	S-RELAP5 Pump Speed Compared to Experimental Data .....	5-67
5.5.5	S-RELAP5 Pressurizer Pressure Compared to Experimental Data .....	5-68
5.5.6	S-RELAP5 Secondary Pressures Compared to Experimental Data .....	5-68
5.5.7	S-RELAP5 Break Flow Compared to Experimental Data .....	5-69
5.5.8	S-RELAP5 Loop Seal Downflow Side Differential Pressure Compared to Experimental Data from Loop 2 .....	5-69
5.5.9	S-RELAP5 Core Collapsed Level Compared to Experimental Data .....	5-70
5.5.10	S-RELAP5 Maximum Clad Temperature Compared to Experimental Data .....	5-70
6.1	S-RELAP5 Primary System Nodalization .....	6-11
6.2	S-RELAP5 Secondary Side Nodalization .....	6-12
6.3	Break Flow Rate for 2.0-Inch Break .....	6-13
6.4	Break Void Fraction for 2.0-Inch Break .....	6-13
6.5	System Pressures for 2.0-Inch Break .....	6-14
6.6	Loop Seal Void Fractions for 2.0-Inch Break .....	6-14
6.7	Combined High Head and Charging Flow for 2.0-Inch Break .....	6-15
6.8	Core Mixture Level and Collapsed Liquid Level for 2.0-Inch Break .....	6-15
6.9	Vapor and Clad Temperatures for Hot Node with 2.0-Inch Break .....	6-16

## Nomenclature

Acronym	Definition
AFW	auxiliary feedwater
ANF	Advanced Nuclear Fuels
ANS	American Nuclear Society
ASCE	American Society of Chemical Engineers
ASME	American Society of Mechanical Engineers
CCFL	counter-current flow limiting
CE-EPRI	Combustion Engineering – Electric Power Research Institute
CFR	Code of Federal Regulations
CHF	critical heat flux
ECC	emergency core coolant
ECCS	emergency core cooling system
EOC	end of cycle
HHSI	high head safety injection
ICAP	International Code Assessment Program
INEEL	Idaho National Engineering and Environmental Laboratory
INEL	Idaho National Engineering Laboratory
ISP	International Standard Problem
KWU	Kraftwerk Union
LBLOCA	large break loss of coolant accident
LHSI	low head safety injection
LOCA	loss of coolant accident
LOCES	Loss-of-Coolant Evaluation Studies
LOF	loss-of-feedwater (or loss-of-fluid)
LOFT	Loss of Fluid Test
MSCV	main steam control valve
MSSV	main steam safety valve
NAI	Numerical Application Inc.
NRC	United States Nuclear Regulatory Commission
PCS	primary cooling system
PCT	peak clad temperature
PWR	pressurized water reactor
RCP	reactor coolant pump

SBLOCA	small break loss of coolant accident
SIAS	safety injection actuation signal
SPC	Siemens Power Corporation
TMI	Three-Mile Island
TRAM	Transient Analysis Method
UPTF	Upper Plenum Test Facility

## 1.0 Introduction

Siemens Power Corporation (SPC) plans to use the S-RELAP5 (Reference 2) code for analysis of small break loss of coolant accidents for Westinghouse and Combustion Engineering PWRs. The NRC has previously reviewed and accepted the SPC methodology using the ANF-RELAP and TOODEE2 codes for small break LOCA analysis for PWRs (Reference 1). The revised evaluation model is an evolutionary outgrowth of SPC's existing methodology and conforms to the requirements for ECCS analysis set forth in 10 CFR 50.

The objective in using S-RELAP5 is to apply a single, advanced, industry recognized code for all analyses, including LOCA and non-LOCA events. Using a single code that has had extensive review permits the development of one base input deck for the analysis of all events for a particular application. The benefits of using a single code include ease of use by engineers, reduced maintenance requirements on developers, improved quality of both code and applications, and reduction of resources for the NRC review of associated methodology.

S-RELAP5 is a modification of ANF-RELAP. The modifications were made primarily to accommodate large and small break LOCA modeling. A hot rod model has been incorporated within the S-RELAP5 code itself. The hot rod model includes fuel models from the approved fuel design code, RODEX2 (References 3 and 4) and the approved swelling and rupture model (Reference 5) from the hot rod model code TOODEE2. The hot rod heat-up calculation is performed as part of the S-RELAP5 system calculation resulting in a single, consistent calculation using one code.

## 2.0 Summary

The purpose of this report is to document and demonstrate the adequacy of a revised SPC methodology using S-RELAP5 for performing SBLOCA analysis. The code and component models were benchmarked against test data to demonstrate the acceptability of the models for SBLOCA analysis. An example plant calculation was performed to estimate the effects of the new model in licensing situations and to provide a base calculation for sensitivity studies. Finally, sensitivity studies were performed using the example calculation to demonstrate the code stability and the methodology insensitivity to typical modeling changes encountered during analysis.

Section 3.0 presents a detailed description of the SBLOCA scenario and describes the methodology using S-RELAP5 and its application. The description emphasizes the phenomenology determining the outcome of the event.

Section 4.0 describes the model changes made to ANF-RELAP that create the S-RELAP5 SBLOCA evaluation model. The S-RELAP5 code includes changes to the following:

- Multi-dimensional capability
- Energy equations,
- Numerical solution of hydrodynamic equations
- Equation of state for steam in a non-condensable mixture
- Hydrodynamic constitutive models
- Heat transfer model
- Choked flow
- Counter-current flow limiting
- Component models
- Fuel model.

Section 5.0 presents the validation benchmark cases for the SBLOCA evaluation model. These benchmark cases use comparisons with measured test data and sensitivity studies to validate the SBLOCA model. The tests used specifically for SBLOCA assessment are:

- Two-dimensional bundle tests with flow blockage
- The Semiscale S-UT-8 test
- The boil-off portion of the LOFT LP-SB-03 test

- A loop seal clearing test performed in the Upper Plenum Test Facility (UPTF)
- The BETHSY 9.1b small break test (ISP-27)

Results from the two-dimensional validation cases demonstrated the general capability of S-RELAP5 to predict two-dimensional flow phenomena in these single-phase tests. The Semiscale S-UT-8 and LOFT LP-SB-3 benchmarks are validations retained from the previous SBLOCA model submittal and demonstrate high pressure, low velocity heat transfer and reflux condensation. Comparisons with the UPTF loop seal clearing test shows that S-RELAP5 conservatively predicts this important event for SBLOCA analysis. The BETHSY integral test demonstrates the capability of S-RELAP5 to predict the overall SBLOCA behavior and to yield conservative temperature results.

An example calculation for a three-loop Westinghouse PWR is presented in Section 6.0. This calculation demonstrates the methodology and provides the base case used for sensitivity studies.

Table 2.1 shows the results from the example calculation using the revised model and similar results using the currently approved SBLOCA evaluation model (Reference 1). The PCT result is similar to the earlier licensing calculations.

**Table 2.1 Comparison Between Previous and Proposed Methodologies**

<b>Methodology</b>	<b>PCT (°F)</b>	<b>Maximum Local Oxidation (%)</b>
S-RELAP5, 2-inch break (new)	1634	1.1
Approved model, 2-inch break (old)	1649	3.0

Using the example base case plant input, sensitivity study calculations were performed for the following:

- Time step size
- Restarting
- Loop seal biasing
- Pump model
- Radial flow loss coefficients
- Nodalization

PCT results from the sensitivity studies are shown in Table 2.2. The results show that the S-RELAP5-based SBLOCA methodology is well converged and has a small sensitivity to all the parameters investigated. The sensitivity of the previous model to radial flow loss coefficients does not exist for the new methodology; therefore the requirement to perform sensitivity calculations in licensing analysis on this parameter is eliminated from the new methodology.



**Table 2.2 Sensitivity Studies Summary**



### 3.0 **Small Break LOCA Evaluation Model Description**

#### 3.1 ***Event Description***

Loss of coolant accidents (LOCAs) are defined as postulated accidents that would result from the loss of reactor coolant, at a rate in excess of the capability of the normal reactor coolant makeup system, from piping breaks in the reactor coolant pressure boundary. The piping breaks are postulated to occur at various locations and include a spectrum of break sizes. Loss of significant quantities of reactor coolant would prevent heat removal from the reactor core, unless the water is replenished. General Design Criterion 35 requires each PWR to be equipped with an Emergency Core Cooling System (ECCS) that refills the vessel in a timely manner to satisfy the requirements of the regulations for ECCS given in 10 CFR Part 50, §50.46 and Appendix K to 10 CFR Part 50.

The postulated SBLOCA is defined as a break in the PWR primary coolant system pressure boundary having a break area equal to or less than 10 % of the cross sectional area of the cold leg or vessel inlet pipes. This range of break areas encompasses the range of penetrations in the primary system boundary. Small breaks can involve relief and safety valves, charging and letdown lines, drain lines and instrumentation lines.

##### 3.1.1 Limiting Break Conditions

There are several locations at which the break could occur. The break location that produces the greatest challenge to the acceptance limits is in the cold leg pipe at the discharge side of the pumps. Breaks at higher elevations will change from liquid to steam flow much sooner and will lose inventory much less rapidly. The discharge side of a pump results in the greatest pressure drop between the core exit and the top of the downcomer, thereby depressing the core level and increasing the period of core uncover. The limiting break size, which produces the highest PCT, depends on the ECCS. For C-E plants, it is generally in the neighborhood of 2 % of the cold leg pipe area. For Westinghouse plants, it can be less than 1 %.

Immediately after the break, the primary coolant system (PCS) undergoes a rapid depressurization with a reactor trip occurring when the pressure falls to the low-pressurizer pressure trip setpoint. The safety injection actuation signal occurs when the PCS pressure reaches the safety injection actuation signal setpoint, which is usually lower than the reactor trip setpoint. This signal initiates operation of the ECCS. Only the HHSI system will deliver flow

initially. The LHSI will not activate for this event, as the system pressure will always exceed the LHSI shut-off head. For most break sizes, the PCS pressure will usually eventually fall below the accumulator pressure. The flow from the accumulator terminates the challenge to the acceptance limits.

The principal ECCS component mitigating all break sizes is the HHSI and the worst single failure is usually the assumed loss of a diesel generator, which results in disabling of one HHSI pump and one motor driven auxiliary feedwater pump. Typically, a limited number of HHSI pumps are allowed to be out of service for maintenance. Most often, only one HHSI pump is assumed available for each analysis. A delay for the start-up of the emergency diesel generator is included in the HHSI system response.

SBLOCA transients fall into one of three categories, depending on the size of the break in the PCS. The smallest breaks are characterized by inventory losses that are less than the flow from the HHSI pump. In this case, core uncovering is insignificant and there is little, if any, heat-up of the fuel. The largest breaks are characterized by a rapid de-pressurization of the PCS. In this case, PCS pressure falls rapidly to the accumulator pressure and both core uncovering and hot rod heatup are limited. HHSI pumps have a limited effect for this category of SBLOCA.

Intermediate breaks are generally the most limiting because the rate of inventory loss from the primary system is large enough that the HHSI pumps cannot preclude significant core uncovering. The slow de-pressurization of the PCS extends the time required to reach the accumulator pressure and can even result in the pressure remaining above the accumulator pressure. The duration of the uncovering is maximized by a break in this intermediate range. During uncovering the heat transfer from the hot rod is limited and the decay heat causes the uncovered portion of the rod to heat up.

The break size and the configuration and capacity of the ECCS are the dominant factors that dictate the SBLOCA transients. The auxiliary feedwater (AFW) system is also a factor, with the effect becoming more pronounced as the break size is decreased. For plants where charging pumps are considered safety grade, charging pump flow may be included with the ECCS flow. Therefore, depending upon plant design and geometry, differences in limiting break size can occur. For some plants the limiting break size can be much larger than for others.

The peak cladding temperature is expected to occur at End of Cycle (EOC) burnup conditions. This is due to the dominant effect of a top-skewed EOC axial power distribution and a larger actinide decay heat at EOC.

### 3.2 *Limiting Break Scenario*

The phenomena which occur during the small break LOCA event have been studied and reported in Reference 6. The SBLOCA scenario developed during this process was for a Westinghouse 4-loop PWR, but because of the similarity of design features is also applicable to PWRs of 3-loop Westinghouse design as well as Combustion Engineering (CE) designed PWRs.

The small break transient is characterized by five time periods: blowdown, natural circulation, loop seal clearance, boil-off, and core recovery. While the duration of each period is break size and system dependent, the small break LOCA transient can be described as follows:

**Blowdown:** On initiation of the break, there is a rapid decompression of PCS. Reactor trip is initiated on a low pressurizer pressure setpoint. Pump trip occurs either automatically based on the assumption that off-site power is lost coincident with the reactor trip or as a result of operator action. A safety injection signal occurs when the primary pressure decreases below the pressurizer low-low pressure setpoint, and safety injection flow begins after a signal delay time. The PCS remains liquid solid for most of the blowdown period, with phase separation starting to occur in the upper head, upper plenum, and hot legs near the end of this period. During the blowdown period, the break flow is single-phase liquid only. Eventually the rapid depressurization ends when the PCS reaches a pressure just above the steam generator secondary side pressure.

**Natural Circulation:** At the end of the blowdown period, the PCS reaches a quasi-equilibrium condition which can last for several hundred seconds depending on break size. During this period the loop seals remain plugged and the system drains top down with voids beginning to form at the top of the steam generator tubes and continuing to form in the vessel upper head and top of the vessel upper plenum region. Decay heat is removed by the steam generators during this time. Vapor generated in the core is trapped within the PCS by liquid plugs in the loop seals, and a low quality flow exits at the break. This period is referred to as the natural circulation period.

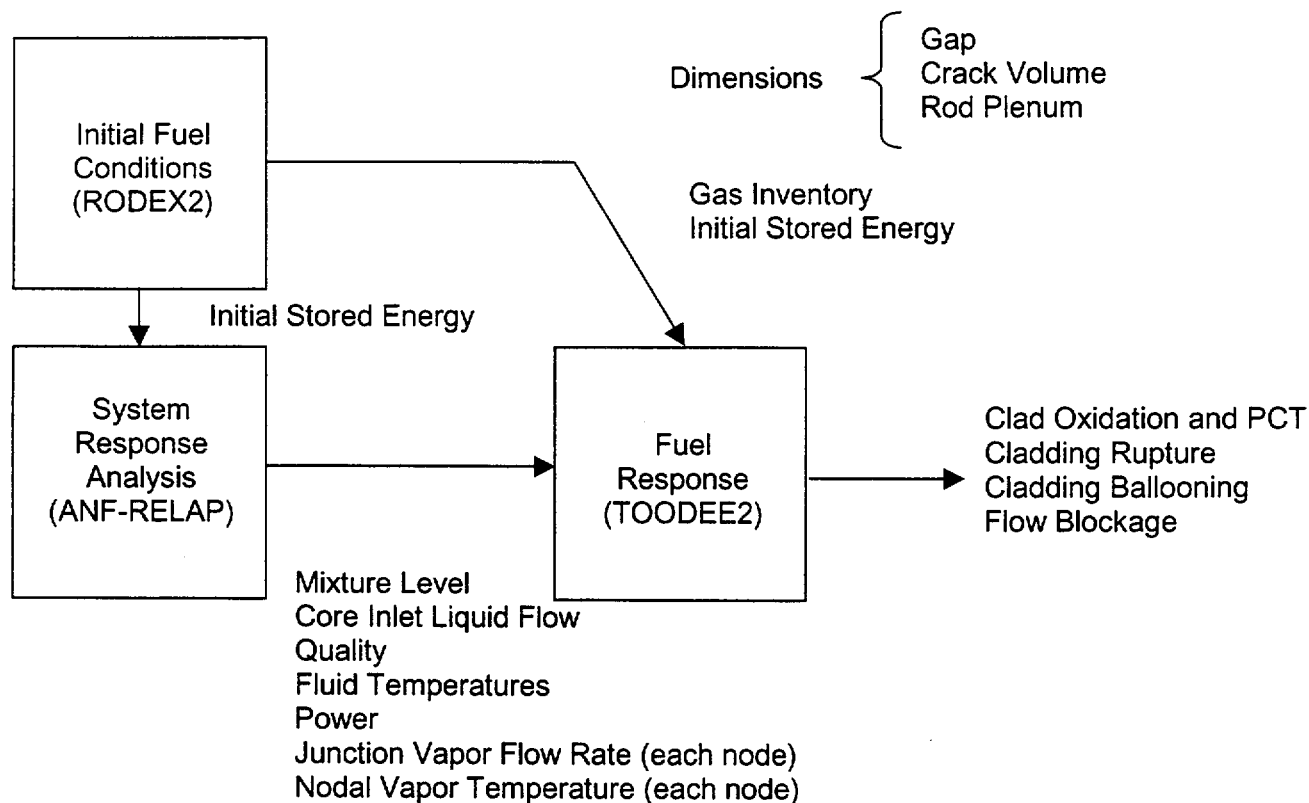
**Loop Seal Clearance:** The third period is the loop seal clearance period. When the liquid level in the downhill side of the steam generator is depressed to the elevation of the top of the horizontal loop seal piping, steam previously trapped in the PCS can be vented to the break. The break flow, previously a low quality mixture, transitions to primarily steam. Prior to loop seal venting, the inner vessel mixture level can drop rapidly, resulting in a short core uncover. Following loop seal venting, the core recovers to about the cold leg elevation, as pressure imbalances throughout the PCS are relieved.

**Boil-Off:** Following loop seal venting, the vessel mixture level will decrease. In this period, the decrease is due to the boil-off of the liquid inventory in the reactor vessel. The mixture level will reach a minimum, in some cases resulting in a deep core uncover. The boil-off period ends when the core liquid level reaches this minimum. At this time, the PCS has depressurized to the point (usually the accumulator setpoint) where ECC flow into the vessel matches the rate of boil-off from the core.

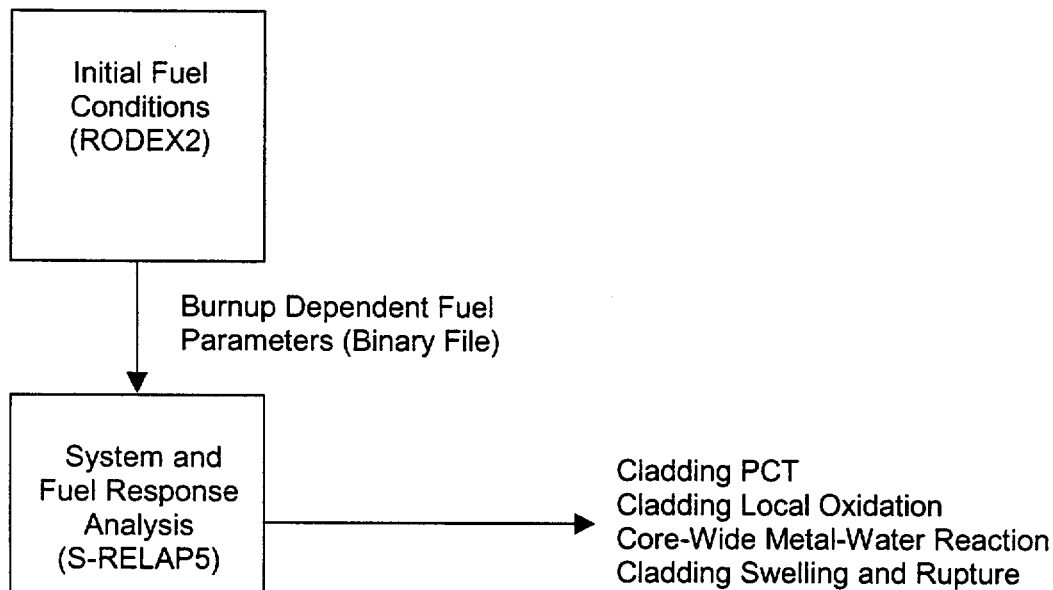
**Core Recovery:** The core recovery period extends from the time at which the inner vessel mixture reaches a minimum in the boil-off period, until all parts of the core quench and are covered by a low quality mixture. The small break LOCA is considered over, and the calculation is terminated when the temperature transient in the core has been terminated, and the safety injection flow exceeds the break flow.

### 3.3 ***Methodology Description***

Two principal computer codes are used to analyze the SBLOCA event. Initial conditions as a function of fuel burnup for the hot rod and the core are calculated using RODEX2 to determine the effects of exposure on the fuel and rod properties. The SBLOCA transient response is calculated using S-RELAP5, which in addition to calculating the overall response, also calculates the hot rod temperature transient using the RODEX2 fuel models and the NUREG-0630 swelling and rupture models embedded in the code. Figure 3.1 schematically shows the simplification made to the methodology by incorporating RODEX2 and TOODEE2 models into S-RELAP5. The hot rod calculations are described in Section 4.0.



**SPC Old SBLOCA Evaluation Model**



**SPC New SBLOCA Evaluation Model**

**Figure 3.1 Schematic of Old and New SPC Small Break Models**

### 3.3.1 System Modeling

All of the PCS loops and the SGs in the S-RELAP5 model of a plant are explicitly modeled to enhance the accuracy of the calculation. A typical SBLOCA S-RELAP5 reactor vessel nodalization and loop piping for a 3-loop Westinghouse plant is illustrated in Figure 6.1. The nodalization for steam generator secondary system is depicted in Figure 6.2. Deviation from this nodalization would be necessary for plants that have the SI system directly connected to the cold legs or other geometrical differences from the example PWR.

The reactor primary and secondary coolant systems are modeled. Primary system modeling includes: the pressurizer, reactor coolant pumps, hot- and cold-leg piping, the reactor vessel and internals, the steam generator, the accumulators, and the HHSIs. Secondary modeling includes the steam generator secondary, feedwater, isolation valves, relief valves, and steam lines. Generally, the nodalizations are fairly conventional, with the exception of components that can have a large effect on the SBLOCA outcome. The components for which special modeling approaches were used are discussed next.

#### 3.3.1.1 Loop Seal Modeling

The loop seal region begins at the exit of the steam generator and ends at the entrance to the pump impeller region. Modeling of the loop seal region is important for breaks in the cold-leg piping located downstream of the pump discharge. Details of loop seals vary between plant designs. The similarity between loop seals designs is that they consist of a descending piping segment connected from the steam generator exit plenum to a horizontal piping segment. The horizontal piping is then connected to an ascending piping segment which connects to the reactor coolant pump.

[

]

The horizontal and ascending segments are each modeled with single volumes. [

]

The ascending section responds to carry-over from the horizontal section. Modeling this as a single volume results in relatively smooth behavior and provides agreement with tests performed at the Upper Plenum Test Facility (Reference 7). The testing and comparisons are discussed in Section 5.4 below.

[

]

### 3.3.1.2 Main Coolant Piping

Each piping loop of the PCS is modeled separately. The components of each loop include the following:

- hot-leg piping
- a pressurizer (if applicable)



- the steam generator inlet plenum
- the steam generator tubes
- the steam generator exit plenum
- the cross-over piping from the steam generator to the pump (loop seal)
- the primary coolant recirculation pump
- an accumulator or safety injection tank
- ECCS connections
- the cold leg piping from the pump to the vessel

#### 3.3.1.3 Reactor Coolant Pumps

The pumps have a number of different effects on the SBLOCA as the event progresses. Initially, when they are operating and coasting down, they provide flow to the core and raise the pressure at the break location. This increased pressure reduces the reactor vessel coolant inventory prior to loop seal clearing. After the pumps coast down, they constitute an additional resistance in the vent path for the steam from the core. The pump pressure drop is calculated from the pump speed and the pump performance data in the form of homologous head and torque curves. Since the lowest point of the pump discharge to the cold leg is usually elevated above the bottom of the cold leg, the pumps also inhibit HHSI flow from flowing backward into the loop seal. [

]

[

]

#### 3.3.1.4 Downcomer Modeling

[

]

#### 3.3.1.5 Upper Vessel

During the period in which the upper vessel region is losing liquid inventory, the region between the core exit and the hot legs will interact with the core. [

]

### 3.3.2 Core Modeling

The behavior of the liquid mixture level in the hot region surrounding the hot rod is the most significant factor in SBLOCA. Although most influenced by other models, the core liquid mixture level can be affected by the modeling of the core itself.

#### 3.3.2.1 General Hydraulic Modeling

[

]

#### 3.3.2.2 Radial Loss Coefficients

[

]

### 3.3.2.3 Heat Structures

[

]

## 3.4 **SBLOCA Analysis**

The purpose of the SBLOCA analysis is to demonstrate that the criteria stated in 10 CFR 50.46(b). These criteria are as follows:

- 1) The calculated maximum fuel element cladding temperature shall not exceed 2200°F.
- 2) The calculated local fuel rod cladding oxidation shall nowhere exceed 17% of the total cladding thickness before oxidation.
- 3) The calculated total amount of fuel element cladding which reacts chemically with water or steam shall not exceed 1% of the Zircaloy within the heated length of the core.
- 4) The cladding temperature transient shall be terminated at a time when the core geometry is still amenable to cooling.

- 5) The core temperature shall be reduced and decay heat shall be removed for an extended period of time, as required by the long-lived radioactivity remaining in the core.

S-RELAP5 is the principal computer code used for analysis of the SBLOCA event. Before the analysis can be performed, S-RELAP5 requires initial fuel rod conditions. The rod conditions are calculated by RODEX2 where the fuel burn-up is taken to the desired burnup, usually end of cycle conditions. The RODEX2 results at the desired burnup are transferred to S-RELAP5. A steady state calculation using S-RELAP5 is made that initializes the system model to plant operating conditions. After assuring the steady state calculation is representative of the plant operating conditions, the SBLOCA transient is performed. In addition to calculating the overall system thermal-hydraulic response, S-RELAP5 also concurrently calculates the hot rod temperature transient using the hot rod input including RODEX2 fuel models and the NUREG-0630 swelling and rupture models which were taken from the implementation in the TOODEE2 code.

After calculations and analysis have been made to determine the limiting single failure, a break spectrum is analyzed by making several calculations with varying break sizes. From this calculational set, the results are examined to determine the break size having the greatest PCT or maximum oxidation present. The calculation having the greatest PCT or maximum amount of cladding oxidized in the break spectrum is the limiting SBLOCA break yielding the reportable PCT, and becomes the analysis of record. The results of this analysis are also compared to the criteria in 10 CFR 50.46(b) for reporting purposes.

The results from the sample problem, discussed Section 6.0, shows that little variation in calculated PCT occurs with small changes to the model. Because of this demonstrated convergence, additional sensitivities are not required to be performed during licensing analysis.

#### 4.0 Model Description

The S-RELAP5 (Reference 2) code includes hydrodynamic models, heat transfer and heat conduction models, a fuel model, a reactor kinetics model, control system models, and trip system models. S-RELAP5 uses a two-fluid, nonequilibrium, nonhomogeneous, hydrodynamic model for transient simulation of the two-phase system behavior. The hydrodynamics include many generic component models: pumps, valves, separators, turbines, and accumulators. Also included are the special process models: form loss at an abrupt area change, choked flow, and counter-current flow limiting (CCFL) models.

The S-RELAP5 code evolved from SPC's ANF-RELAP code, a modified RELAP5/MOD2 version (Reference 8), used at SPC for performing PWR plant licensing analyses including small break LOCA analysis, steam line break analysis, and PWR non-LOCA Chapter 15 event analyses. The code structure for S-RELAP5 was modified to be essentially the same as that for RELAP5/MOD3 (Reference 9), with the similar code portability features. The coding for reactor kinetics, control systems and trip systems were replaced with those of RELAP5/MOD3. The majority of the modifications to S-RELAP5 were undertaken to improve its applicability for the realistic calculation of Large Break LOCA (LBLOCA). To a large extent, those models are relevant to analysis of PWR SBLOCA events.

In Section 1.1 of the S-RELAP5 Models and Correlations Manual (Reference 2) there is a list summarizing major modifications and improvements in S-RELAP5. Where appropriate, this list is reproduced herein with additional information specific to SBLOCA.

- 1) Multi-Dimensional Capability. Full two-dimensional treatment was added to the hydrodynamic field equations. The two-dimensional capability can accommodate the Cartesian and the cylindrical (z,r) and (z, $\theta$ ) coordinate systems, and can be applied anywhere in the reactor system. Thus far, SPC has applied two-dimensional modeling to the downcomer, core, and upper plenum. The RELAP5/MOD2 cross-flow modeling also was improved. The application of a two-dimensional component in the downcomer is important for simulating the asymmetric emergency core cooling (ECC) water delivery observed in the UPTF downcomer penetration tests (Reference 10).
- 2) Energy Equations. The energy equations of RELAP5/MOD2 and RELAP5/MOD3 have a strong tendency to produce energy error when a sizeable pressure gradient exists

between two adjacent cells (or control volumes). This deficiency is a direct consequence of ignoring specific energy terms that are difficult to approximate numerically. Therefore, the energy equations were modified to conserve the energies transported into and out of a cell. For analyses involving containment modeling, the new approach is more appropriate numerically. For SBLOCA calculations, no significant differences were calculated in the key parameters such as clad surface temperature, break mass flow rate, void fraction, and others between the two formulations of the energy equations.

- 3) Numerical Solution of Hydrodynamic Field Equations. The reduction of the hydrodynamic finite-difference equations to a pressure equation is obtained analytically by algebraic manipulations in S-RELAP5, but is obtained numerically by using a Gaussian elimination system solver in RELAP5/MOD2 and MOD3. This improvement aids computational efficiency and helps to minimize effects due to machine truncation errors.
- 4) State of Steam-Non-Condensable Mixture. Computation of state relations for the steam-noncondensable mixture at very low steam quality (i.e., the ratio of steam mass to total gas phase mass) was modified to allow the presence of a pure noncondensable gas below the ice point (0°C). The ideal gas approximation is used for both steam and noncondensable gas at very low steam quality. This modification is required to correctly simulate the accumulator depressurization and prevents spurious code failures during accumulator ECCS water injection. For SBLOCA, this model does not have significant impact.
- 5) Hydrodynamic Constitutive Models. Significant modifications and enhancements were made to the RELAP5/MOD2 interphase friction and inter-phase mass transfer models. The constitutive models are flow-regime dependent and were constructed from the correlations for the basic elements of flow patterns such as bubbles, droplets, vapor slugs (i.e., large bubbles), liquid slugs (i.e., large liquid drops), liquid film, and vapor film. When possible and applicable, literature correlations were used as published. Often a constitutive formulation is composed of more than one correlation to cover different flow regimes. Transition flow regimes were introduced to allow a smooth change between two constitutive models. Partition functions for combining different correlations and for

transitions between two flow regimes were developed based on physical reasoning and code-to-data comparisons. Most of the existing RELAP5/MOD2 partition functions were retained in S-RELAP5. The vertical stratification model implemented in ANF-RELAP was further improved. The RELAP5/MOD2 approximation to the Colebrook equation of wall friction factor was replaced by the more appropriate explicit-approximate formulation of Jain (Reference 11).

- 6) Heat Transfer Model. The use of a different set of heat transfer correlations for the reflood model in RELAP5/MOD2 was eliminated. Some minor modifications were made to the selection logic for heat transfer modes (or regimes), single phase liquid natural convection and condensation heat transfer. The Lahey correlations for vapor generation in the subcooled nucleate boiling region were implemented (Reference 12). No changes are made to the RELAP5/MOD2 CHF correlations. [

]

- 7) Choked Flow. The computation of the equation of state at the choked plane was modified. Instead of using the previous time step information to determine the state at the break, an iterative scheme is used. This modification was also implemented in ANF-RELAP. Some minor modifications were also made to the under-relaxation scheme to smooth the transition between subcooled single phase critical flow and two-phase critical flow. The Moody critical flow model (Reference 14) is also implemented and used for Appendix K SBLOCA analyses.
- 8) Counter-Current Flow Limiting. The Kutateladze-type CCFL correlation in ANF-RELAP was replaced by the more general Bankoff form (Reference 15), which can be reduced to either a Wallis-type or a Kutateladze-type CCFL correlation. RELAP5/MOD3 also uses the Bankoff correlation form (Reference 16).
- 9) Component Models. SPC's pump performance degradation model developed from CE-EPRI data was included in the S-RELAP5 pump model. The computation of pump head in the fluid field equations was modified to be more implicit. A containment model was added. With this model, the containment pressure boundary conditions are provided by the approved EXEM/PWR evaluation model code, ICECON, which is run concurrently

with S-RELAP5 using realistic values for parameter input. The accumulator model was eliminated because of its well-known problems. With S-RELAP5, the accumulator is to be modeled as a pipe with nitrogen or air as noncondensable gas. The ICECON containment model is not used in SBLOCA transient analyses.

10) Pump Modeling. [

]

- 11) Fuel Model. The RODEX2 fuel model and the NUREG-0630 clad ballooning and rupture model, as implemented in TOODEE2, have been incorporated into the S-RELAP5 code to calculate the fuel response for transient analyses. Both models have been approved for licensing applications (References 3, 4 and 5). The Baker-Just metal-water reaction model (Reference 18) is used for oxidation during the transient. The oxidation level is set to zero at the start of the transient for the metal-water reaction calculation. The oxidation reported for comparison to the criteria is that calculated with the Baker-Just model and does not include pre-transient oxidation. The S-RELAP5/RODEX2 model does not calculate the burnup response of the fuel. Instead, fuel conditions at the burnup of interest are transferred from RODEX2 to S-RELAP5 via a binary data file from a separate RODEX2 calculation. The data transferred from RODEX2 describes the fuel state at zero power before the transient. A steady-state S-RELAP5 calculation is



required to establish the fuel state at power, which is approximately the same as RODEX2 fuel state at the same power. The clad ballooning and rupture model also accounts for flow diversion in the vicinity of the rupture location in the same way as the TOODEE2 code.

## 5.0 Benchmark Calculations

The S-RELAP5 code was applied to two separate effects and three integral tests to validate code performance under SBLOCA conditions. The tests are summarized in Table 5.1. The tests were chosen to specifically test the two-dimensional model, loop seal clearing, and core heat transfer.

**Table 5.1 Experiment Summary**

<b>Experiment</b>	<b>Description</b>	<b>SBLOCA Relevancy</b>
2-D Flow Tests	Separate effects test with parallel 14x14 bundles, full width, partial height, with one bundle blocked and various flows in the other.	Two-dimensional core model
Semiscale S-UT-8	Scaled PWR integral facility, test series designed to investigate effects of ECCS on SBLOCA.	Core heat-up before loop seal clearing
LOFT LP-SB-3	Scaled PWR integral test facility, test series designed to study core heat transfer during slow boil-off SBLOCA (1.84 inch equivalent).	Core heat transfer during boil-off phase
UPTF-A5RUN11E	Full-scale PWR test facility, test series designed to study loop seal clearing behavior with vapor super heat.	Loop seal clearing
BETHSY Test 9.1b	Scaled PWR integral test facility, test series designed to study SBLOCA without HHSI.	Integral effects: 2-inch equivalent small break, three-loop facility, loop seal clearing

From the table, the applicability range covers relevant break sizes, loop seal clearing, and core heat-up for scenarios of interest.

## 5.1 ***Two-Dimensional Flow Test***

This benchmark calculation compares the two-dimensional component in S-RELAP5 with test data and verifies that the two-dimensional component in S-RELAP5 can be used to model multidimensional flow problems. The tests selected for this comparison are a series of flow blockage tests using test assemblies prototypic of 14x14 Westinghouse assemblies.

### 5.1.1 Test Facility Description

The test data selected for comparison was used to benchmark XCOBRA-IIIC, VIPRE, and THINC-IV (References 19 and 20) for both core flow redistribution and flow redistribution within a single fuel assembly. The original test data is reported in a Westinghouse Advanced Reactor Division document: E. Weiss, *Flow Recovery in a Blocked Fuel Assembly*, ARD-TH-416, October, 1969, the results of which are summarized in Reference 20 and, for subsequent testing by Weiss for a similar configuration, in Reference 21.

The test configuration for both sets of tests by Weiss is shown in Figure 5.1.1. For the bulk of the testing, the gap between the two simulated fuel assemblies was left open (Figure 5.1.2). For the Reference 21 testing, a perforated plate was inserted between the two simulated fuel assemblies (Figure 5.1.3).

The tests consisted of introducing asymmetric flow in the inlet region and measuring flow recovery in the bundle. The test reported in Reference 21 also had the outlet of one assembly blocked. Because of the detail of the measurements and the nearly prototypic geometry, the test results from Reference 20 have become a standard benchmark test for flow redistribution codes.

Reference 20 reported the results for two test configurations in sufficient detail to allow comparison. Nominally, the first configuration has 1100 gpm entering one fuel assembly and 550 gpm in the other. The second configuration has one inlet blocked and 1500 gpm entering the other. In both cases, the exits are open.

The case discussed in Reference 21 is similar, but has a perforated plate inserted between the two assemblies, the inlet and outlet blocked on one assembly, and a nominal total flow of 1300 gpm.

### 5.1.2 S-RELAP5 Model Description

Models for the test section and the boundary conditions for each of three tests were constructed based on the geometry shown in Figure 5.1.1 through Figure 5.1.3. Using the models, local velocities and flows were calculated to compare to the data. A simplified nodalization diagram is given in Figure 5.1.4.

[

]

### 5.1.3 Boundary Conditions

[

]

### 5.1.4 Comparison to Data

References 20 and 21 present axial velocity distribution maps at six different elevations for three tests. The assembly without blockages is Assembly A.

- The inlet flow for Assembly A was nominally 1100 gpm and 550 gpm for Assembly B.
- The inlet flow for Assembly A was nominally 1500 gpm and the inlet to Assembly B was blocked.
- The inlet flow for Assembly A was nominally 1300 gpm and both the inlet and outlet to Assembly B were blocked.

#### 5.1.4.1 Test 1 – 1100/550

Figure 5.1.6 through Figure 5.1.11 compare the reported axial fluid velocities for the test with an inlet flow of 1100 gpm in one side (A) and 550 gpm in the other (B) to those calculated by S-RELAP5. The data for this flow comparison as extracted from Figure 4.3 of Reference 20. The THINC-IV fit starts with a flow split at the zero elevation that has 69% of the flow in Assembly A. This would be a flow split of 1138/512 gpm with the same total flow. Based on the

comparisons to the THINC-IV code, the flow split was really much closer to 1138 to Assembly A and 512 to Assembly B. Test 1 was run using these values.

The comparison of flow velocities at the pitot tube locations with the S-RELAP5 calculations shows, with minor exceptions, excellent agreement. The axial flow fractions are compared in Figure 5.1.12 and also compare well to the data.

#### 5.1.4.2 Test 2 – 1500/0

Figure 5.1.13 through Figure 5.1.18 compare the reported axial fluid velocities for the test with an inlet flow of 1500 gpm on side A and with side B blocked at the inlet to those calculated by S-RELAP5. A calculation of total mass flow, calculated by integrating the velocity profiles, was used to deduce the correct flow for the test. Based on a comparison of the integrated velocity distribution with the integrated S-RELAP5 velocity distribution, the flow split at the inlet should really be about 1281/0 gpm. The comparisons are based on this adjusted value. S-RELAP5 calculates reverse flow near the back wall of the blocked assembly (B). The test data shows reverse flow, or the possibility of reverse flow, with zero velocities from the pitot tubes. The S-RELAP5 results, with minor exceptions are in very good agreement with the measured data.

Figure 5.1.19 compares the reported mass flow fraction in assembly A with that calculated by S-RELAP5. The agreement for this test is not as good as that for the case with the 1100/550 gpm flow split. The points of largest disagreement are Levels 4 through 7. The velocity measurements at these levels did not conserve total mass flow, therefore the difference between the S-RELAP5 predictions and the data may well be much smaller in this region than Figure 5.1.19 indicates.

#### 5.1.4.3 Test 3 – 1300/0

Reference 21 reports a similar test, using the same test rig with a perforated plate inserted between the two test assemblies (Figure 5.1.3). Figure 5.1.20 through Figure 5.1.25 compare the reported axial fluid velocities for this test to those calculated by S-RELAP5. The agreement for these data is reasonably good for all levels. Again, the most significant difference is the ability of S-RELAP5 to calculate reverse flow in the blocked assembly.

### 5.1.5 Comparison to Core Flow Distribution Codes

To assess the quality of the comparison to data, the XCOBRA-IIIC and THINC-IV flow predictions for the test were compared to the S-RELAP5 flow predictions. XCOBRA-IIIC was benchmarked against one case; the case from Reference 20 that had an inlet flow split of 1100/550 gpm.

The THINC-IV fit was extracted from Figure 4.3 of Reference 20. As noted, the flow split for THINC-IV was closer to 1138/512 gpm. The XCOBRA-IIIC benchmark case was run with the inlet flows adjusted for this change in flow distribution and compared to the S-RELAP5 simulation. The results of the rerun, using the current version of XCOBRA-IIIC, the THINC-IV results, and the S-RELAP5 results are compared in Figure 5.1.26. S-RELAP5 compares with data much better than either XCOBRA-IIIC or THINC-IV.

Figure 5.1.27 compares S-RELAP5 to THINC-IV for the 1500/0 gpm inlet case. Over much of the range, S-RELAP5 fits the data about as well as, or better than, THINC-IV. Near the top of the simulated fuel assemblies S-RELAP5 allows the high flow assembly to retain more flow than does THINC-IV.

Overall, S-RELAP5 does as well as or better than, core flow distribution codes licensed by the NRC for core flow and subchannel analysis of PWR cores (such as XCOBRA-IIIC).

### 5.1.6 Conclusions

The key results of this benchmark calculation are the following:

- Radial distributions of axial velocities agree well with data from References 20 and 21.
- Flow splits between simulated bundles agree quite well with measured data from Reference 20.

The key results of comparing of S-RELAP5 with flow blockage data are that the two-dimensional model in S-RELAP5 is sufficient to describe flow redistribution in multidimensional problems and that it does as well as thermal-hydraulic design codes used for PWR core analysis (XCOBRA-IIIC and THINC-IV) in predicting the flows.

**Table 5.1.1 Flow Boundary Conditions for the Cases Evaluated**

Case	Description	Flow to Test Assembly A Lbm/sec	Flow to Test Assembly B Lbm/sec
1	1100/550 gpm	153.00	76.50
1a	1138/512 gpm split	158.28	71.11
2	1500 gpm to one Assembly	208.54	0.0
2a	1281 gpm to one Assembly	178.09	0.0
3	1300 gpm to one Assembly	180.74	0.0



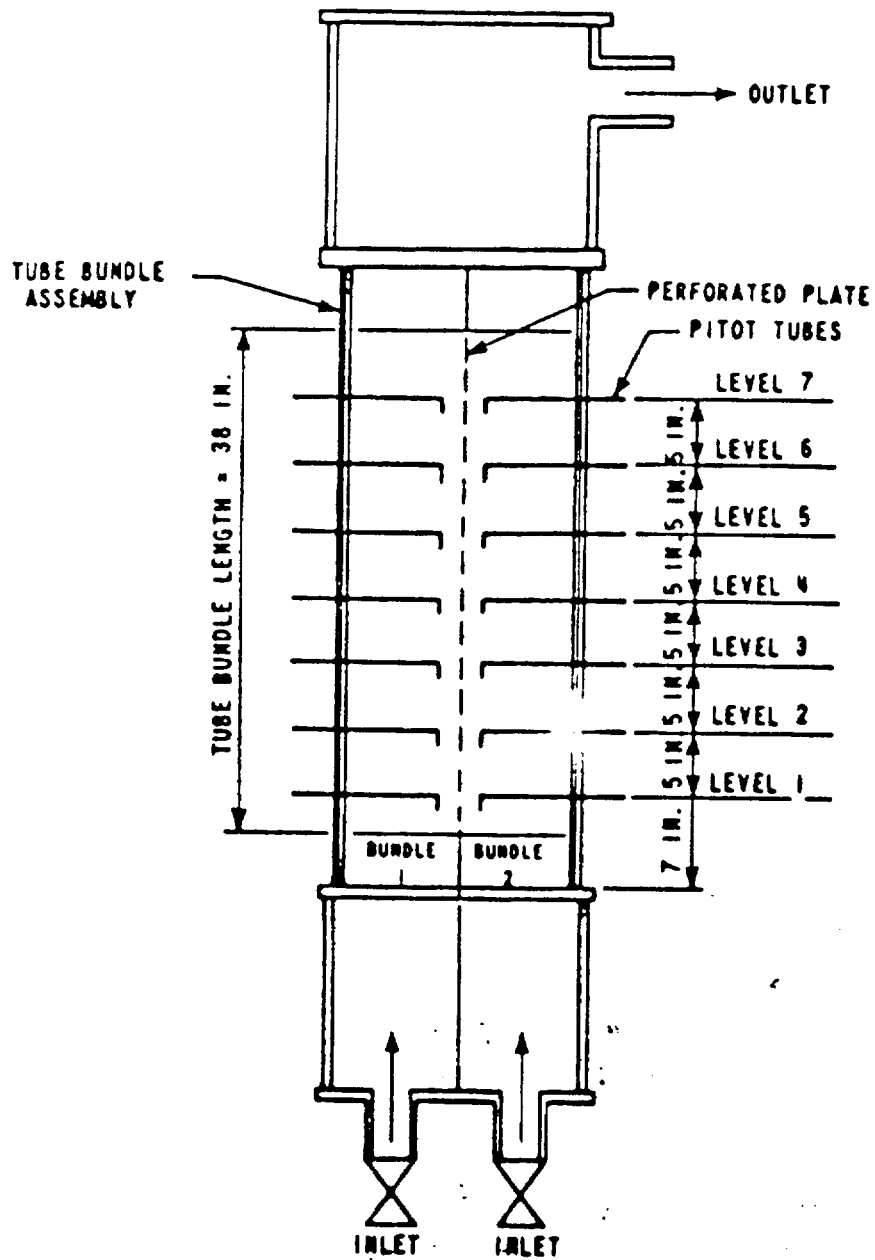


Figure 5.1.1 Test Rig for Flow Blockage Tests Showing Location of Perforated Plate

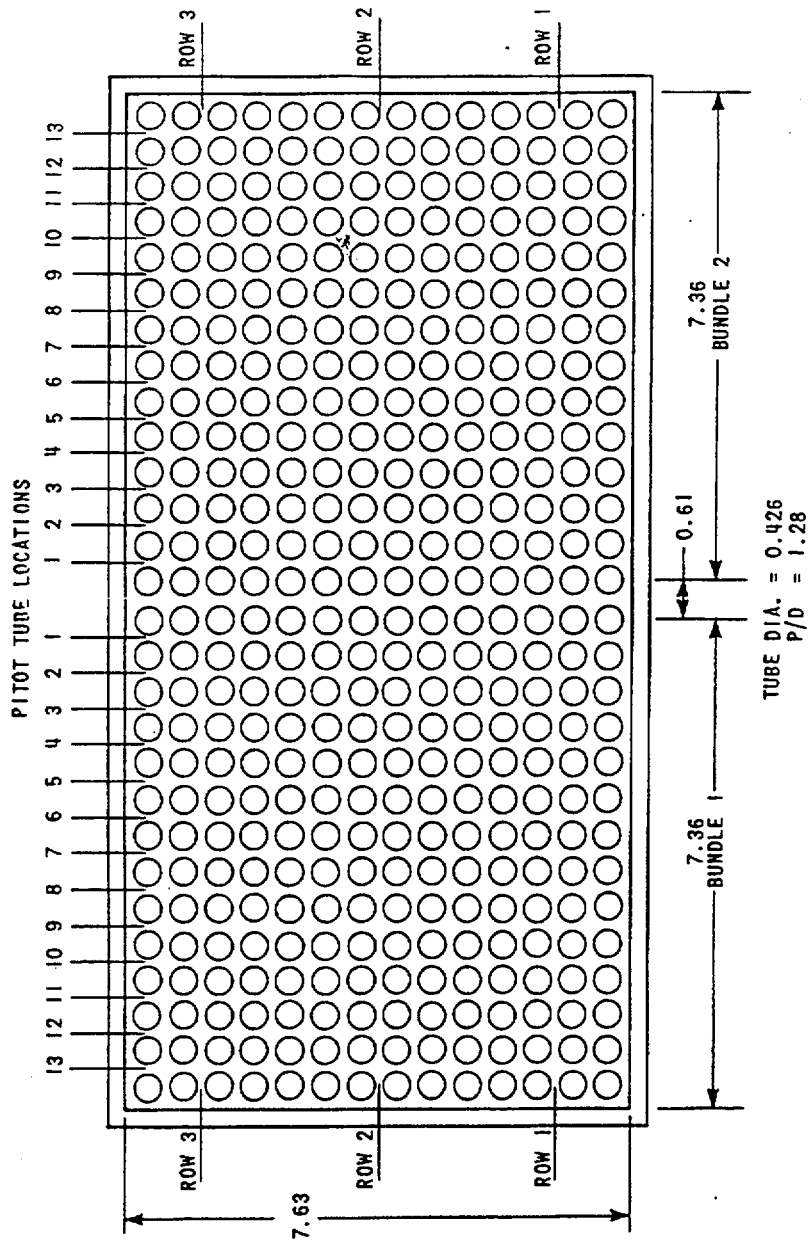


Figure 5.1.2 Cross Sectional View of Test Assemblies Without Perforated Plate Between Test Assemblies

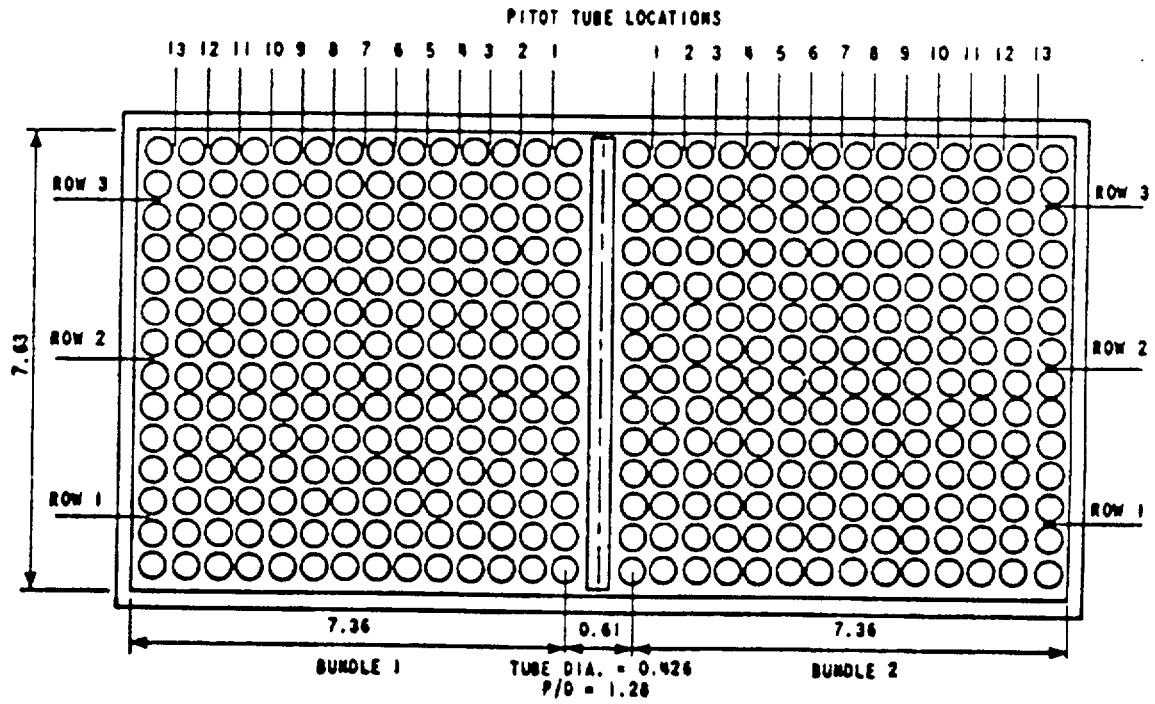
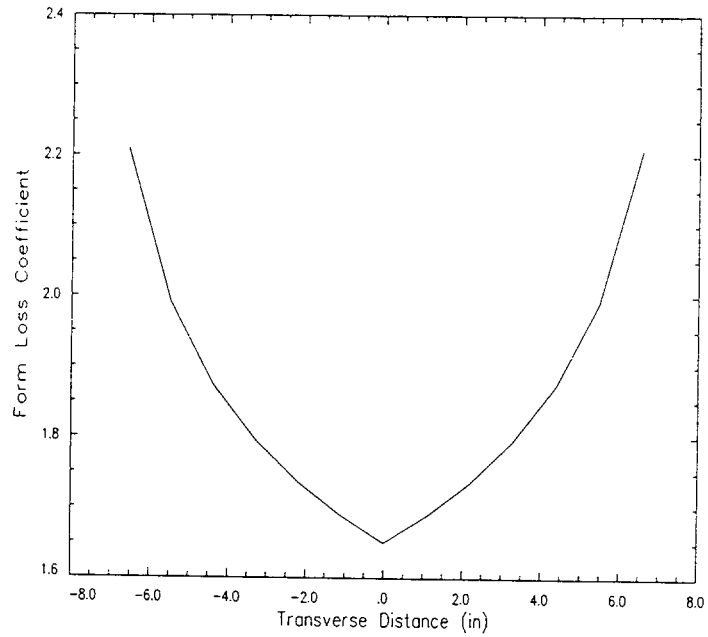


Figure 5.1.3 Cross Sectional View of Test Assemblies with Perforated Plate Between Test Assemblies



**Figure 5.1.4 Nodalization Diagram for S-RELAP5 Modeling of Westinghouse Flow Blockage Tests**



**Figure 5.1.5 Form Loss for Lateral Flow (Typical)**

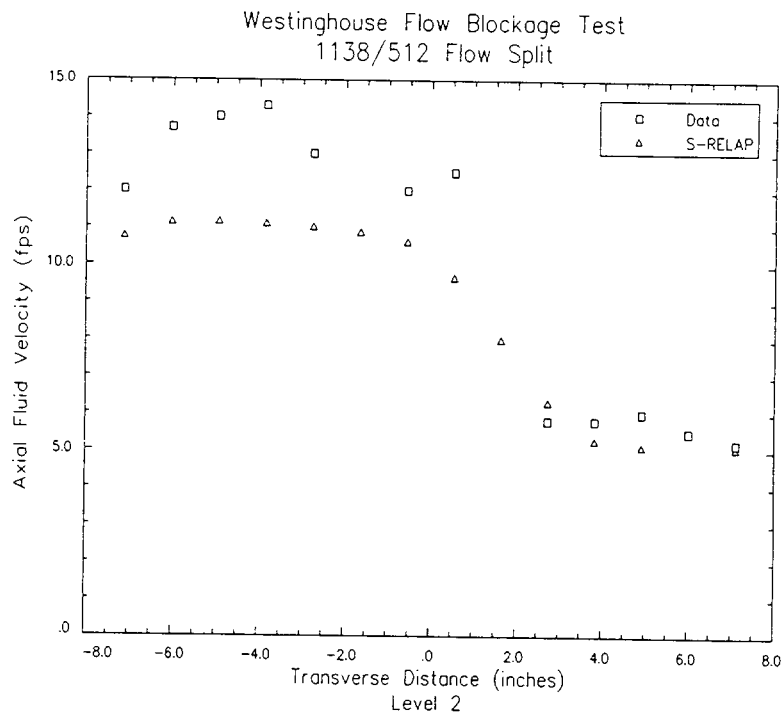


**Figure 5.1.6 Axial Velocities at 7.5-Inches for Asymmetric Flow (1138/512)**

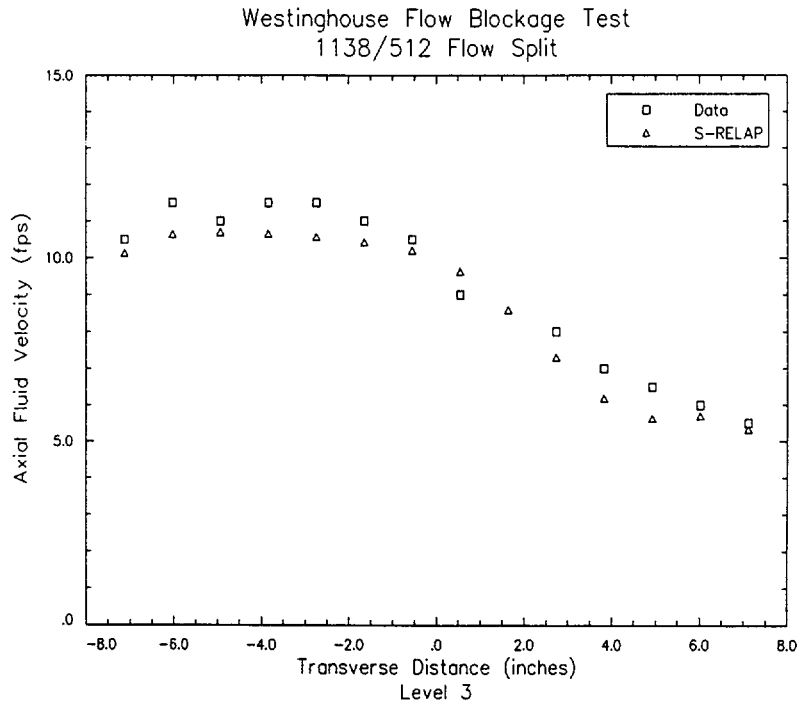


**Figure 5.1.7 Axial Velocities at 12.5-Inches for Asymmetric Flow (1138/512)**

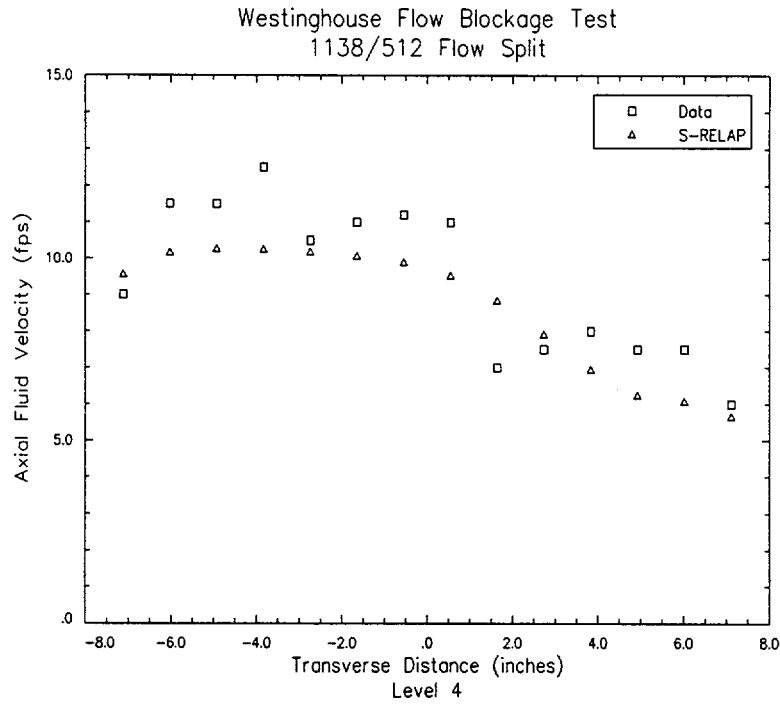


**Figure 5.1.8 Axial Velocities at 17.5-Inches for Asymmetric Flow (1138/512)**

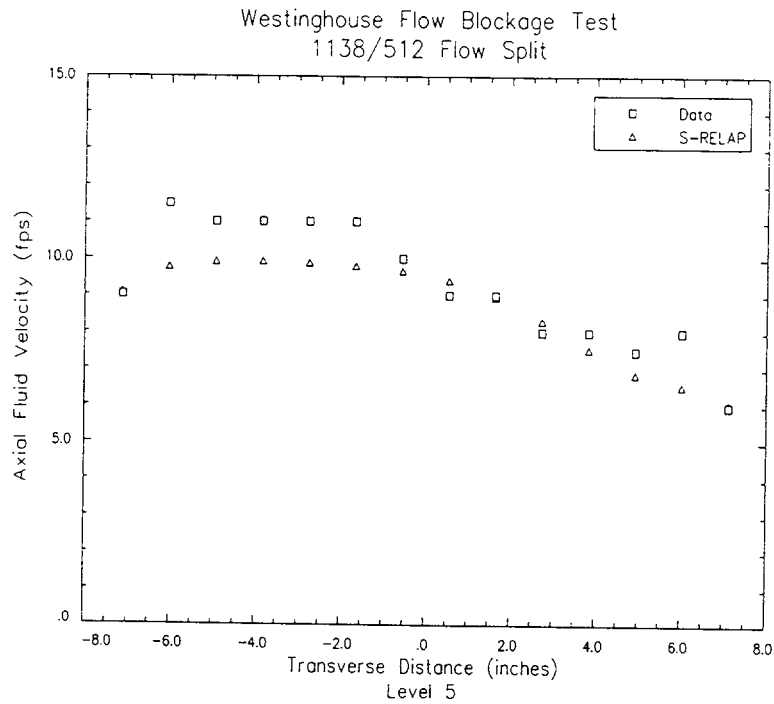


**Figure 5.1.9 Axial Velocities at 22.5-Inches for Asymmetric Flow (1138/512).**

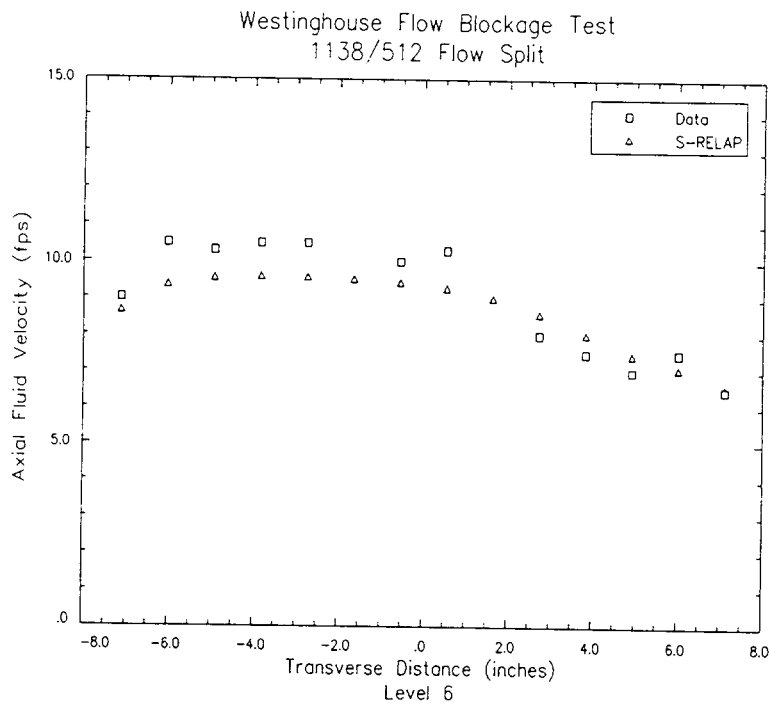


**Figure 5.1.10 Axial Velocities at 27.5-Inches for Asymmetric Flow (1138/512).**

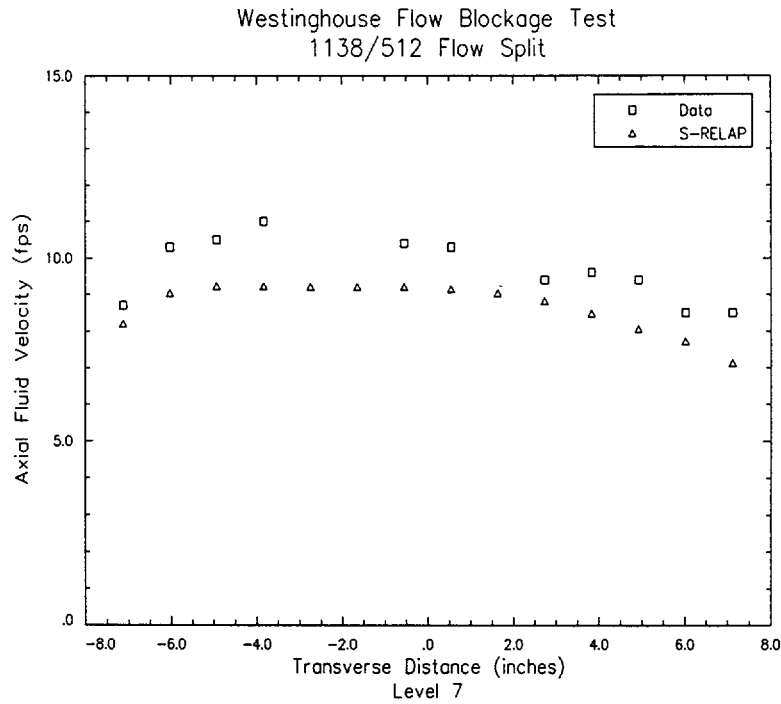


**Figure 5.111 Axial Velocities at 32.5-Inches for Asymmetric Flow (1138/512)**

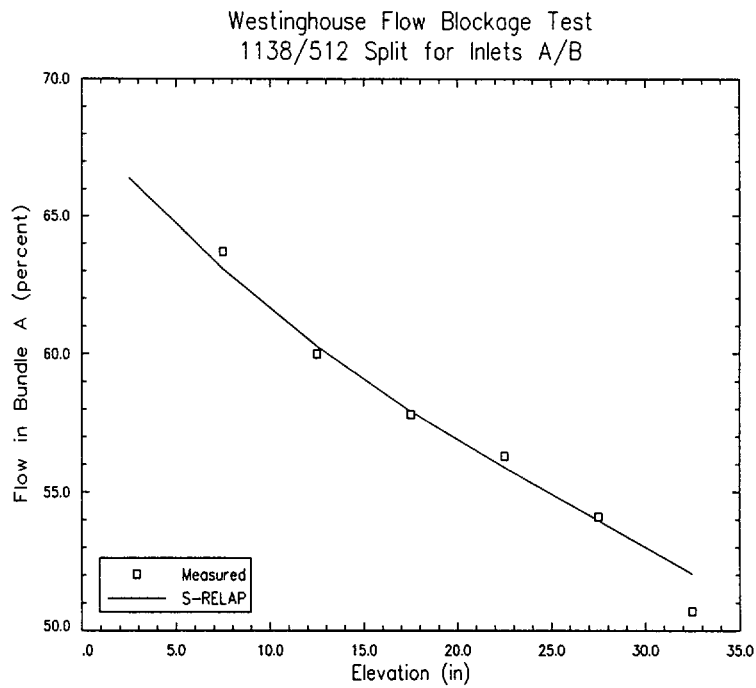


**Figure 5.112 Axial Flow Fractions for Asymmetric Flow (1138/512)**



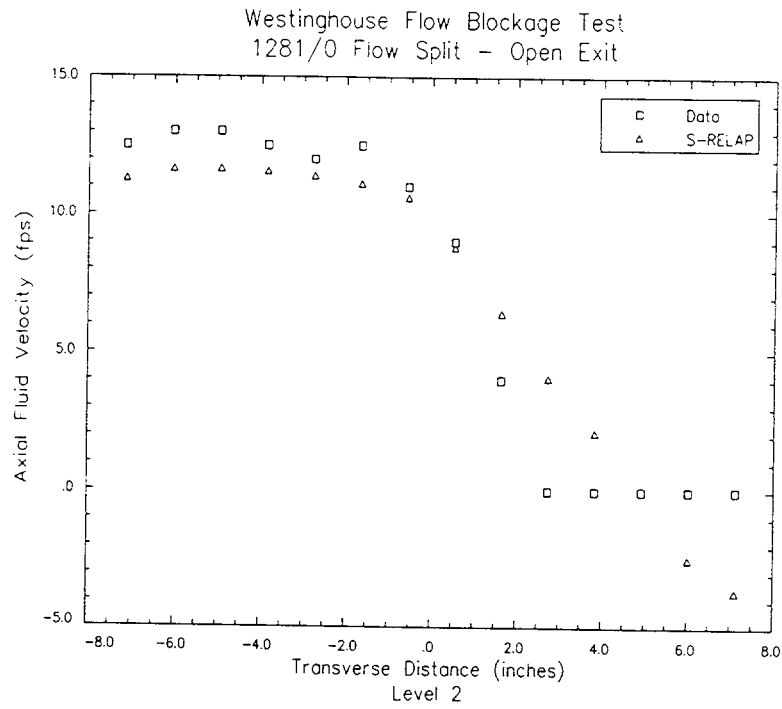


**Figure 5.1.13 Axial Velocities at 7.5-Inches for Asymmetric Flow (1281/0)**

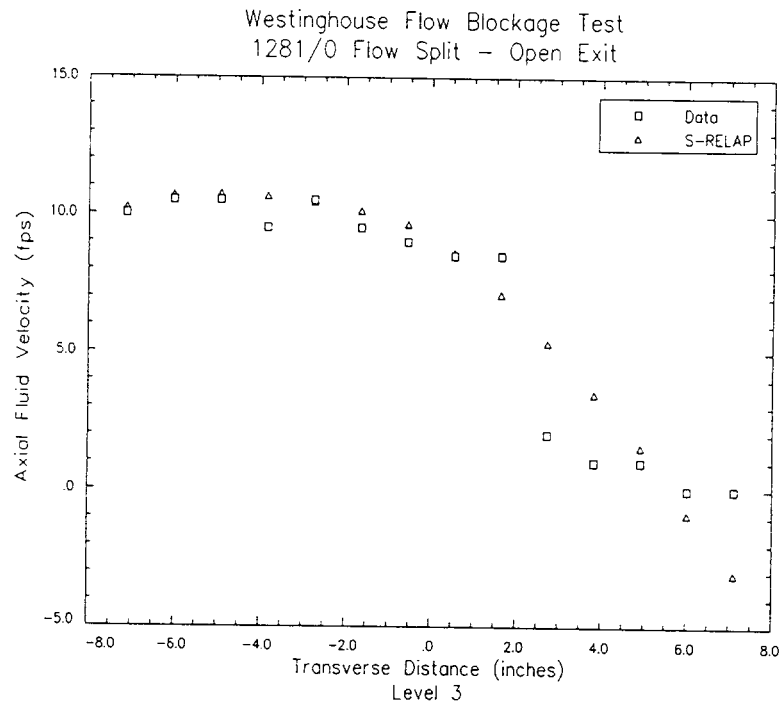


**Figure 5.1.14 Axial Velocities at 12.5-Inches for Asymmetric Flow (1281/0).**

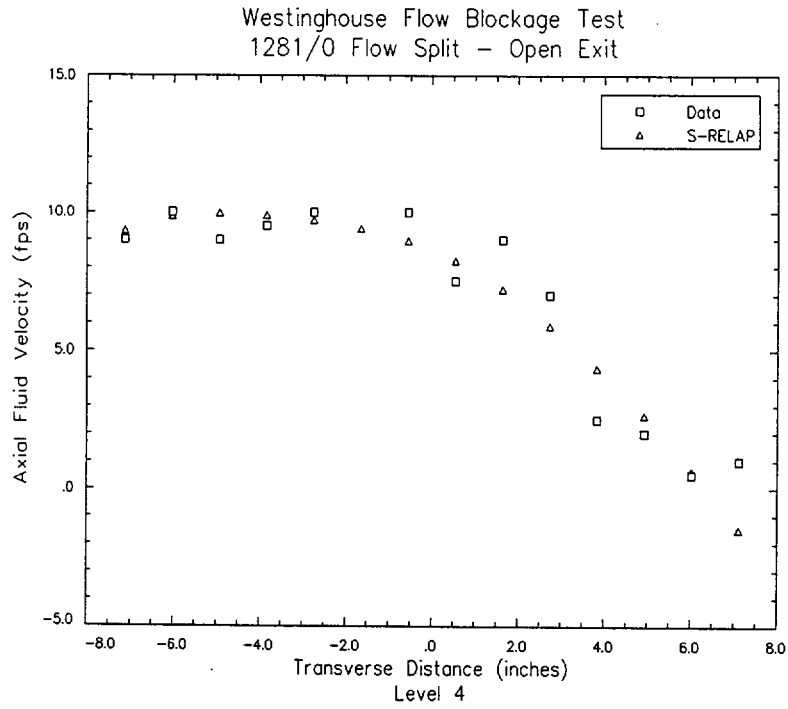


**Figure 5.1.15 Axial Velocities at 17.5-Inches for Asymmetric Flow (1281/0).**

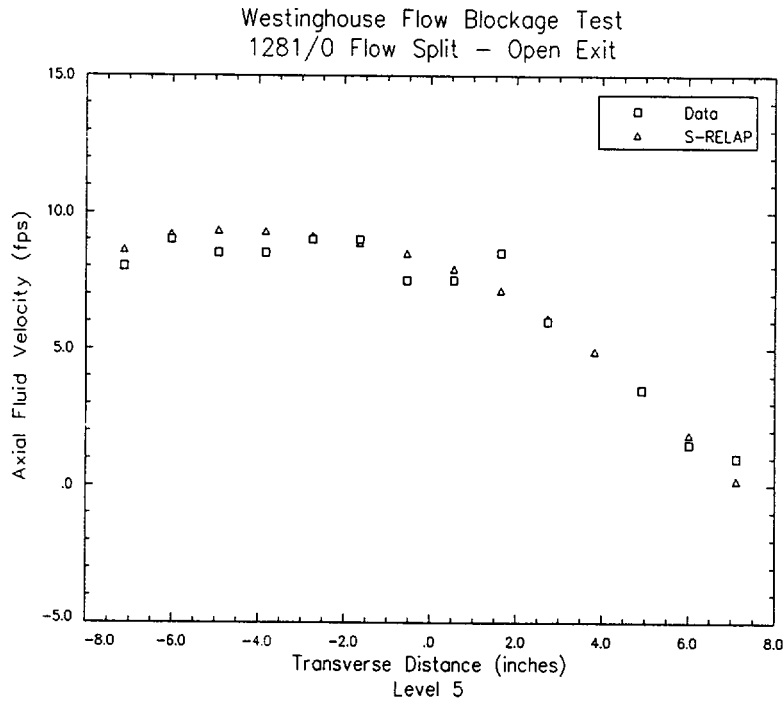


**Figure 5.1.16 Axial Velocities at 22.5-Inches for Asymmetric Flow (1281/0)**

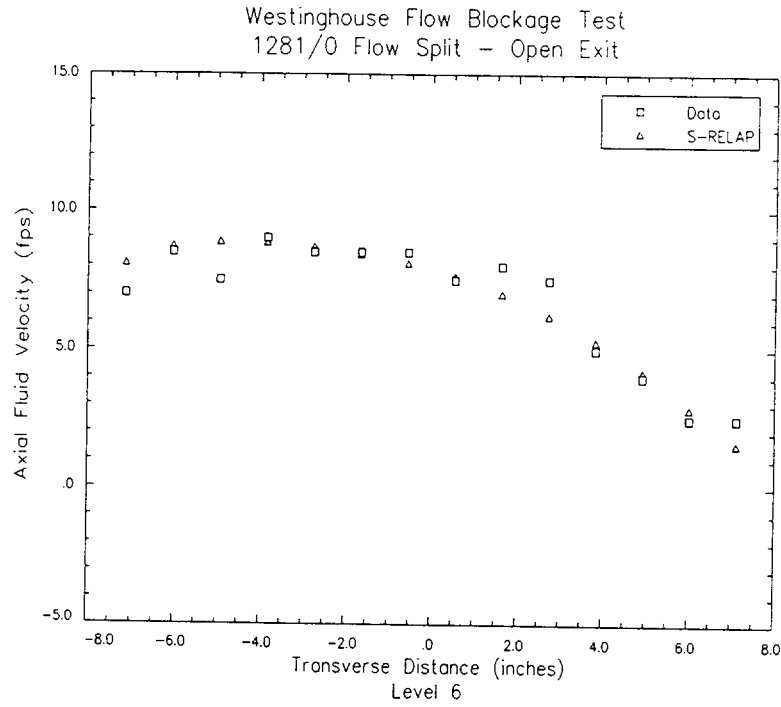


**Figure 5.1.17 Axial Velocities at 27.5-Inches for Asymmetric Flow (1281/0)**

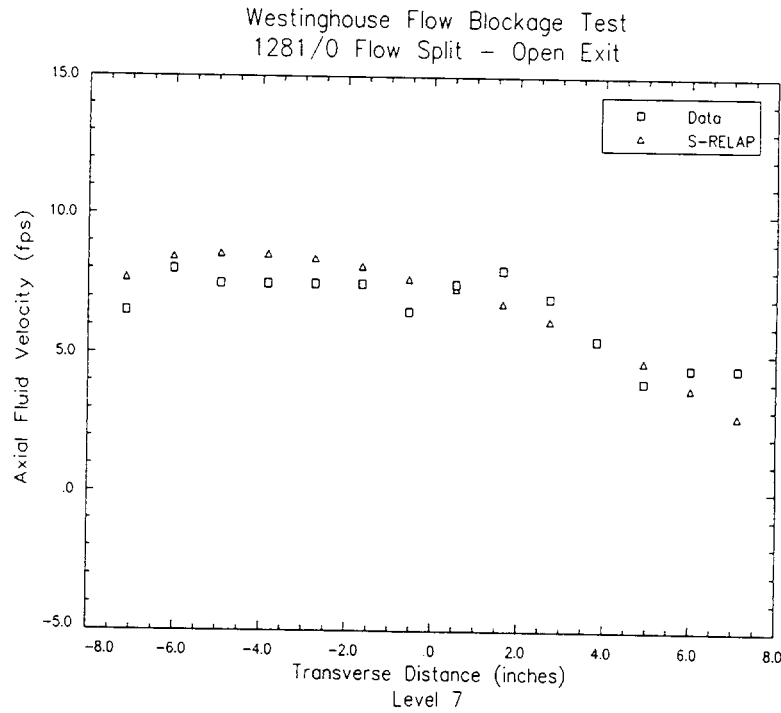


**Figure 5.1.18 Axial Velocities at 32.5-Inches for Asymmetric Flow (1281/0)**

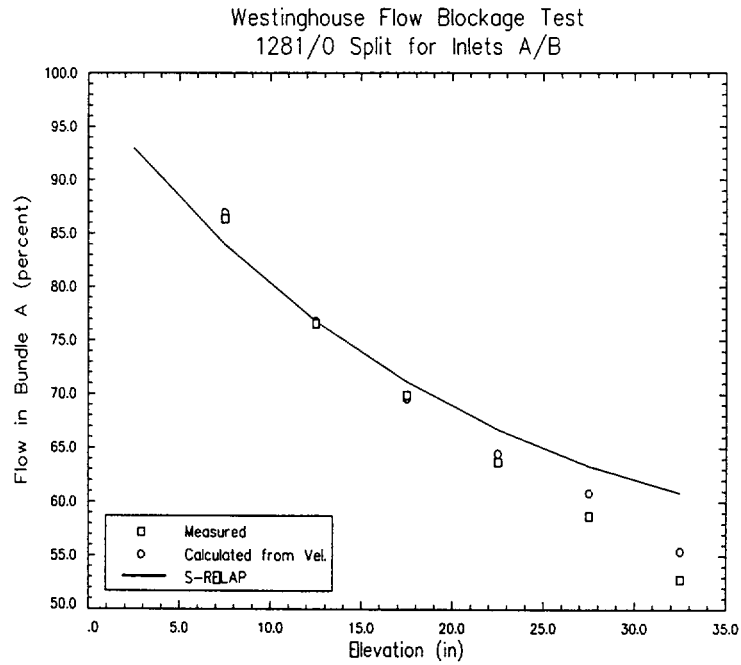


**Figure 5.119 Axial Flow Fractions for Asymmetric Flow-Blocked Inlet Comparison of S-RELAP5 to Flow Data and Flow Fractions Based on Velocities**

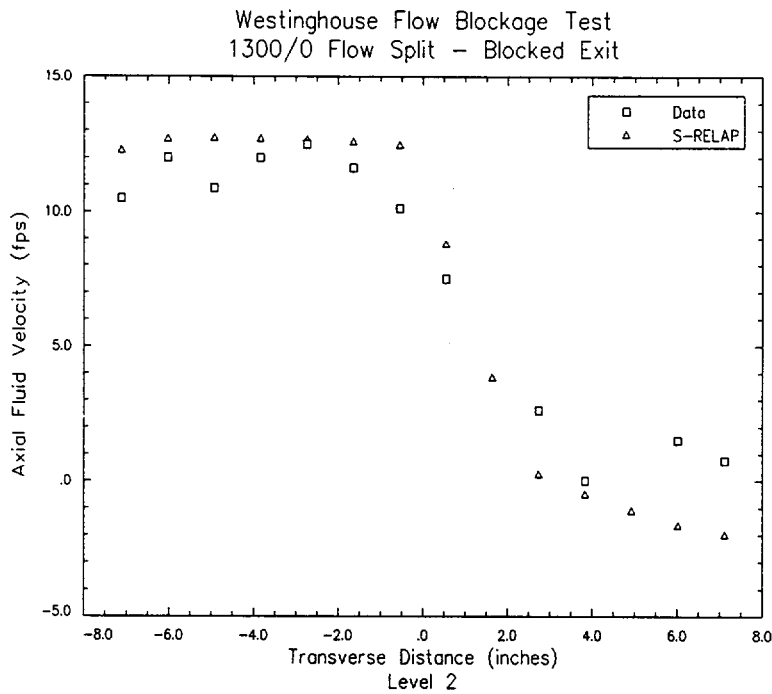


**Figure 5.120 Axial Velocities at 7.5-Inches for Asymmetric Flow (1300/0) – Blocked Exit for Assembly B**

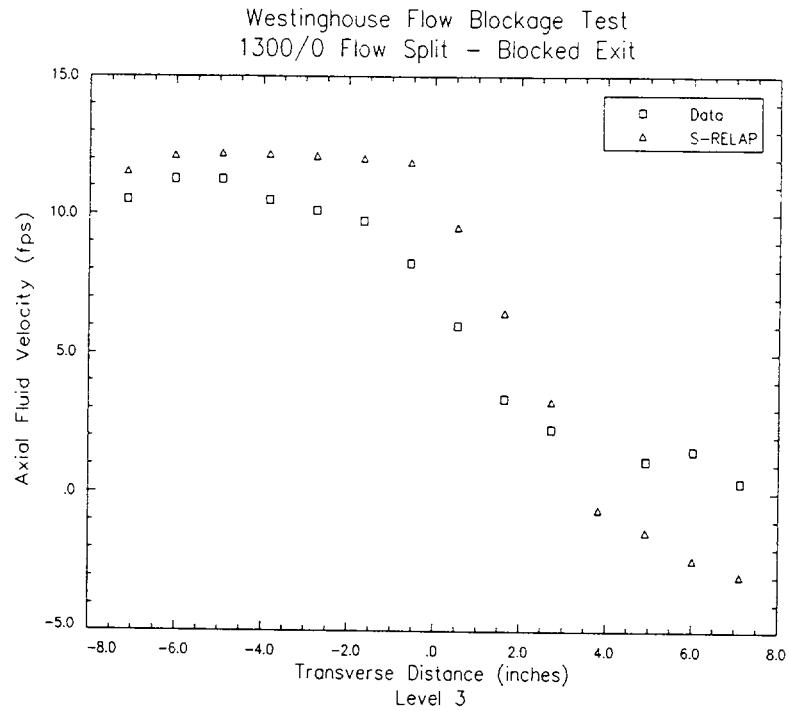


**Figure 5.1.21 Axial Velocities at 12.5-Inches for Asymmetric Flow (1300/0) – Blocked Exit for Assembly B**

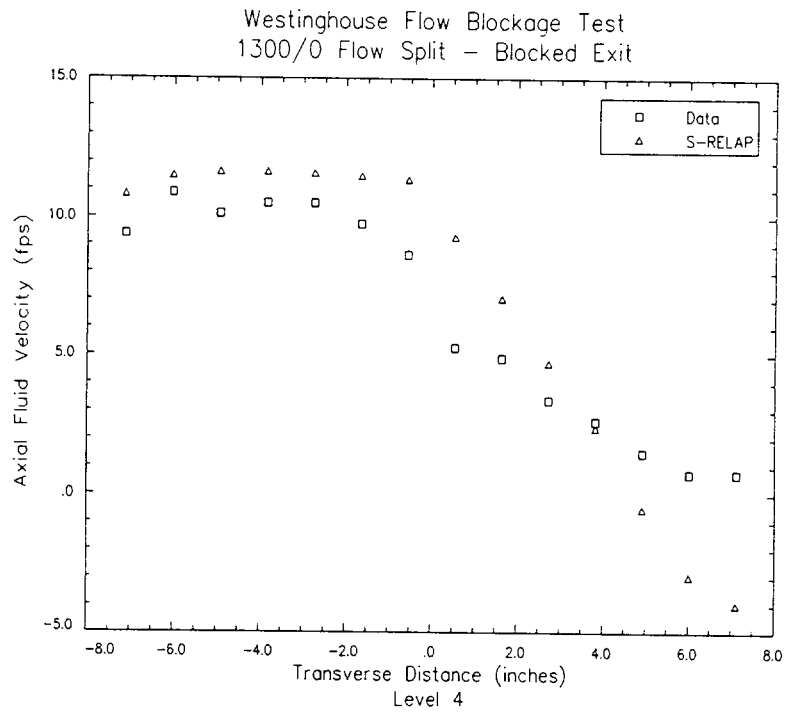


**Figure 5.1.22 Axial Velocities at 17.5-Inches for Asymmetric Flow (1300/0) – Blocked Exit for Assembly B**

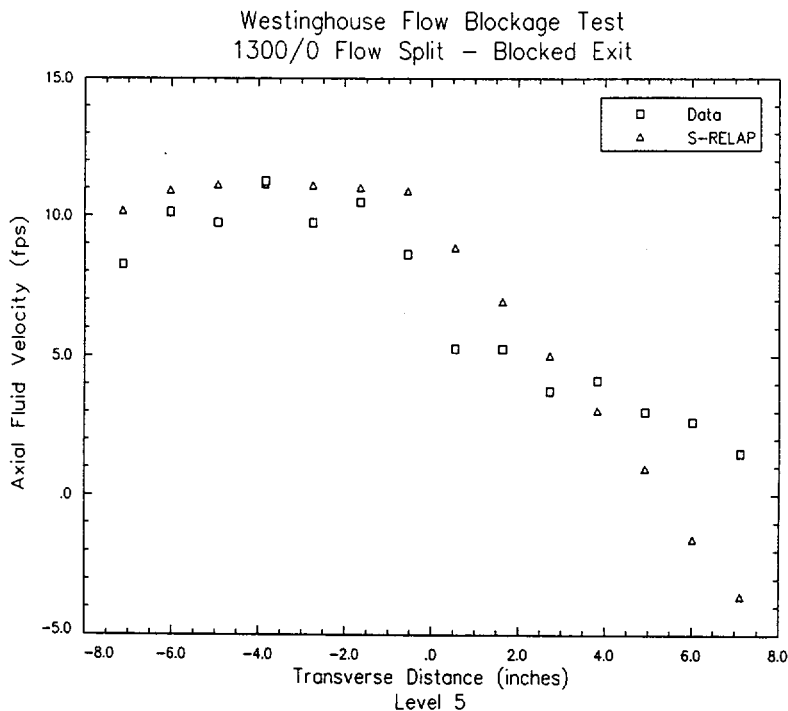


**Figure 5.1.23 Axial Velocities at 22.5-Inches for Asymmetric Flow (1300/0) – Blocked Exit for Assembly B**

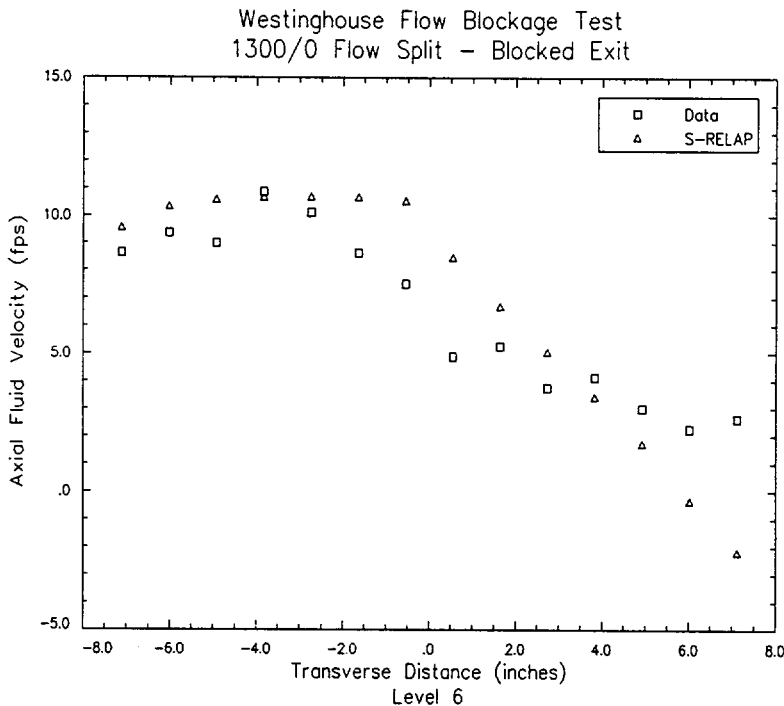


**Figure 5.1.24 Axial Velocities at 27.5-Inches for Asymmetric Flow (1300/0) – Blocked Exit for Assembly B**

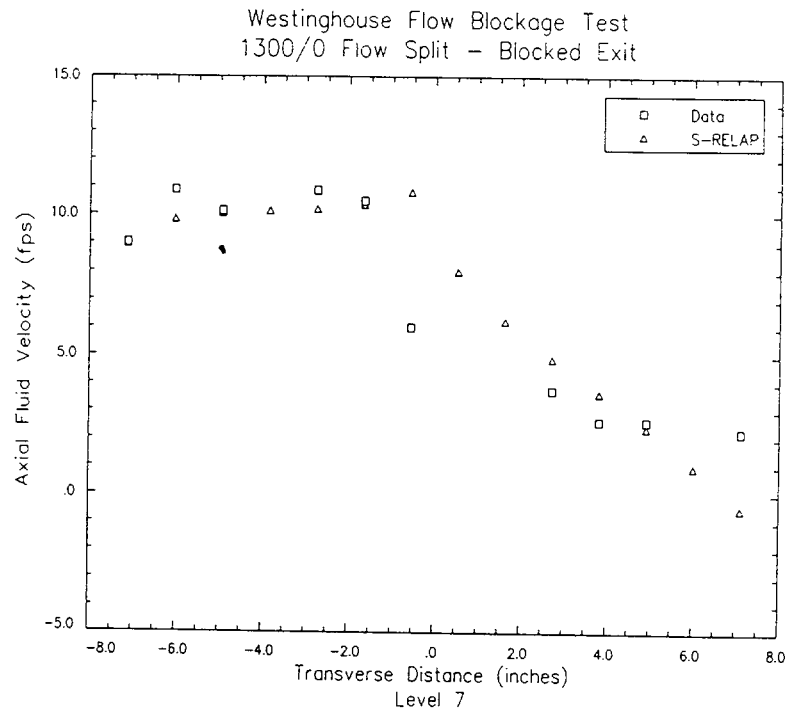


**Figure 5.1.25 Axial Velocities at 32.5-Inches for Asymmetric Flow (1300/0) – Blocked Exit for Assembly B**

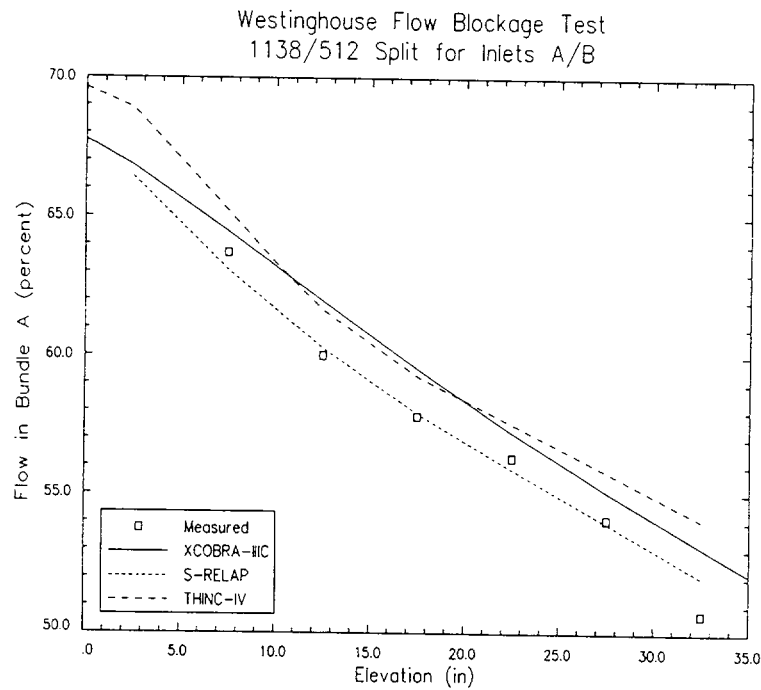


**Figure 5.1.26 Comparison of S-RELAP5 with THINC-IV for Asymmetric Flow (1138/512)**

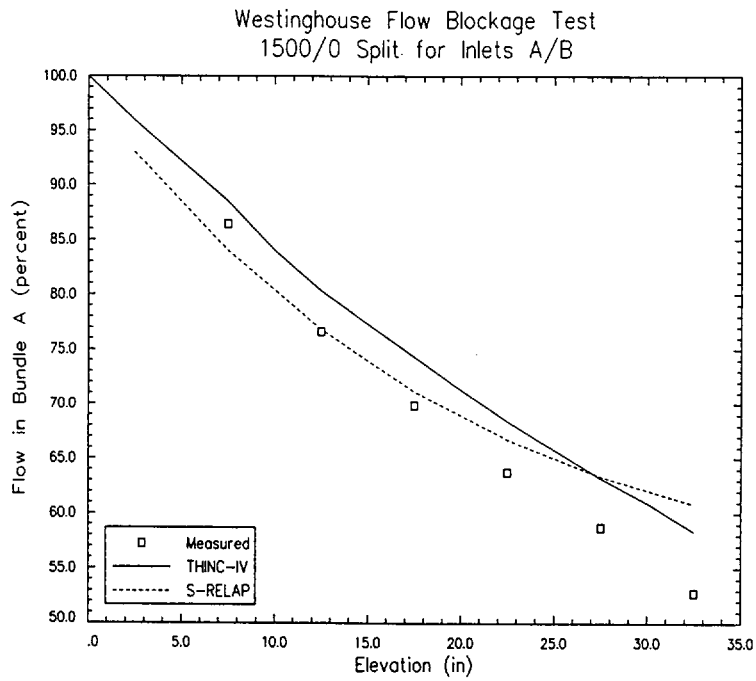


**Figure 5.1.27 Comparison of S-RELAP5 with THINC-IV for Asymmetric Flow (1500/0)**



## 5.2 **Semiscale Test S-UT-8**

The S-UT series of small break tests was performed in the Semiscale Mod-2A test facility at INEEL. The base series of tests was designed to investigate the effect of ECCS on a SBLOCA in a PWR with an upper-head injection system. Test S-UT-8 was added to the series as a variation of the baseline test, S-UT-6. The S-UT-8 test was characterized by deep core uncovering due to increased amounts of liquid held up in the upflow side of the steam generators, compared to test S-UT-6. The primary differences between the tests were that S-UT-8 had significantly less bypass flow from the downcomer to the upper plenum (1.5% for S-UT-8, 4% for S-UT-6). The decreased bypass flow contributed to the deep core uncovering by increasing the steam flow to the steam generators thereby increasing condensation potential, and to delay the downflow side draining of liquid from the steam generator. The S-UT-8 test was simulated with S-RELAP5 to demonstrate that S-RELAP5 could reproduce the liquid hold-up in the upflow side of the steam generator and cause a subsequent deep core uncovering.

### 5.2.1 Test Facility Description

The Mod-2A system was scaled to have a core power and system fluid volume 1/1700 of a four-loop PWR. The intact loop had three times the fluid volume and loop mass flow of the broken loop and represented three of the four operational loops. ECCS included a high-pressure injection system, passive accumulators, and a low-pressure injection system. The test facility is illustrated in Figure 5.2.1.

The flow passing from the downcomer to the upper plenum by way of the upper head was reduced to about 1.5% in S-UT-8, compared to 4.0% in S-UT-6. Reference 23 showed that prolonged flooding in the ascending tubes of the steam generators caused the long, deep core uncovering seen in S-UT-8. Table 5.2.1 shows the sequence of events for the S-UT-8 test.

**Table 5.2.1 Sequence of Events for Semiscale Test S-UT-8**

Event	Test (sec)	S-RELAP5 (sec)
Break initiation	0.	0.
Steam flow valves closed	unknown	9.2
SG feedwater flow stopped		
Intact loop	unknown	9.2
Broken loop	unknown	9.2
HHSI began (trip 508)	35.	33.
Core heatup began	168	142
Downflow side of intact loop SG tubes drained	170	148
Upflow side of intact loop SG tubes drained	225	200
Core temperatures recover	240	~270

**5.2.2 S-RELAP5 Model Description**

The S-RELAP5 model, shown in Figure 5.2.2, was derived from a model originally developed at INEEL and was used by SPC in 1986 for ANF-RELAP simulations of test S-UT-8 (Reference 1). The model was modified for this analysis to incorporate model changes, where applicable, from using the recently developed methodology presented in this report.

[

]

### 5.2.3 Boundary Conditions

Test S-UT-8 was initiated by opening the break valves. Core power was tripped on low pressurizer level and followed a programmed decline simulating decay heat in an operating reactor. The feedwater and steam line valves were closed coincident with the core power trip. Pump trip and coastdown occurred shortly thereafter. ECCS actuation occurred on low primary system pressure; injection was only to the intact loop. Reference 23 contains a comprehensive discussion of S-UT-8.

### 5.2.4 Comparison to Data

The event sequences for the test and the S-RELAP5 simulation are compared in Table 5.2.1, and the comparisons to measured data are summarized in Table 5.2.2. In some cases, the test reports do not include certain event times. These are marked "unknown" in the table. Overall, the event times show general agreement.

Figure 5.2.3 compares the calculated and measured primary system pressure over the first 300 seconds of the test. The primary system pressure calculated by S-RELAP5 is slightly above the measured pressure until about 270 seconds. This is because of the over-predicted steam generator pressures, shown in Figure 5.2.4. The steam generator pressures were over-predicted due to valve closure rate and feedwater cessation uncertainties from the S-RELAP5 calculation. The over-predicted steam generator pressure contributed to event timing discrepancies, but did not invalidate the comparisons to measured data.

Figure 5.2.5 compares the experimental and calculated amounts of mass expelled out the break. The agreement between the two is excellent for the first 75 seconds of the transient. After that the calculated amount of mass expelled is slightly lower than the measured amount due to the break uncovering earlier in transient than the data indicates. [

]

Figure 5.2.6 shows the collapsed level in the ascending tubes for the intact steam generator and Figure 5.2.7 shows the collapsed level in the descending side of the steam generator. S-RELAP5 agrees very good with the ascending side data, and fair with the descending side data. The data show increasing levels from 50 to 100 seconds, while only the ascending side

from the S-RELAP5 calculation shows the increase. Both comparisons show S-RELAP5 leading the data, which is consistent with the early break uncovering time calculated by S-RELAP5. These figures show that S-RELAP5 adequately simulates the holdup of liquid in the steam generator tubes.

Figure 5.2.8 shows the collapsed level in the core. The drop in level calculated by S-RELAP5 at 100 seconds is caused by the early transition from single to two phase break flow. The early break flow transition and the lack of liquid hold-up in the down-flow side of the steam generator also causes an earlier core dryout in the simulation. The heatups for both the calculation and the test begins when the collapsed levels fall below 180 cm. The calculated level did not drop as far as the measured level and began recovering sooner. However the measured level reached 180 cm on recovery before 250 seconds and the simulated level did not reach 180 cm until about 270 seconds. Thus, the heat-up period for the simulation was much longer.

The effects of the earlier and longer dryout are shown in Figure 5.2.9, the cladding temperature at the 6-foot (1.83 m) elevation. The S-RELAP5 temperatures shown for comparison are calculated from nodes spanning the 6 foot elevation and are taken from mesh points within the structure that approximate the thermal-couple location. The slightly higher calculated temperature between 50 and 150 seconds is due to the slightly higher primary pressure and corresponding saturation temperature. The measured dryout at this elevation occurred at 168 seconds. In the simulation, the S-RELAP5 dryout occurred approximately 25 seconds earlier. The peak temperature from S-RELAP5 is greater than the experimental temperature.

#### 5.2.5 Conclusions

Table 5.2.2 summarizes the results obtained in this analysis. PCTs have been rounded to the next highest whole number.

**Table 5.2.2 Summary of Calculated PCTs.**

Parameter	Time, s	PCT, K (°F)
Measured PCT	226	682 (768)
S-RELAP5	254	698 (797)

S-RELAP5 approximated the early hydraulic behavior seen in the experiment; a deep core uncovering due to holdup of liquid in the up-flow side of the steam generator and CCFL at the core outlet. The calculated core mid-plane temperature response agreed well with the data. In the core mid-plane, S-RELAP5 predicted CHF to occur sooner than it actually occurred and predicted PCTs which are close to, yet above, the data. These results indicate that S-RELAP5 can simulate the core heat-up prior to loop seal clearing in SBLOCA events.

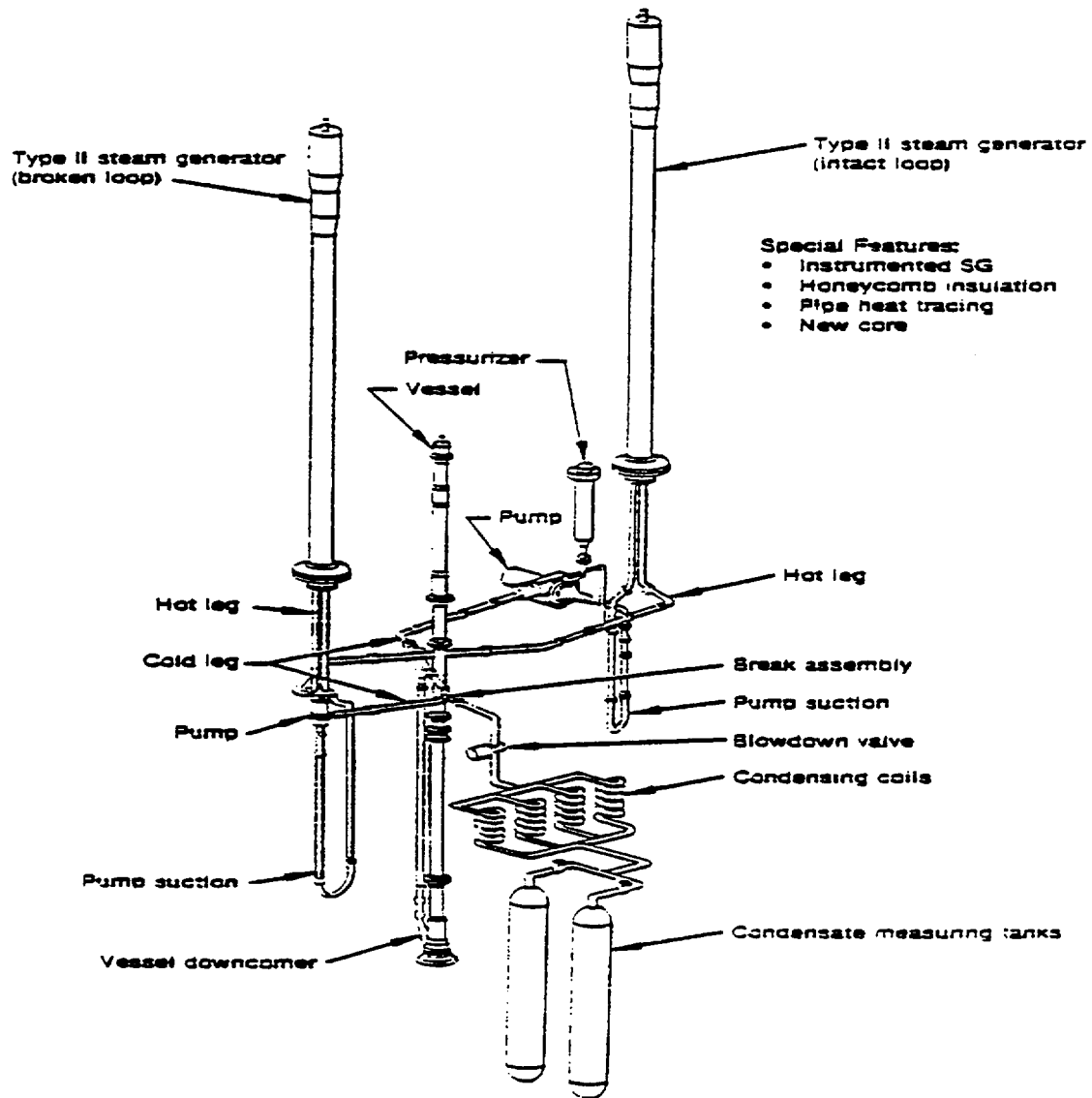
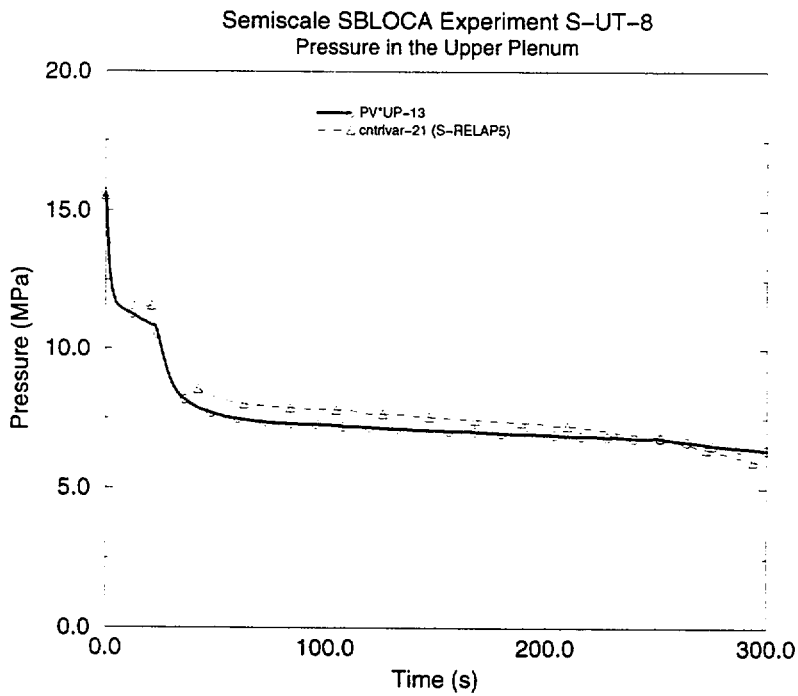


Figure 5.2.1 Isometric of the Semiscale Mod-2A Facility



**Figure 5.2.2 S-RELAP5 Nodalization for S-UT-8 Simulations**



**Figure 5.2.3 Primary System Pressure (Upper Plenum)**

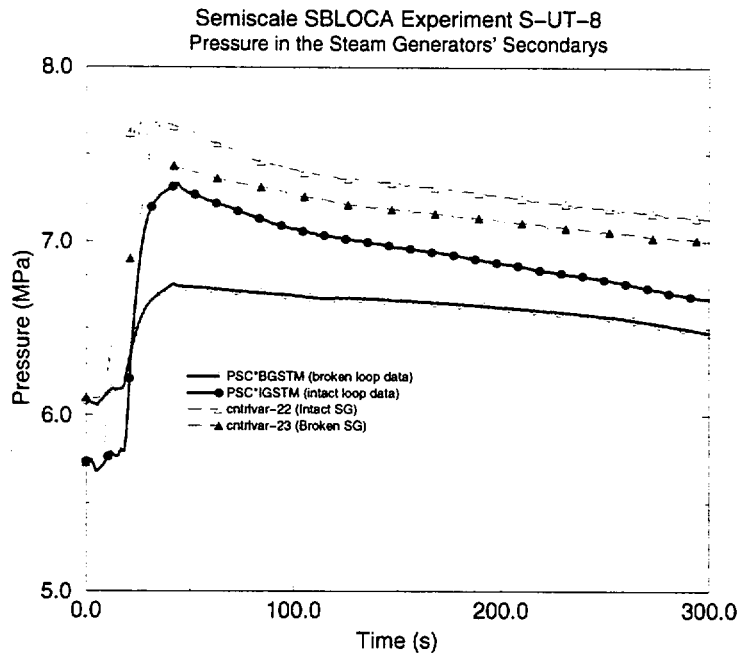


**Figure 5.2.4 Secondary Side Pressures**



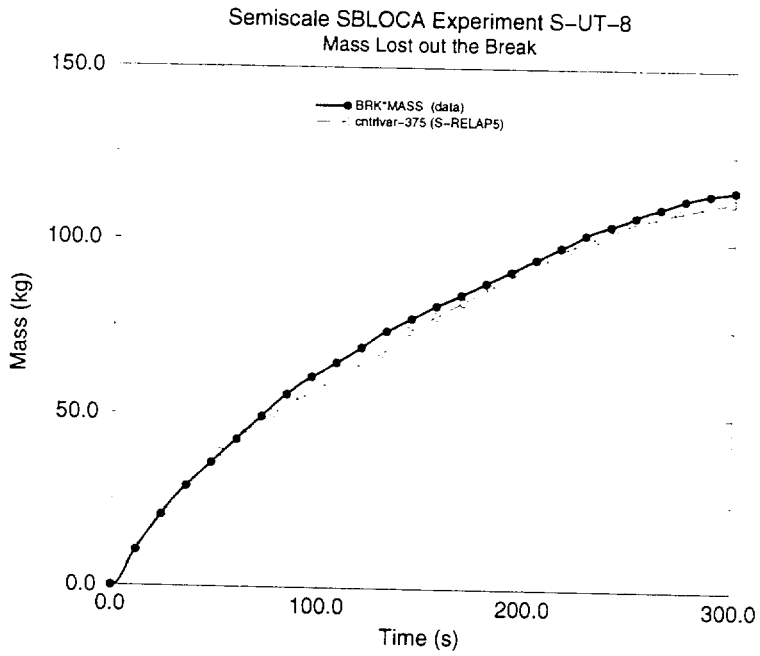


Figure 5.2.5 Integrated Break Flow

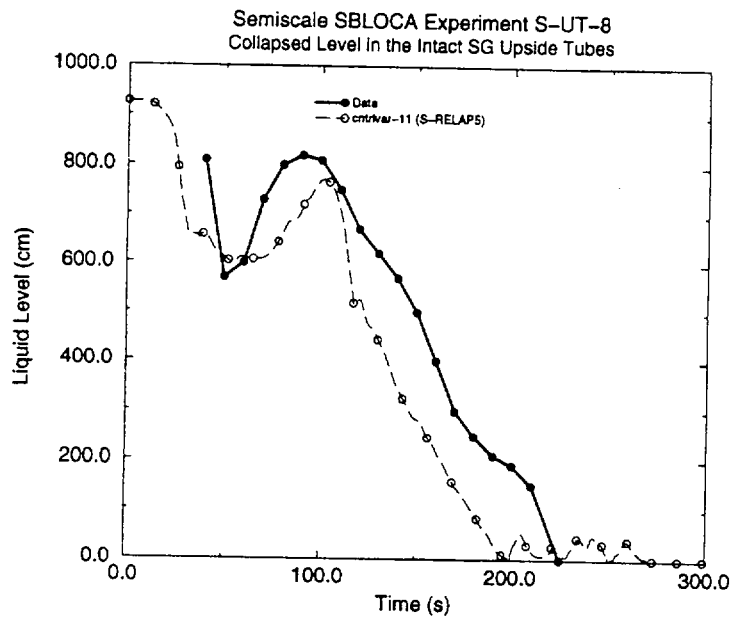


Figure 5.2.6 Collapsed Level in the Intact SG Upflow Tubes

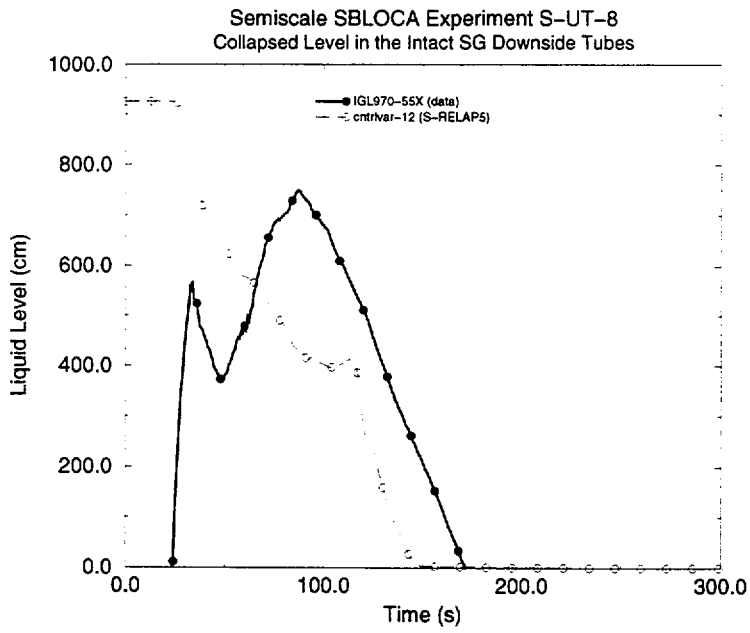


Figure 5.2.7 Collapsed Level in the Intact SG Downflow Tubes

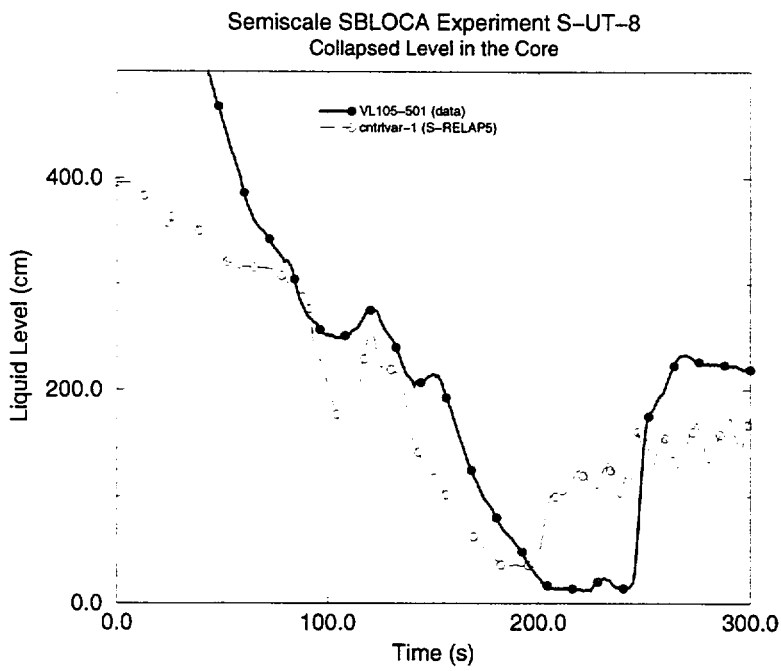


Figure 5.2.8 Collapsed Level in the Core

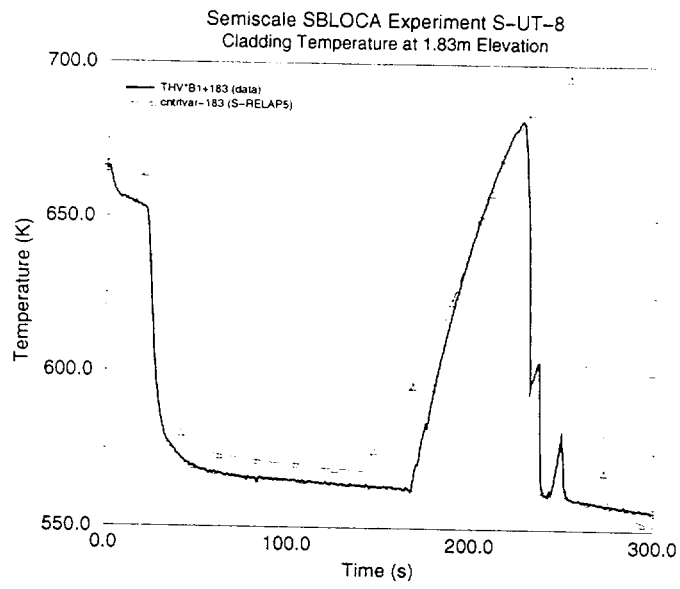


Figure 5.2.9 Core Mid-Plane Cladding Temperature

### 5.3 **LOFT LP-SB-03**

The LP-SB-3 test was the last test studying small-break phenomena at the loss of fluid test (LOFT) facility. One objective of this test was to investigate core heat transfer when core uncover occurs during relatively slow boil-off conditions (Reference 24). This section briefly describes the test facility, the test conditions for the LP-SB-3 test, and the S-RELAP5 simulation model, and compares calculated results from S-RELAP5, previous ANF-RELAP calculations, and measured data.

#### 5.3.1 Test Facility Description

The LOFT facility was designed to simulate the major components and system responses of a full-scale PWR during a LOCA. The experimental facility includes five major systems that are instrumented so system variables can be measured and recorded during an experiment. The systems include the reactor vessel, the intact loop, the broken loop, the blowdown suppression system, and the ECCS. The system of interest for this application, the reactor vessel, is shown in Figure 5.3.1. Reference 25 describes the LOFT system in more detail.

#### 5.3.2 S-RELAP5 Model Description

The period of interest for a boil-off investigation is approximately 1500 seconds starting at 3500 seconds into the transient. Therefore, an abbreviated system model was developed to simulate the core boil-off period exclusively. [

]

Heat structures representing the hot rod, hot assembly, and outer core region were initialized to conditions equal to the experimental values at 3500 seconds. Also, the hydrodynamic components were set to the experimental condition at 3500 seconds. A steady-state calculation was made to establish two-phase conditions in the core region similar to those found in the experiment. A transient calculation was made for 1500 transient seconds and the calculated results were shifted approximately 3500 seconds to the time frame of core boil-off by matching the measured and calculated dryout times.

### 5.3.3 Event Description

The description of the test is given in Reference 26. The experiment was initiated by opening the break valve in the intact-loop cold-leg break line. The reactor scrammed at a primary system pressure of 2057.6 psia at 9.2 seconds. The steam generator control system responded to the reactor scram by isolating the feedwater flow to the steam generator and the steam flow out of the steam generator. The main feedwater pump power was terminated at 9.4 seconds and the main feedwater valve was isolated at 10.8 seconds. The main steam control valve (MSCV) began closing at 9.5 seconds and was fully closed at 21 seconds. The secondary system pressure increased sharply after reactor scram because of the feedwater shutoff and MSCV closure. The first cycle of MSCV occurred at 87.5 seconds to keep the secondary side pressure between 1032 and 932 psia. The MSCV cycled four times, with the last cycle occurring at 1030 seconds. Fluid saturation conditions were reached in the piping to the break at about 100 seconds.

**Table 5.3.1 Event Sequence**

Event	Test (sec)
Break initiation, intact-loop cold-leg break line	0.
Reactor scram	9.2
SG main feedwater pump trip	9.4
SG main feedwater valve closed	10.8
Pump tripped	1600
Break uncovered	1612
Core heatup began	3800
Break isolated	4742
Initiation of 'feed and bleed'	5415
Experiment end time	6845

At 875 seconds, the rate of pressure increase slowed abruptly. The primary coolant pumps tripped at 1600 seconds. The reduction of the pump head caused an uncovering of the break at 1612 seconds.

As the liquid level fell in the core, the upper part of the core started to heat up at 3800 seconds. The break was isolated at 4742 seconds, when the highest indicated cladding temperature reached 1000 °F.

The cladding temperature continued to rise until the highest indicated value reached 1300 °F at 5415 seconds. A secondary system feed-and-bleed operation was initiated at that time by fully opening the MSCV bypass valve and operating the main feedwater pump. This action caused a very rapid cool down and depressurization of the secondary system while the fuel clad temperature continued to increase, reaching the maximum value of 1318 °F at 5422 seconds. The primary system started depressurizing and cooling down at that time. The primary system pressure reached the accumulator setpoint at 5558 seconds, at which time the accumulator injection began.

At 6785 seconds, the pressure fell low enough that the low-pressure injection pump started injecting, and the experiment was terminated at 6845 seconds.

#### 5.3.4 Comparison to Data

The results from this calculation are shown in Figure 5.3.3 through Figure 5.3.6. For comparison, results calculated using ANF-RELAP also are shown. The over-predicted temperature at the 28 inch elevation shown in Figure 5.3.5 is due to a cooling mechanism in the experiment not modeled in the code calculation. The overall comparison between S-RELAP5 and measured data is acceptable under the conditions assumed for this calculation.

[

]

System mass responses also were compared for the code calculations. Both cases started with approximately the same total mass. At the end of the transient calculations, the PCS contained about 4% more mass in the S-RELAP5 run than in the ANF-RELAP run. However, throughout the transient, S-RELAP5 has a slightly higher mass flow out of the core and higher flow into the downcomer compared to ANF-RELAP. Also, the mass flow exiting the system was slightly lower from S-RELAP5 compared to

ANF-RELAP. Overall, these differences are small and considered insignificant, however they do cause slight differences in direct comparisons.

#### 5.3.5 Conclusions

The results of comparisons between S-RELAP5 and ANF-RELAP showed significant differences (more than 50 °F) between the calculated results at the 28-inch elevation. The temperature comparisons at the 49-inch elevation showed insignificant differences. The mixture level plots show that the boil-off rates calculated from both codes are very similar, but small differences exist at specific locations. Overall, the comparisons show little difference between ANF-RELAP and S-RELAP5 as applied to the LOFT LP-SB-3 test. The comparisons between measured data and S-RELAP5 show the code is capable of calculating the expected boil-off and fuel heatup during the SBLOCA event in a conservative manner.

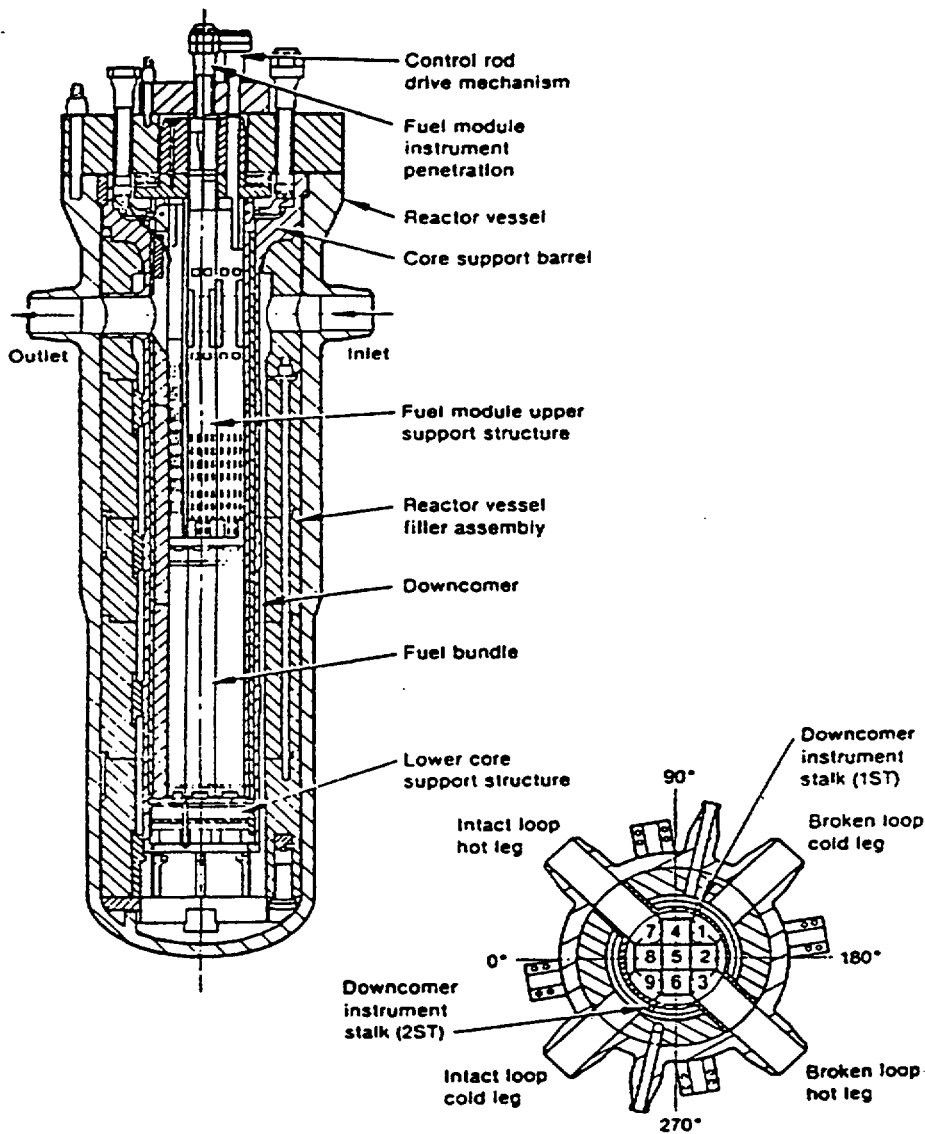
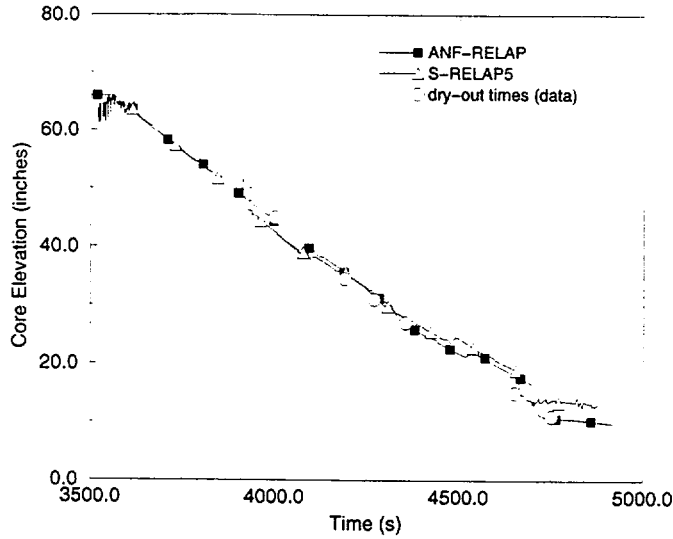


Figure 5.3.1 LOFT Reactor Vessel Assembly.





**Figure 5.3.2 Primary System Nodalization**



**Figure 5.3.3 S-RELAP5 Mixture Level Using Two-Dimensional Core Model Compared to LOFT Data and ANF-RELAP Calculation**

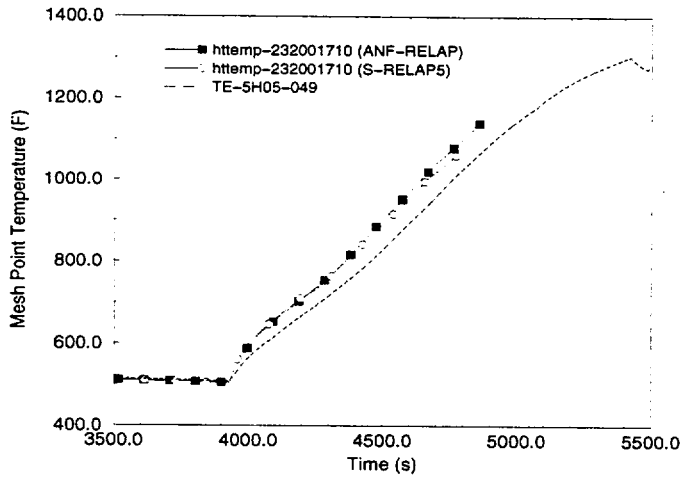


**Figure 5.3.4 S-RELAP5 Clad Temperatures at the 49-Inch Elevation Using Two-Dimensional Core Model Compared to LOFT Data and ANF-RELAP Calculation**

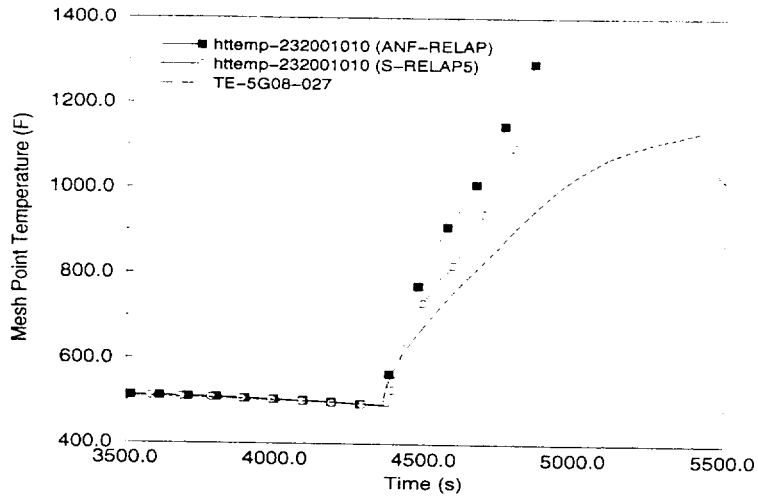


**Figure 5.3.5 S-RELAP5 Clad Temperatures at the 28-Inch Elevation Using Two-Dimensional Core Model Compared to LOFT Data and ANF-RELAP Calculation**

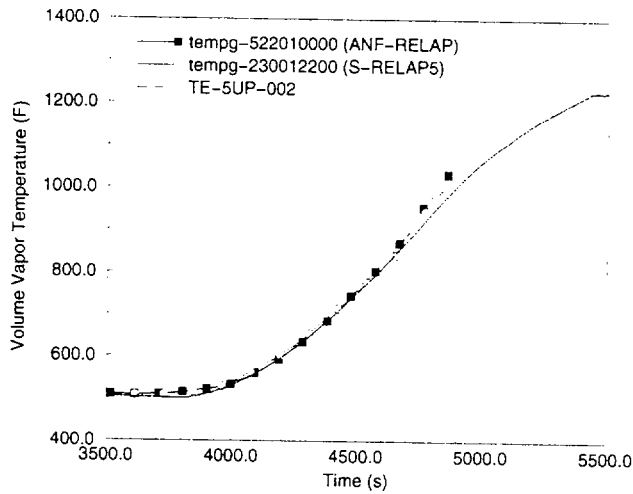


**Figure 5.3.6 S-RELAP5 Steam Temperatures at the Core Exit Using Two-Dimensional Core Model Compared to LOFT Data and ANF-RELAP Calculation**

## 5.4 *UPTF Loop Seal Clearing*

In 1991 Siemens performed (on a proprietary basis) the TRansient Accident Management (TRAM) test series A5 tests in the UPTF (References 7 and 27 through 29). This series consisted of full-scale integral and separate-effects tests, designed to evaluate loop seal behavior during a SBLOCA. The loop seal and pump configuration for the UPTF facility is similar to that for Westinghouse and Combustion Engineering PWRs. Separate-effect test (A5RUN11E) from this series was selected as the most appropriate test to evaluate the ability of S-RELAP5 to model this behavior.

Test A5RUN11E was one of two available UPTF tests with appropriate steam mass flow through the loop seal for SBLOCA and substantial steam superheat. After loop seal clearing, the steam flow through the loop seal is expected to be substantially superheated. The system pressure for this test, however, is lower than what is expected in a plant calculation. As a result, the steam is less dense with higher superficial velocities than expected in a SBLOCA plant calculation. These higher velocities should generate higher interfacial drag with the horizontally stratified liquid trapped in the loop seal and provide a bounding calculation.

### 5.4.1 Test Facility Description

UPTF is a full-scale PWR test facility designed to explore a number of thermal-hydraulic phenomena during various postulated accident scenarios. The facility consists of four separate loops with steam generator simulators and reactor coolant pump simulators, a reactor vessel with a core simulator, a containment simulator, and a variety of ECCS injection systems. Figure 5.4.1 is a schematic of the facility. The portion of the system relevant to the test used in this analysis consists of the piping from the second loop steam generator through the pump (including loop seal) and the cold-leg piping from the pump to the vessel downcomer. Figure 5.4.2 shows this portion of Loop 2 with selected key measurement instrumentation locations. The downcomer pressure measurement shown in Figure 5.4.2 (JAA01CP002L), actually is located at the outlet of the cold-leg for Loop 1, not at the outlet for Loop 2. Figure 5.4.3 shows the locations of important measurement instrumentation in the loop seal.

For test A5RUN11E, increasing the reactor coolant pump simulator resistance in the other three loops to infinity isolated the second loop. The system was pressurized to 320 kPa (46.4 psia) and filled with saturated steam. The vessel also was filled to 4 meters (13.12 ft) with saturated

liquid. For the entire transient, the broken loop vent valve in the cool leg for Loop 4 was open to the containment simulator. System pressure was controlled by adjusting the containment pressure.

The test results are summarized in Figure 5.4.5 through Figure 5.4.9. At 2 seconds, steam injection into the containment simulator and system pressure control began. The system pressure control lowered the system pressure to about 310 kPa (45.0 psia) at about 30 seconds. At about 72 seconds, superheated steam injection into the steam generator in Loop 3 began. At the same time, slightly subcooled liquid water injection into the steam generator simulator side of the loop seal in Loop 2 began. The pressure controller allowed the system to pressurize to between 340 kPa and 350 kPa (49.3 and 50.8 psia) in response to the mass and energy addition to the system. Because the downcomer and core simulator were partially filled with liquid, steam injected into the steam generator simulator in Loop 3 was forced through the loop seal in Loop 2. During this period the loop seal in Loop 2 partially filled with liquid. [

]

At approximately 230 seconds, the liquid water injection into the loop seal was cut off and loop seal clearing began as steam was forced through the loop seal. At about 400 seconds the loop seal clearing test ended and the steam injection rate was ramped down. The liquid remaining in the loop seal then collapsed into the horizontal section. [

]

At about 470 seconds, liquid and steam injection began again. The steam injection rate was only about two-thirds of what it was for the first test. The pump side of the loop seal again filled to a collapsed level between 1.0 meter to 1.2 meters (3.28 and 3.94 ft) At about 625 seconds, the liquid water injection was stopped and the second loop seal clearing test began. At about 790 seconds, the second loop seal clearing test ended and the steam injection rate was reduced, allowing the liquid trapped in the loop seal to collapse into the horizontal section. [

]

#### 5.4.2 S-RELAP5 Model Description

The S-RELAP5 model used for this analysis consists of the piping from the second loop steam generator simulator to the pump simulator (including the loop seal), the pump simulator, the cold-leg piping from the pump simulator to the vessel downcomer and the first downcomer volume. This analysis includes a sensitivity study on loop seal steam generator side nodalization and maximum time step. Two different nodalizations for the piping on the steam generator side of the loop seal were examined. [

]

#### 5.4.3 Boundary Conditions

This analysis simulates only a portion of the larger UPTF system by specifying boundary conditions for the portion being modeled. The boundary conditions consist of inlet steam mass flow rate and temperature, injected water mass flow rate and temperature, and outlet (downcomer) pressure. Figure 5.4.5 through Figure 5.4.7 show the boundary conditions used to drive the S-RELAP5 simulation and the test data corresponding to these boundary conditions. The model was initialized at equilibrium as filled with saturated steam at a pressure of 320 kPa (46.4 psia).

#### 5.4.4 Comparison to Data

Comparing the calculated levels and pressure drops (Figure 5.4.8 and Figure 5.4.9) demonstrates that the calculated loop seal clearing was similar to the data. [

]

The accurate liquid inventory in the loop seal is given by the data in the period immediately following each test, when the liquid collapses into the bottom of the loop seal. [

]

The second test had a lower steam mass flow rate and, as a consequence, more liquid remains trapped in the loop seal. The steam generator side level was approximately the same, but the pump side level was much higher. A significant amount of liquid, compared to the high flow test, was entrained in the pump simulator causing the high level and pressure drop in this test. [

]

The comparisons of S-RELAP5 predictions with test A5RUN11E data show S-RELAP5 predicts loop seal clearing adequately. It also predicts a larger amount of liquid remaining in the loop seal after clearing than was measured in the test and a higher differential pressure across the loop seal after clearing. In a PWR SBLOCA transient, the pressure drop across a cleared loop will affect the levels in the core and downcomer. As the pressure drop increases, the core level will decrease which can increase the PCT.

#### 5.4.5 Sensitivities

In addition to benchmarking the base model to the measured data, sensitivity studies were performed to demonstrate the impact of the loop seal nodalization and the time step used in the calculation. [

] Figure 5.4.11 and Figure 5.4.12 compare the S-RELAP5 calculations with the data.

The sensitivity of the S-RELAP5 calculations to time step was evaluated with the base model. Maximum time steps of 100 ms, 10 ms and 5 ms were used. Figure 5.4.8, Figure 5.4.9, and Figure 5.4.13 through Figure 5.4.16 compare the collapsed level and pressure drop to the data.

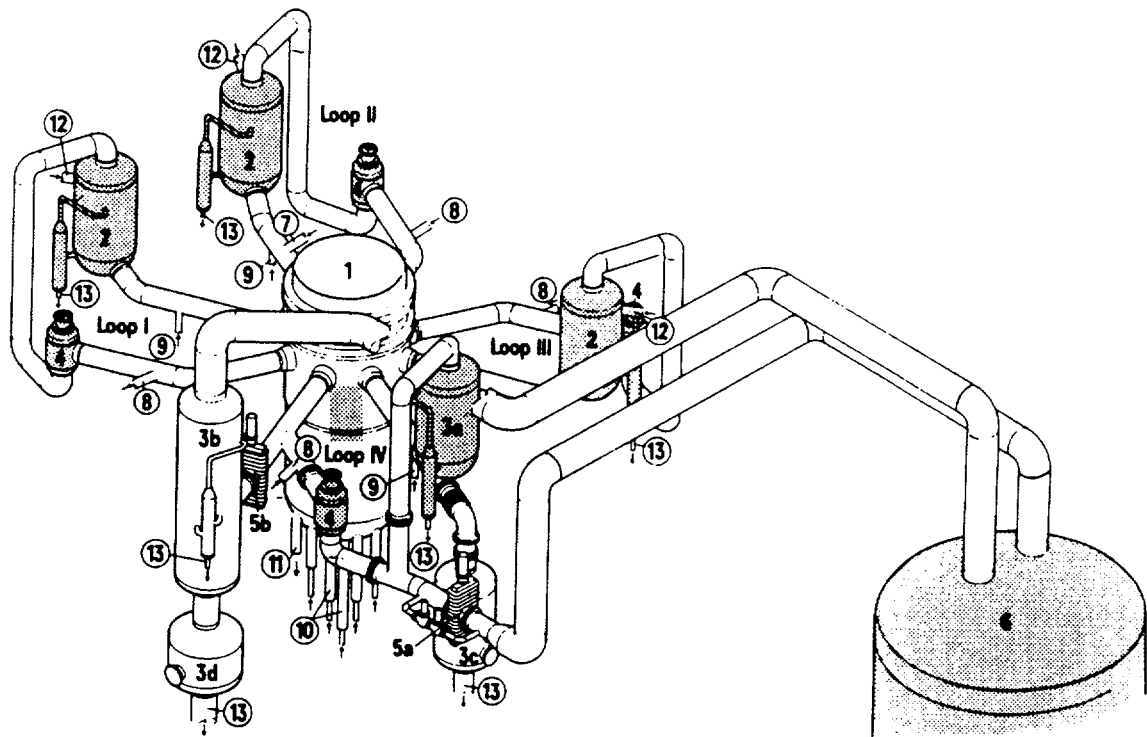
The loop seal behavior is not particularly sensitive to changes in nodalization or to time step and is consistently conservative for the two nodalizations used.

#### 5.4.6 Conclusions

The pressure drop across a loop seal and the quantity of liquid remaining in a loop seal after loop seal clearing from this test were compared to the predicted values for the test using S-RELAP5. The S-RELAP5 simulation of the loop seal was based on the SBLOCA modeling. Finally, different nodalizations and time steps were used to evaluate the sensitivity of the SBLOCA model to these modeling parameters.

Compared to the UPTF data, S-RELAP5 tends to predict a larger quantity of liquid in the loop seal in the post-clearing period. It also predicts a larger pressure drop. The predicted behavior was found to be relatively insensitive to time step size and to volume lengths. Both the larger quantity of liquid and larger pressure drop can cause higher PCTs to be calculated for SBLOCA analysis, hence is conservative.






- |    |  |      |                                  |
|----|--|------|----------------------------------|
| 1  | Test Vessel  | (7)  | Surgeline-Nozzle                 |
| 2  | Steam Generator Simulator<br>(Intact Loop)                           | (8)  | ECC-Injection Nozzles (Cold Leg) |
| 3a | Steam Generator Simulator / Water Separator<br>(Broken Loop Hot Leg) | (9)  | ECC-Injection Nozzles (Hot Leg)  |
| 3b | Water Separator<br>(Broken Loop Cold Leg)                            | (10) | Core Simulator Injection Nozzle  |
| 3c | Drainage Vessel for Hot Leg  | (11) | TV-Drainage Nozzle               |
| 3d | Drainage Vessel for Cold Leg   | (12) | Steam Injection Nozzle           |
| 4  | Pump Simulator   | (13) | Drainage Nozzle                  |
| 5a | Break Valve (Hot Leg)  |      |                                  |
| 5b | Break Valve (Cold Leg)   |      |                                  |
| 6  | Containment Simulator  |      |                                  |
-  Simulator

Figure 5.4.1 Upper Plenum Test Facility

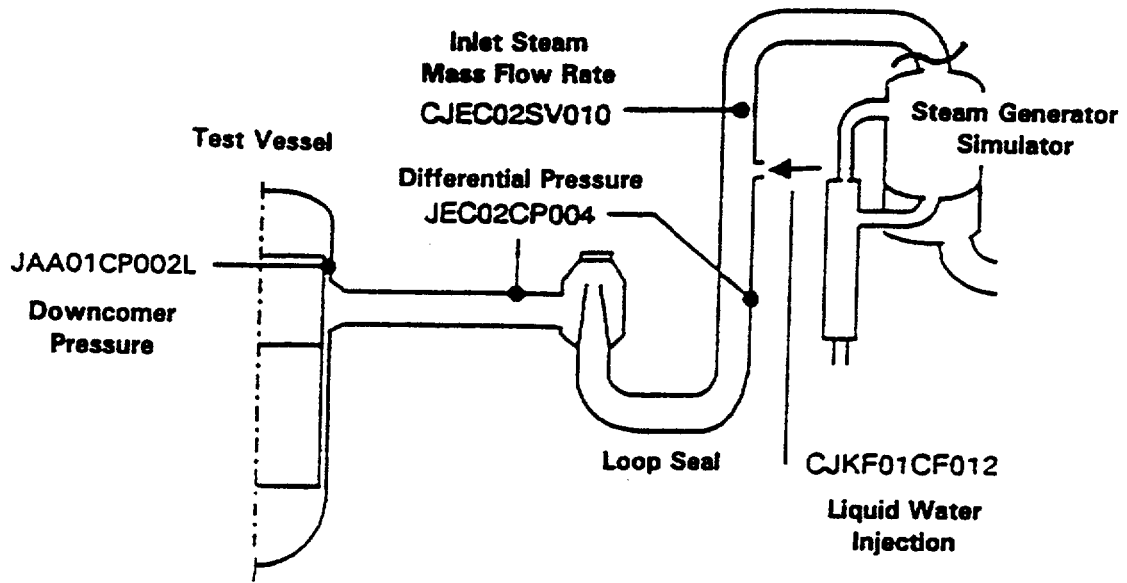


Figure 5.4.2 Configuration and Instrumentation for Loop 2

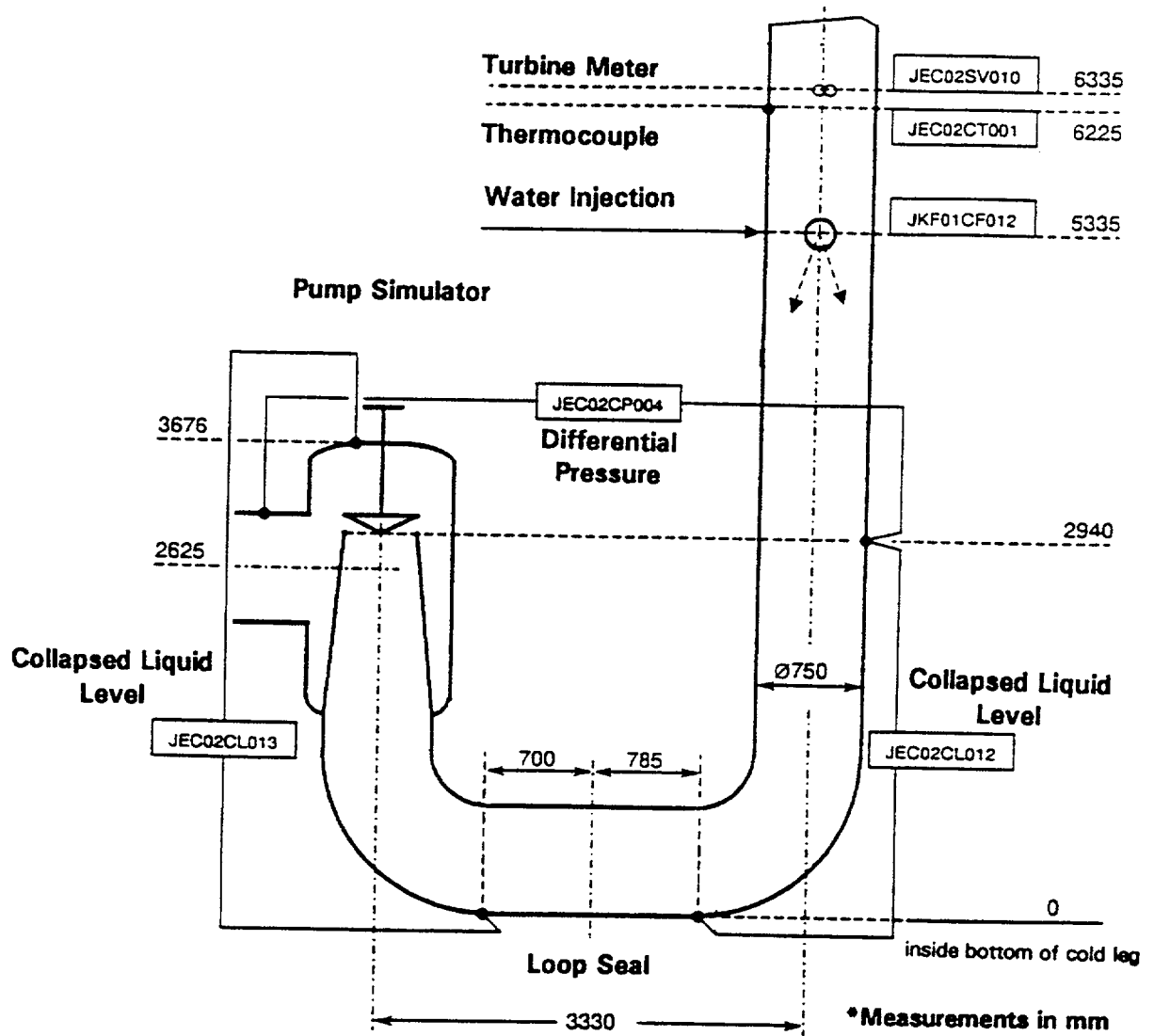


Figure 5.4.3 UPTF Loop 2 Loop Seal Configuration and Instrumentation



**Figure 5.4.4 Loop Seal Nodalization with 13 Volumes**

**Figure 5.4.5 Cold-Leg Outlet Pressure Boundary Condition for  
S-RELAP5 Model UPTF Test A5RUN11E**

**Figure 5.4.6 Cross-Over Leg Inlet Steam and Water Injection Mass  
Flow Rate Boundary Conditions for S-RELAP5 Model UPTF Test  
A5RUN11E**

**Figure 5.4.7 Cross-Over Leg Inlet Steam and Water Injection  
Temperature Boundary Conditions for S-RELAP5 Model UPTF Test  
A5RUN11E**

**Figure 5.4.8 Comparison of Loop Seal Collapsed Liquid Level to  
Data from UPTF Test A5RUN11E-Base Model 10 ms Time Step**

**Figure 5.4.9 Comparison of Differential Pressure Across Loop Seal  
to Data from UPTF Test A5RUN11E-Base Model with 10 ms Time  
Step**

**Figure 5.4.10 Loop Seal Nodalization with 10 Volumes**

**Figure 5.4.11 Comparison of Loop Seal Collapsed Liquid Level to Data from UPTF Test A5RUN11E—Alternative Model with 10 ms Time Step**

**Figure 5.4.12 Comparison of Differential Pressure Across Loop Seal to Data from UPTF Test A5RUN11E—Alternative Model with 10 ms Time Step**



**Figure 5.4.13 Calculated Comparison of Loop Seal Collapsed Liquid Level to Data from UPTF Test A5RUN11E-Base Model with 100 ms Time Step**

**Figure 5.4.14 Comparison of Differential Pressure Across Loop Seal to Data from UPTF Test A5RUN11E-Base Model with 100 ms Time Step**

**Figure 5.4.15 Calculated Comparison of Loop Seal Collapsed Liquid Level to Data from UPTF Test A5RUN11E - Base Model with 5 ms Time Step**

**Figure 5.4.16 Comparison of Calculated Differential Pressure Across Loop Seal to Data from UPTF Test A5RUN11E - Base Model with 5 ms Time Step**

## 5.5 **BETHSY**

Test 9.1b at the BETHSY test facility (Reference 30) is an integral benchmark test for SBLOCA analyses. It simulates the typical limiting break size and location in a PWR. This test simulates many of the major phenomena in SBLOCA transients in PWRs, such as loop seal clearing, core level depression, core heat up and refill, and break flow. It provides an extensive database for assessing the various thermal hydraulic models in system computer codes and has been designated as International Standard Problem (ISP) 27 for the international code assessment program (ICAP) community during the code development stage of RELAP5/MOD2 and RELAP5/MOD3 (References 31 and 32).

S-RELAP5 was used to simulate the phenomena, including primary and secondary system pressures, core collapsed level, integrated break flow mass, loop seal clearing, and ECCS injection.

### 5.5.1 Test Facility Description

BETHSY is a test facility designed to represent a 3-loop 2775-MWt Westinghouse-type PWR. It is scaled such that the heights are preserved and the volume is scaled by a factor of 1/100. The primary and secondary systems have design pressures of 17.2 (2495 psia) and 8 MPa (1160 psia) respectively. The core simulator has 428 full-length heater rods and 29 guide tubes. The heater rods simulate a 17x17 fuel design. Other components in the primary system include a core bypass, an external downcomer, three piping loops, reactor coolant pumps, and a pressurizer. The secondary system consists of three steam generators with 34 U-tubes each. The flow rates and temperatures for the main and auxiliary feedwater systems are adjustable.

The ECCS includes HHSIs, LHSIs, and accumulators. The ECCS water can be injected in the cold-legs or at other locations such as the hot-legs, the top of downcomer, or the lower and upper plena. In addition, trace heaters are installed in the primary coolant system and steam generators to compensate for the excessive heat loss due distorted ratio between volume and surface area.

Figure 5.5.1 shows the principal components of the BETHSY facility. Reference 30 describes the BETHSY facility in more detail.

### 5.5.2 S-RELAP5 Model

The S-RELAP5 input model used to simulate the BETHSY SBLOCA is based on a RELAP5/MOD3 model developed at INEEL (Reference 33). The input model was modified for use with S-RELAP5 and to incorporate SPC modeling guidelines for SBLOCA.

[

]

The schematic noding diagram is shown in Figure 5.5.2. The following specific features were incorporated in the S-RELAP5 model

[

2.

]

### 5.5.3 Boundary Conditions

The event was initiated by opening a 2-inch break located at the cold-leg centerline on the discharge side of the pump. HHSI was assumed to be unavailable, which ensured core

uncovery and fuel rod heat up. When the cladding temperature reached 723 K (842 °F), an “ultimate procedure” was instituted that involved a steam generator dump to atmosphere to depressurize the primary system below the accumulator pressure and the shut-off head of the LHSI. The test was considered over when the reactor primary system was in a condition where the residual heat removal system could be actuated.

The power and pump speeds from the data were used as boundary conditions for the analysis. Figure 5.5.3 and Figure 5.5.4 show the core power versus time and pump speed versus time, respectively.

#### 5.5.4 Comparison to Data

Table 5.5.1 compares the calculated and measured chronology of key events. The comparison demonstrates that S-RELAP5 can simulate the major phenomena of a SBLOCA transient in a PWR. The maximum clad temperature predicted by S-RELAP5 was 1035 K (1403 F), which is conservative compared to the measured value of 995 K (1331 °F). The calculated time of PCT was 3030 seconds, which agrees well with measured value of 3050 seconds.

Figure 5.5.5 through Figure 5.5.10 compare the predictions from S-RELAP5 with the data. The S-RELAP5 calculated results include a time shift to remove the 100 second steady state calculation performed before transient initiation. In general, the calculation results compare well with data.

Figure 5.5.5 compares calculated and measured pressure response for the primary system. The emptying of the pressurizer drives the initial, rapid depressurization. During the slow, quasi-steady pressure plateau extending to 2560 seconds, the pressure is the saturation pressure for the primary coolant. The pressure differences after about 750 seconds reflect the differences in the core exit temperature during this period. At about 2560 seconds, the ultimate procedure was initiated, which led to further depressurization.

Figure 5.5.6 compares calculated and measured pressure response for the secondary system. The calculation and data agree very well, except for the depression in the secondary pressure between 500 and 1500 seconds. This depression is caused by a loss of recirculation in the secondary side of the steam generators and the consequent subcooling in the risers (Reference 30). This is also the period where the break flow is considerably under-predicted.

Figure 5.5.7 compares calculated and measured break flow. The calculation did not predict the increase in break flow rate in the period between 500 and 1500 seconds. The subcooling in the risers caused a decreased temperature, and possibly a decreased void fraction, at the break during this period. These contributed to the increased mass flow from the break during the 500 to 1500 second time frame. After 1500 seconds, the measured break flow dropped considerably in magnitude, while the calculated mass flow was considerably larger from 1500 to 2000 seconds. Beyond 2000 seconds, the calculated flow decreased in magnitude until it coincided with the measured break flow at 2500 seconds. The initially under-predicted then over-predicted mass flows caused the loops seals to uncover later than measured, while the core uncovering and subsequent heat-up occurred slightly earlier than measured. Overall, the comparison with data is reasonable.

Figure 5.5.8 shows the loop seal clearing behavior by comparing calculated and measured differential pressure on the descending leg of Loop 2. The behavior before the 2560 seconds (ultimate procedure) shows two major aspects of loop seal behavior. The first is the rapid drop when loop seal clearing occurred. While the drop is significant, it does not reduce to zero. As liquid falls back in to the loop seal, a pressure differential of from 5 to 10 kPa (0.7 to 1.5 psia) remains. As the liquid clears the loop, the pressure differential finally drops to zero. In the uncleared loops, the pressure differential of 10 kPa (1.5 psia) remains until the ultimate procedure begins. S-RELAP5 predicts a later loop seal clearing than was observed. This is consistent with the break flow rates, because the break uncovers when the loop seal clears. The post-clearing behavior for this case, while delayed reflects the data quite well.

Figure 5.5.9 compares calculated and measured collapsed core level. This particular comparison is one of the critical comparisons for the SBLOCA outcome. The calculated level agrees very well with data, both qualitatively and quantitatively.

Figure 5.5.10 compares calculated and measured clad temperatures at the PCT node. The calculated results reflect the slightly early, deeper collapsed level response for S-RELAP5 compared to the data. The calculated PCT was about 1035 K (1403 °F), as compared to the measure value of 995 K (1331 °F). The calculated time of PCT was 3030 seconds compared to the measure time of 3050 seconds.

#### 5.5.5 Conclusions

The S-RELAP5 code was assessed against the BETHSY Test 9.1b (ISP 27). S-RELAP5 simulates the various observed major phenomena well, including primary and secondary system pressures, core collapsed level, break flow, loop seal clearing, and ECCS injection. [

] S-RELAP5 was shown to closely predict the loop seal clearing process and the post-clearing behavior observed in the test. Finally, the maximum clad temperature was conservatively predicted to be about 1035 K (1403 °F) as compared to data of 995 K (1331 °F). The calculated PCT time of occurrence was 3030 seconds which agrees well with data of 3050 seconds. Therefore, the present results support the use of S-RELAP5 for PWR SBLOCA analyses.

**Table 5.5.1 Chronology of Main Events**

Event	Event Time, s	
	Measured	Calculated
Transient starts	0	0
Scram signal occurs	41	33
Pressurizer empties	50	48
Safety injection signal generated (P = 11.9 M Pa)	54	50
Core power decay starts 17 seconds after scram signal	58	50
Aux. feedwater starts (30 seconds after SI signal)	82	80
Pump coastdown starts 300 seconds after SI signal	356	350
Pump stops	971	970
First core exposure begins	1830	2000
First loop seal clears in Loop 2	1944	2150
Ultimate Procedure Starts	2562	2562
Loop seal reforms in Loop 2	2750	2650
Accumulator injection starts	2962	2915
Second loop seal clears in Loop 2	3040	3045
Second loop seal reforms in Loop 2	3680	3800
Accumulator isolates	3831	3900
LHSI starts	5177	5154



**Table 5.5.2 Initial Conditions for BETHSY Test 9.1b**

Parameter	Units	Measured
<b>PRIMARY LOOP</b>		
Core differential temperature	K	3.58
Primary pressure	MPa	15.51 ± 0.09
Core inlet temperature	K	559.85 ± 0.5
Primary loop flow rate	kg/s	50.0 ± 5
Pump rotational speed	rpm	2940 ± 30
Core power	kW	2857 ± 30
Pressurizer pressure	MPa	15.51 ± 0.09
Pressurizer level	m	4.08 ± 0.1
Primary mass inventory	kg	1960
<b>SECONDARY SYSTEM</b>		
Steam dome pressure	MPa	6.91 ± 0.04
Feedwater flow rate/SG	kg/s	0.52
Downcomer level	m	13.45 ± 0.05
Recirculation ratio/SG	-	20 ± 2
Secondary mass inventory/SG	kg	820 ± 30
<b>EMERGENCY CORE COOLING</b>		
Accumulator pressure	MPa	4.18 ± 0.04
Accumulator temperature	K	290.15 ± 1
Accumulator liquid volume	m <sup>3</sup>	0.286
<b>EXTERNAL CIRCUITS</b>		
Trace heating	kW	107.5 ± 2
Pump connected cooling circuits	kW	25 per pump

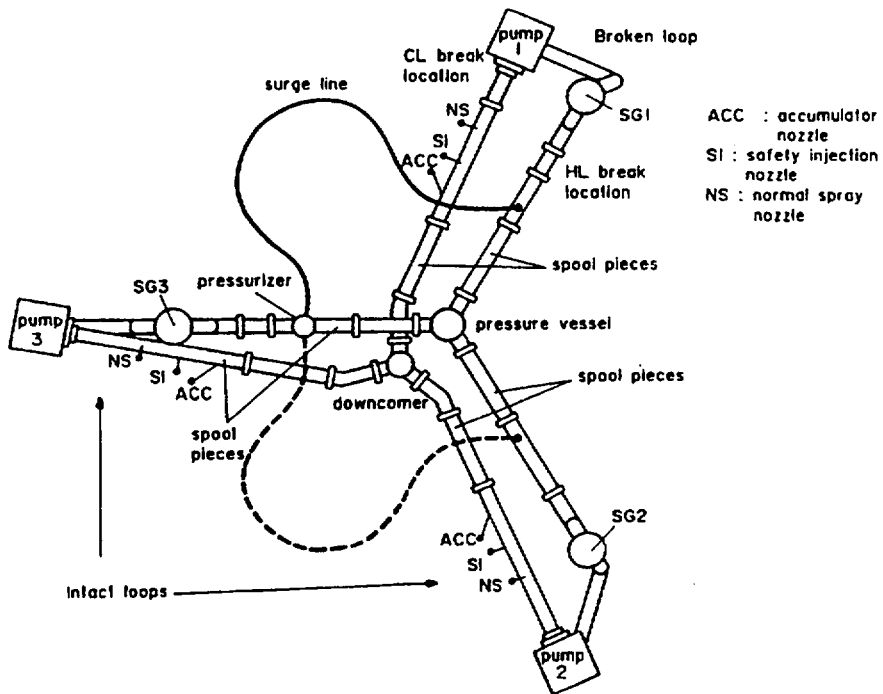


Figure 5.5.1 Schematic of BETHSY 3-Loop Configuration



**Figure 5.5.2 S-RELAP5 Nodalization of BETHSY Facility**

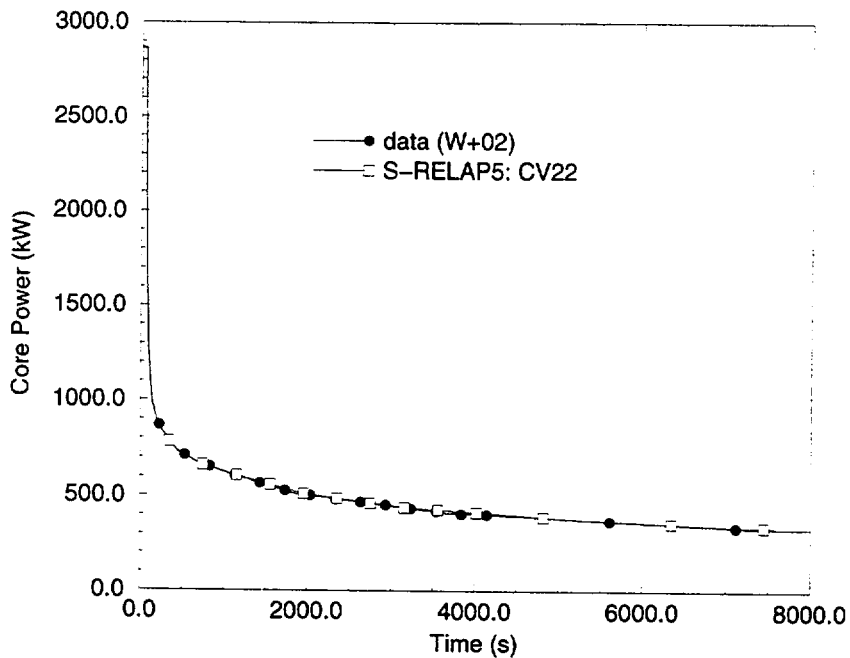


Figure 5.5.3 S-RELAP5 Core Power Compared to Experimental Data

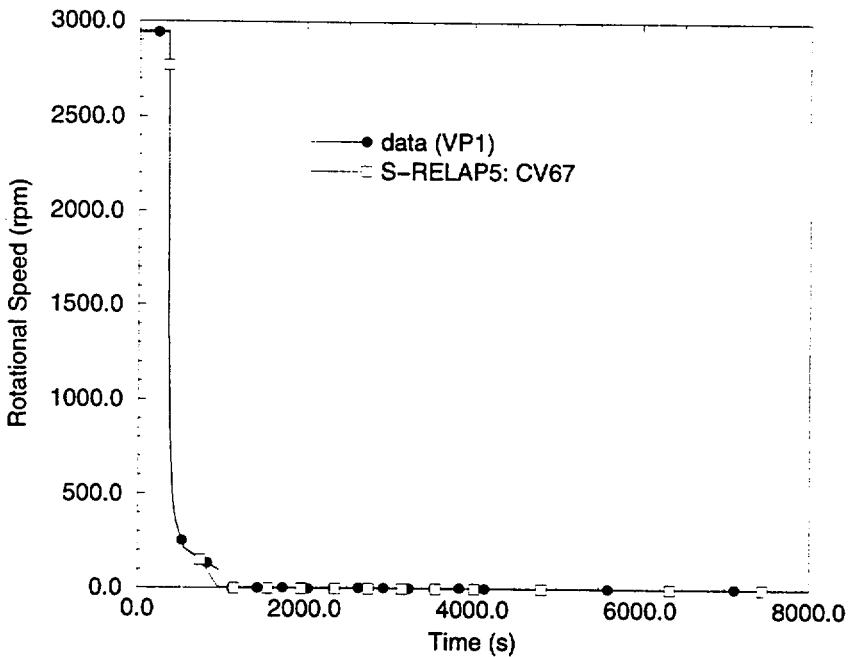
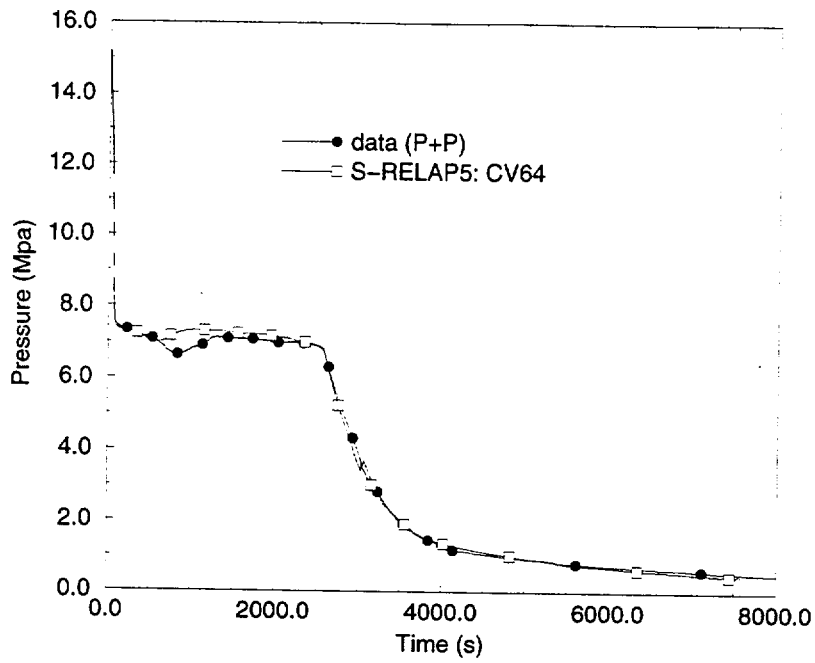
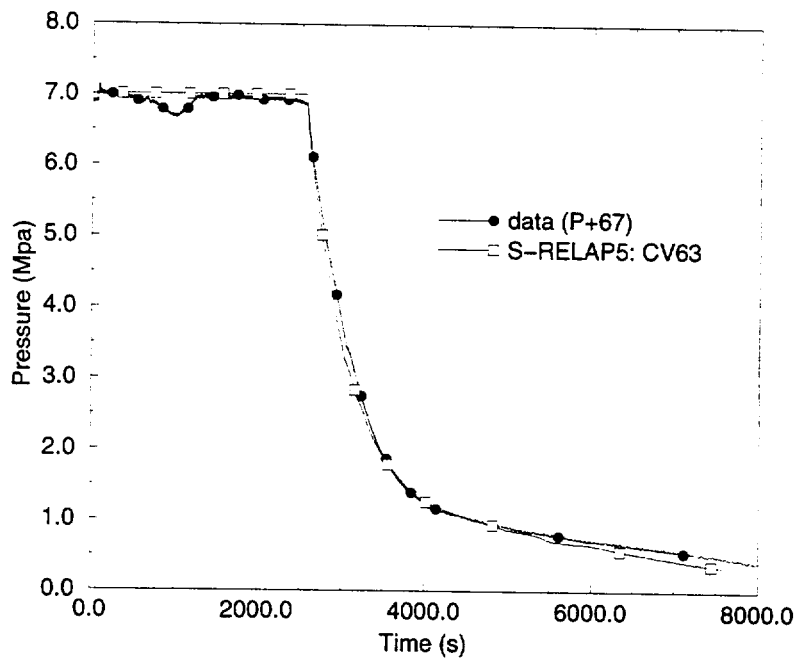


Figure 5.5.4 S-RELAP5 Pump Speed Compared to Experimental Data



**Figure 5.5.5 S-RELAP5 Pressurizer Pressure Compared to Experimental Data**



**Figure 5.5.6 S-RELAP5 Secondary Pressures Compared to Experimental Data**

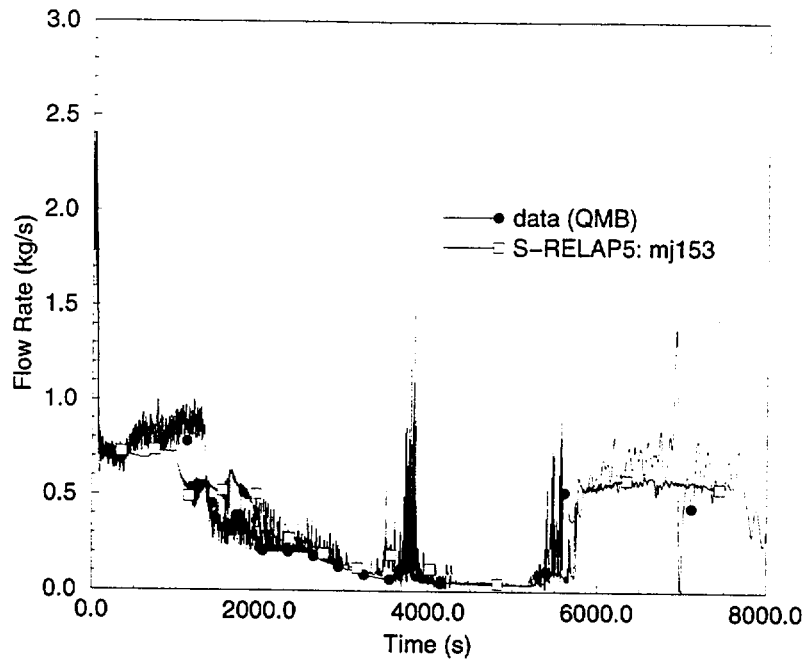


Figure 5.5.7 S-RELAP5 Break Flow Compared to Experimental Data

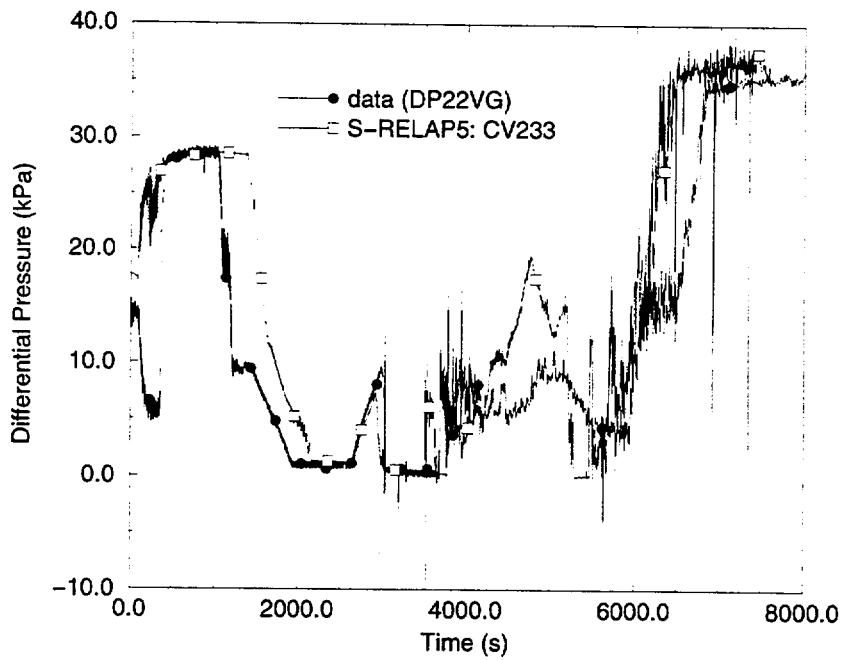


Figure 5.5.8 S-RELAP5 Loop Seal Downflow Side Differential Pressure Compared to Experimental Data from Loop 2

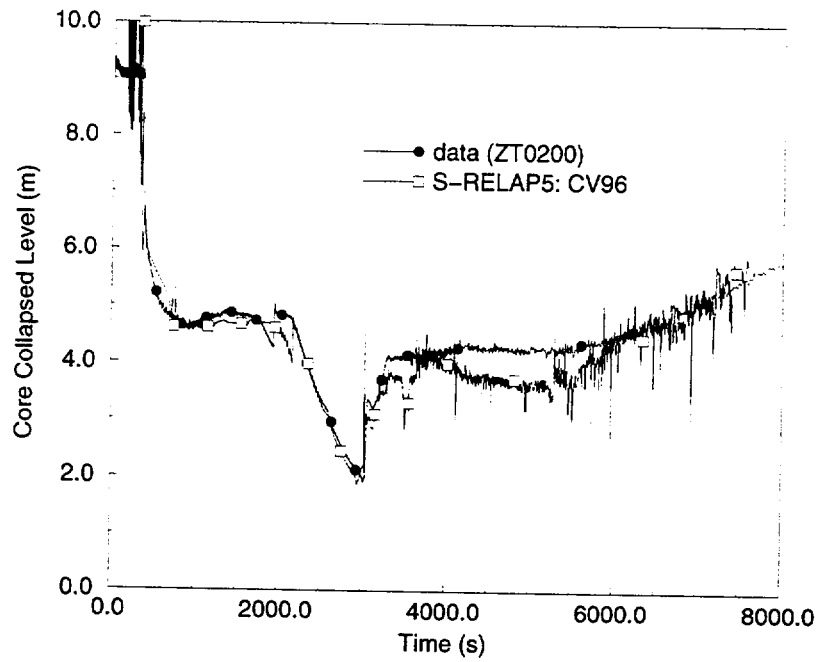


Figure 5.5.9 S-RELAP5 Core Collapsed Level Compared to Experimental Data

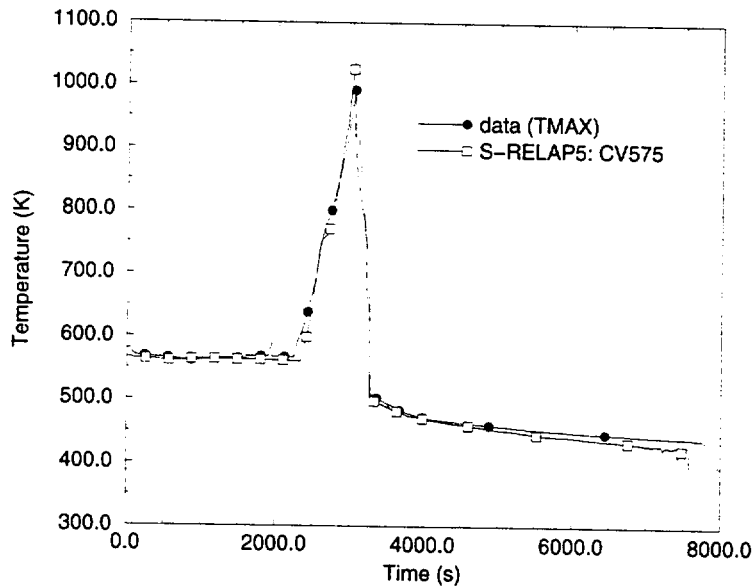


Figure 5.5.10 S-RELAP5 Maximum Clad Temperature Compared to Experimental Data

## 6.0 Methodology Example

The example calculation is presented which shows the application of the S-RELAP5 SBLOCA methodology to a 2300-MWt, Westinghouse-designed PWR with 3 hot-legs, 3 cold-legs, and 3 vertical U-tube steam generators. The reactor vessel contains a downcomer, upper and lower plena, and a reactor core containing 157 fuel assemblies. The hot-legs connect the reactor vessel with the vertical U-tube steam generators. Feedwater is injected into the downcomer of each steam generator. There are three auxiliary feedwater pumps (AFW); two motor driven and one turbine driven. The ECCS contains three HHSI pumps, three accumulators, and two LHSI pumps.

### 6.1 *S-RELAP5 Model*

The reactor coolant system of the plant is nodalized in the S-RELAP5 model into control volumes interconnected by flow paths. The model includes 3 accumulators, a pressurizer, and three steam generators with both primary and secondary sides modeled. All the loops were modeled explicitly to provide an accurate representation of the plant.

Figure 6.1 and Figure 6.2 are nodalization diagrams for the primary and secondary systems.

Decay heat was determined from reactor kinetics equations with actinide and decay heating as prescribed by Appendix K.

The calculations assumed loss of off-site power concurrent with reactor scram. The single failure criterion required by Appendix K was satisfied by assuming the loss of one diesel generator, which resulted in the disabling of one HHSI pump, one LHSI pump, and one motor-driven auxiliary feedwater pump. In addition, one HHSI pump was assumed to be off line for service, leaving only one active HHSI pump. Initiation of the HHSI system was delayed the maximum expected value beyond the time of SIAS to account for the time required for startup of the diesel generator, switching, and valve sequencing. The disabling of a motor-driven auxiliary feedwater pump left one motor-driven pump and the turbine-driven pump available. The motor-driven pump actuation setpoint was based on low steam generator level plus a delay. No credit was taken for the turbine-driven AFW.

In the analysis, the RCPs tripped at reactor scram, coincident with the loss of off-site power. Steam generator tube plugging was set to 6% symmetrically.



The axial power shape used was a conservatively top-skewed (EOC) shape. The power in the hot rod was at the technical specification peaking limits.

[

]

The limiting case was identified via a break spectrum analysis.

## 6.2 ***Break Spectrum***

A range of break sizes was analyzed for breaks located in the pump discharge cold-leg as a part of the sample problem. These included 1.5-inch, 2.0-inch, and 2.5-inch-diameter breaks. The 2.0-inch break produced the limiting PCT (Table 6.1).

The 1.5-inch break was small enough that HHSI flow was sufficient to prevent any significant core uncover. The primary system lost mass for the first 6000 seconds, then began recovering. Core uncover began at about 4800 seconds and a brief core heatup occurred in the 5000 to 7200 second period. The HHSI flow exceeded the boil-off rate and the core recovered. At the end of the simulation, the primary system was gaining mass at the rate of about 1 lbm/s and the vessel downcomer was filled to the cold-leg nozzle elevation.

The 2.5-inch break was large enough to cause the system to depressurize to the accumulators injection pressure fairly rapidly. Although uncover occurred much sooner, the amount of time spent uncovered was relatively short. The large amount of liquid injected by the accumulators between 1800 and 2500 seconds terminated the core heatup. When the calculation was terminated only about 10% of the accumulators' inventory had been injected.

The 2.0-inch break was the limiting break. The core uncover was delayed compared to the 2.5-inch break, but the rate of depressurization to the accumulator setpoint was much lower and the amount of time the hot rod spent uncovered was greater.

### 6.3 **2-Inch Break Base Case**

The sequence of events for this case is presented in Table 6.2. The 2-inch break caused a longer period of core uncover than the 1.5-inch and 2.5-inch breaks. Cladding temperatures rose steadily during the 1100 seconds between core uncover and accumulator injection. The calculation was terminated at 3500 seconds.

The break flow is plotted in Figure 6.3. The break flow is driven by the system pressure and the void at the break. Until loop seal clearing occurs, it mirrors the primary pressure. At that time, the flow transitions from liquid to steam and the mass flow out the break drops precipitously (see Figure 6.4).

Figure 6.5 shows the pressure traces for the PCS and the three steam generators. The behavior is typical of limiting SBLOCA events. The primary pressure drops rapidly to saturation, then again falls rapidly as the core level drops and the boil-off rate decreases.

Figure 6.6 shows the voids in the ascending legs of the loop seals. [ ] only one loop cleared (Loop 1) at 1184 seconds.

After the initial clearing, the loop seal experienced some carryover of liquid from the horizontal segment of the seal for a period, then re-cleared.

Figure 6.7 shows the combined HHSI flow for this case. As the system depressurizes because of the core boil-off, the HHSI flow increases.

The core collapsed level and core mixture levels are shown in Figure 6.8. The difference between the two shows the presence of two-phase flow in the core. The uncovering of the core at about 1900 seconds is clearly shown.

Figure 6.9 shows the cladding and vapor temperatures corresponding to the node with the maximum PCT of 1634 °F. The core is heating until the accumulator injects at 3080 seconds. The temperature then begins to recover to saturation.

With the core flooded, the boil-off rate and the system pressure rise. The pressure rise reduces HHSI flow, and if the pressure rises sufficiently, the accumulator flow will cease. Eventually, a second heat-up will occur. However, at this later time the decay heat will be lower and the temperature excursion will be far smaller.

#### 6.4 ***Sensitivity Studies***

The sensitivity studies described in this section address a set of variations expected to have little effect on the outcome. The figure of merit for the sensitivity studies is the difference in PCT between a designated base case and the resulting sensitivity case. The results of the sensitivity study are reported and summarized in Table 6.3. In all cases expected to have minimal impact, the change in PCT is 5 °F or less. This reflects a stable, converged methodology.

##### 6.4.1 Time Step Size

The nominal time step size recommended for transient calculations is 0.01 seconds. For the sensitivity case, the maximum time-step size was halved to 0.005 seconds. The run started from the same steady-state as the original run. [

]

#### 6.4.2 Restart

Sensitivity studies were conducted to show the sensitivity of PCTs to the choice of steady-state restart number and to restarting a transient. Neither of these changes will have a significant effect on the results.

The first sensitivity run was conducted by rerunning the 2-inch break simulation and restarting from 600 seconds of steady-state rather than 300 seconds of steady state. [

]

The second sensitivity run restarted the base calculation at 1000 seconds (200 seconds before loop seal clearing) and rerunning the 1000 – 3500-second part of the simulation. [

]

#### 6.4.3 Loop Seal [

]

[

]

#### 6.4.4 Pump Model

[

]

#### 6.4.5 Radial Flow Form Loss Coefficients

This study was performed to show insensitivity of core radial flow loss coefficients on the outcome of the SBLOCA event. [

] These results show that the PCT calculated is insensitive to form loss in the horizontal direction. Therefore, form loss sensitivity studies are not required as part of the SBLOCA licensing analysis.

#### 6.4.6 Nodalization Studies

Three nodalization studies were performed to test model performance. A simple test was to renumber connections between the cold legs and downcomer. The PCT calculated by S-RELAP5 should be insensitive to how the components are numbered in the model. The net change in calculated PCT was 0 °F (no change).

[

]

#### 6.4.7 Summary

A sample analysis to determine the limiting break size was made by applying the revised SBLOCA methodology to a three-loop Westinghouse PWR. RODEX2 was used to determine fuel burn-up conditions at EOC. S-RELAP5 was used to calculate the maximum hot rod temperature. The results of the study showed that the 2 inch break case was limiting with a PCT of 1634 °F.

Furthermore, sensitivity studies were performed using the three-loop Westinghouse PWR to show that the solution was converged with respect to time step size, restart application, loop seal biasing, pump application, core radial flow, and nodalization. Results of the study show that the S-RELAP5-based SBLOCA methodology is well converged and has a very small sensitivity to all the parameters investigated. Therefore, the requirement to perform sensitivity calculations in licensing analysis is unnecessary.

**Table 6.1 Break Spectrum Results  
Summary**

<b>Break Size (diameter in inches)</b>	<b>PCT (°F)</b>
1.5	940
2.0 (base 2.0-inch case)	1634
2.5	1491

**Table 6.2 Event Sequence for 2.0-Inch Break**

Event	Time (s)
Break initiation	0.0
Reactor and RCP trip (505, 515)	38
SIAS trip (trip 509). 28.5s must elapse to get pumps on-line	63
HHSI began (trip 560)	217
Motor-driven AFW initiation (trip 1615)	111
Loop seal clearing – Loop 1 (Void 226-8 >0.97),	1184
Loop seal clearing – Loop 2 (component 326),	---
Loop seal clearing – Loop 3 (component 426 - broken leg),	---
Break uncover (junction 885) (trip 568)	1277
Accumulator injection (trip 562)	3080
PCT occurs (1646 °F, H.S. 1721, node 28)	3084
Steam generator level recovered (trip 1611)	-
End of calculation	3500



**Table 6.3 Sensitivity Studies**





**Figure 6.1 S-RELAP5 Primary System Nodalization**



**Figure 6.2 S-RELAP5 Secondary Side Nodalization**

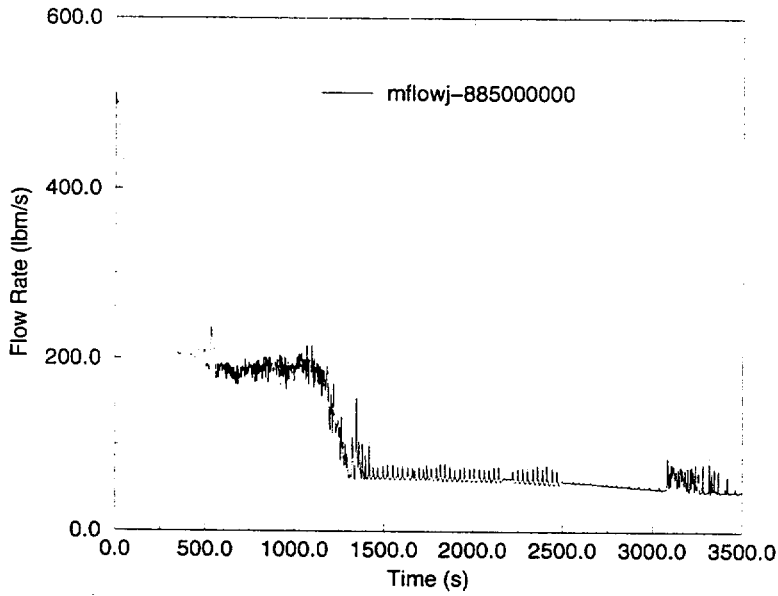


Figure 6.3 Break Flow Rate for 2.0-Inch Break

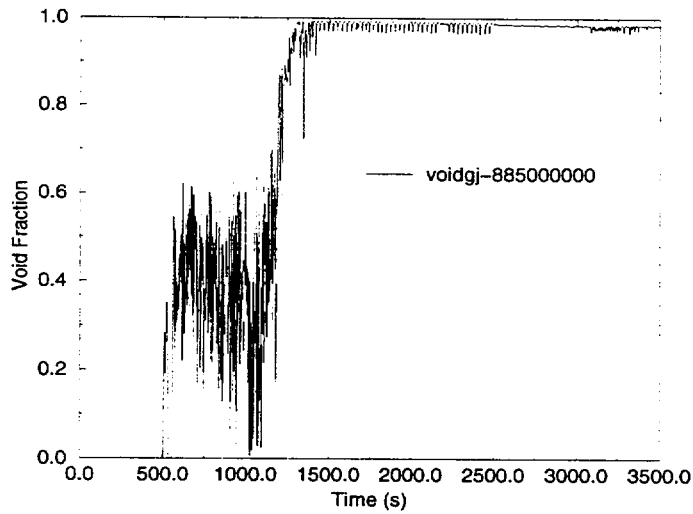


Figure 6.4 Break Void Fraction for 2.0-Inch Break

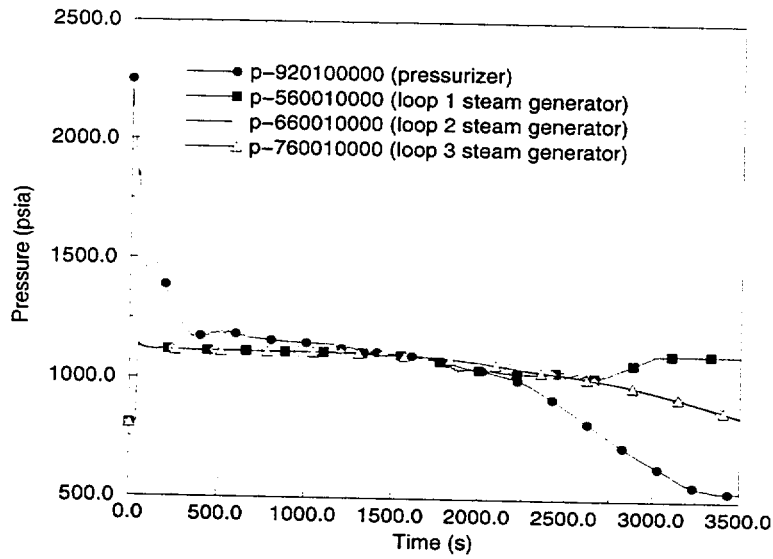


Figure 6.5 System Pressures for 2.0-Inch Break

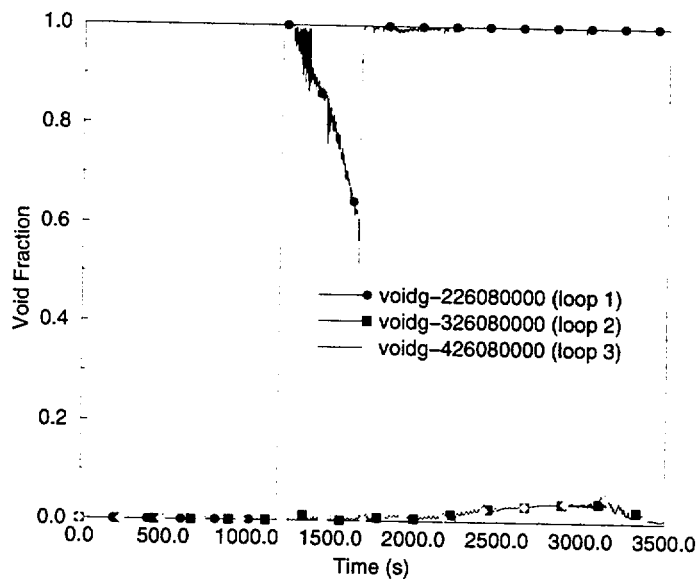


Figure 6.6 Loop Seal Void Fractions for 2.0-Inch Break

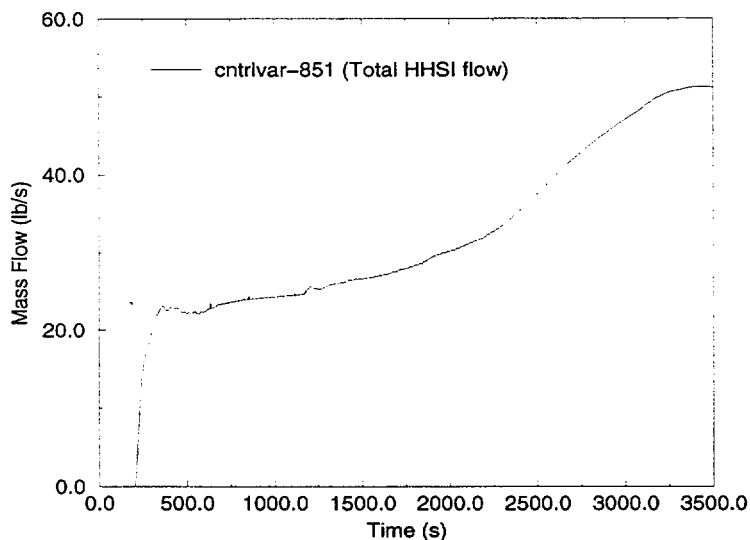


Figure 6.7 Combined High Head and Charging Flow for 2.0-Inch Break

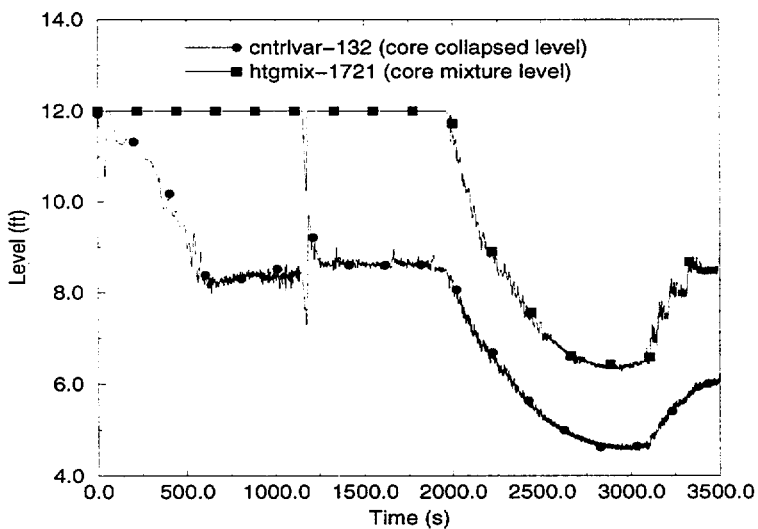
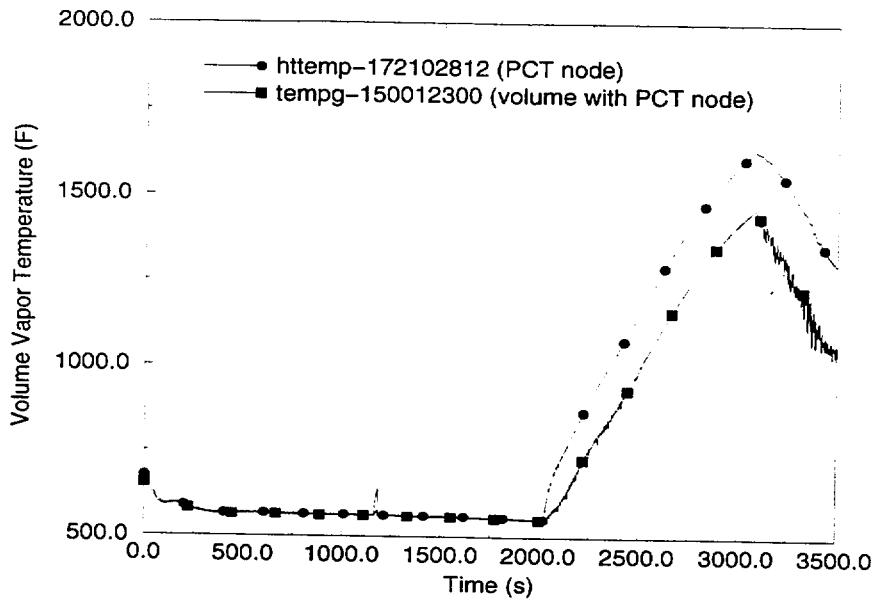


Figure 6.8 Core Mixture Level and Collapsed Liquid Level for 2.0-Inch Break



**Figure 6.9 Vapor and Clad Temperatures for Hot Node with 2.0-Inch Break**

## 7.0 References

1. XN-NF-82-49 (P) (A), Revision 1 Supplement 1 *Exxon Nuclear Company Evaluation Model Revised EXEM PWR Small Break Model*, Siemens Power Corporation, December 1994.
2. EMF-2100(P) Revision 1, *S-RELAP5 Models and Correlations Code Manual*, Siemens Power Corporation, December 1999.
3. XN-NF-81-58(P) (A), Supplements 1 and 2, Revision 2, *RODEX2 Fuel Thermal-Mechanical Response Evaluation Model*, Exxon Nuclear Company, March 1984.
4. ANF-81-58(P)(A) Revision 2 Supplements 3 and 4, *RODEX2 Fuel Thermal-Mechanical Response Evaluation Model*, Advanced Nuclear Fuels Corporation, June 1990.
5. XN-NF-82-07(P)(A), Revision 1, *Exxon Nuclear Company ECCS Cladding Swelling and Rupture Model*, Exxon Nuclear Company, November 1982.
6. S. M. Bajorek, A. Ginsberg, D. J. Shimeck, K. Ohkawa, M. Y. Young, L. E. Hochreiter, P. Griffin, Y. Hassan, T. Fernandez, D. Speyer, "Small Break Loss of Coolant Accident Phenomena Identification and Ranking Table (PIRT) for Westinghouse Pressurized Water Reactors", Ninth International Topical Meeting on Nuclear Reactor Thermal Hydraulics (NURETH-9), San Francisco, California, October 3-8, 1999.
7. "UPTF-TRAM Versuch A5, Freiblasen des Pumpenbogens Einzeleffekt- und Integralversuche, Quick Look Report," NT33/94/011, Siemens AG, Erlangen, Germany, Power Generation Group (KWU), December 1994.
8. V. H. Ransom, *RELAP5/MOD2 Code Manual, Vol. 1: Code Structure, Systems Models, and Solution Methods*, NUREG/CR-4312, EGG-2396, Rev. 1, March 1987.
9. The RELAP5 Development Team of INEL, *RELAP5/MOD3 Code Manual, Vol. 1: Code Structure, Systems Models, and Solution Methods*, NUREG/CR-5535, INEL-95/0174, August, 1995.
10. 2D/3D Program Upper Plenum Test Facility, *UPTF Test No.6 Downcomer Countercurrent Flow Test*, Quick Look Report, U9 316/89/2, Siemens KWU March 1989; *UPTF Test No.7 Downcomer Countercurrent Flow Test*, Quick Look Report, E314/90/003, Siemens KWU, March 1990.
11. A. K. Jain, "Accurate Explicit Equation for Friction Factor," *ASCE J. Hydraulics Div.*, 102, pp. 674-677, 1976.
12. R. T. Lahey, Jr., "A Mechanistic Subcooled Boiling Model," *Proceedings of Sixth International Heat Transfer Conference*, Volume 1, pp. 293-297, 1978.
13. M. J. Thurgood, *Recommendation for Determining the Uncertainty in the Peak Clad Temperature Calculated by RELAP5/MOD2/ANF for a Loss-of-Coolant Accident*, NAI Report.



14. F. J. Moody, "Maximum Flow Rate of a Single Component, Two-Phase Mixture," *Journal of Heat Transfer, Trans. ASME*, 87, pp. 134-142, 1965.
15. S. G. Bankoff, R. S. Tankin, M. C. Yuen, and C. L. Hsieh, "Countercurrent Flow of Air/Water and Steam/Water Through a Horizontal Perforated Plate," *International Journal of Heat and Mass Transfer*, Vol. 24, pp. 1381-1395, 1981.
16. The RELAP5 Development Team of INEL, *RELAP5/MOD3 Code Manual Vol. 4: Models and Correlations*, NUREG/CR-5535, INEL-95/0174, August, 1995.
17. *Pump Two-Phase Performance Program*, EPRI NP-15556, Vols. 1-8, September 1980.
18. L. Baker and L. C. Just, *Studies of Metal-Water Reactions at High Temperature: III. Experimental and Theoretical Studies of Zirconium-Water Reaction*, ANL-6548, 1962.
19. C. W. Stewart, et al, *VIPRE Code Manual: Volume 3, Programmer's Manual*, Battelle Pacific Northwest Laboratory, June 1981.
20. H. Chelemer, P. T. Chu & L. E. Hochreiter, *THINC-IV – An Improved Program for Thermal-Hydraulic Analysis of Rod Bundle Cores*, WCAP 7956, Westinghouse Electric Corporation, June 1973.
21. E. Weiss, R. A. Markley & A. Battacharyya, "Open Duct Cooling-Concept for the Radial Blanket Region of a Fast Breeder Reactor," *Nuclear Engineering and Design, Volume 16*, PP 175-386, 1971.
22. I. E. I'Delchik, et al, *Handbook of Hydraulic Resistance*, Second Edition, Revised and Augmented.
23. *Vessel Coolant Mass Depletion During a Small-Break LOCA*, EGG-SEMI-6010, Sept. 1982.
24. *Experimental Analysis and Summary Report on OECD LOFT Experiment LP-SB-3*, OECD LOFT-T-3905, December 1985.
25. D. L. Reeder, LOFT System and Test Description (5.5 ft Nuclear Core 1 LOCES), NUREG/CR-0247, TREE-1208, July 1978.
26. *Quick Look Report on OECD LOF Experiment LP-SB-03*, OECD LOFT-T-3604, March 1984.
27. "Freiblasen Des Pumpenbogens Einzeleffekt- und Integralversuche, Versuchsdatenbericht," S554/93/007, Siemens AG, Erlangen, Germany, Power Generation Group (KWU), September 1993.
28. "UPTF-TRAM Test Group A Test Results, Analysis," *Working Group of Experts Meeting*, Mannheim, Germany, Siemens AG, December 6-8, 1993.

29. "UPTF-TRAM Test Instrumentation, Measurement System Identification, Engineering Units and Computed Parameters," S554/92/013, Siemens AG, Erlangen, Germany, Power Generation Group (KWU), November 1992
30. P. Clement, Chataing, T., and Deruaz, R., "Final Comparison Report for International Standard Problem 27," French original report on BETHSY Test 9.1b.
31. S. Lee, B. D. Chung, and H. J. Kim, "Assessment of BETHSY Test 9.1b Using RELAP5/MOD3," NUREG/IA-0103, June 1993. Korea's ICAP report on BETHSY Test 9.1b
32. P. A. Roth, C. J. Choi, and R. R. Schultz, *Analysis of Two Small Break Loss-of-Coolant Experiments in the BETHSY Facility Using RELAP5/MOD3*, EGG-NE-10353, Idaho National Engineering Laboratory, July 1992.
33. Transmittal package from Carolee McKenzie (INEEL) to W. S. Yeung "FIN A6102 – Transmittal of ISP 26 and ISP 27 Data – CCK-03-94," dated May 13, 1994. Package included data tapes, work books, and input decks for ISP26 and ISP27.
34. M. Jakob, "Heat Transfer and Flow Resistance in Cross Flow of Gases Over Tube Banks," *Trans. ASME*, Vol. 60, pp 384-386, 1938.

## Appendix A Core Radial Loss Coefficient Development

[



## Distribution

J. S. Holm, 26/USNRC (12)

e-mail notification only

DM Brown  
KE Carlson  
H Chow  
RE Collingham  
RL Feuerbacher  
KR Greene  
RC Gottula  
RG Grummer  
TM Howe  
SE Jensen  
AB Meginnis  
WT Nutt  
LD O'Dell  
PWR Neutronics  
PWR Safety Analysis